

3.2.4 Mel Kuntz

Spatial and Temporal Models

Figures 3.2.4-1 and 3.2.4-2 present the logic trees describing the basic structure of the spatial and temporal models developed by Mel Kuntz (MK) for PVHA-U. MK specified different models for the 10,000-year assessment and for the 1-My assessment. For the 10,000-year assessment (Figure 3.2.4-1), the past events that form the basis for the spatial and temporal models are restricted to events younger than 4 Ma. For the 1-My assessment, older events are also considered relevant, and two sets of models are developed: one based on events younger than 4 Ma and the other based on events younger than 12 Ma. Table 3.2.4-1 lists all the past events in the region of interest judged relevant by MK to any of his spatial and temporal models. The table lists events within each of two spatial zones, described below. The table includes alternative interpretations of some events, along with the probability MK assigned to each interpretation. In combination, twelve unique interpretations of the number of past events younger than 4 Ma were identified, and 196 unique interpretations of the number of past events younger than 12 Ma in the region of interest were identified. These are represented schematically in the second node of each logic tree: separate spatial and temporal models are fitted to each of these alternative event sets. The probability for each event set is calculated from the probabilities given to different interpretations as summarized in Table 3.2.4-1.

Several alternative approaches to modeling the spatial distribution of future events were specified: (1) a locally homogenous zones model with a single Crater Flat zone and a larger background zone, and (2) a spatial smoothing model using kernel density estimation combined with estimates based on the interpretation of various geology data sets. Two data sets are used: lithostatic pressure and tomography, as shown in Figure 3.2.4-1.

Figure 3.2.4-3 illustrates the two zones defined for the spatial zones model: the Crater Flat zone and the larger region of interest. In the locally homogenous zones model, events are assumed to occur within each of these zones at different rates, and the spatial distribution of events within each zone is homogenous. MK defined the rate transition between the two zones as gradual, with uncertainty in the transition distance. This uncertainty is represented conceptually by the 5th, 50th, and 95th percentiles of the transition distance as shown along the top branch of the logic tree. In model implementation, the transition distance was approximated by a 9-point distribution, to ensure proper representation of the tails of the assessed distribution.

As shown by the top branch of the logic tree in Figure 3.2.4-1, a homogenous Poisson temporal model is used in conjunction with the locally homogenous zones spatial model. The rate within each zone for the homogenous Poisson model is estimated based on the number of relevant events and the age of the oldest such event using the approach described in Section 3.1. Uncertainty in that rate is represented by the last node in the logic tree. The values on each branch of this node are conditional on the zone (i.e., the rate is different in each zone), but it is represented in the figure with a single node in the logic tree.

Based on the most likely event set from Table 3.2.4-1, the means of the estimated rates are $5.3e-7$ events per year in the Crater Flat spatial zone and $1.0e-6$ events per year in the region of interest outside the Crater Flat spatial zone. Note that these are rates in regions of greatly

differing areas, and that the rates are spatially varying, so direct comparison of the rates is difficult. The average rate density (the rate divided by the area of the zone or region) is higher in the Crater Flat zone than in the background, although the rate of events in the region of interest is higher than the rate in the Crater Flat zone.

For the kernel density estimate for the 10,000-year assessment, MK specified a single parameterization of the kernel density estimator: a Gaussian kernel with a bandwidth of 5 km, fit based on the post-4 Ma events in the Crater Flat zone only, and with past events weighted by the inverse of the age of the event. For the 1-My assessment, the same kernel function and bandwidth are used, fit to all relevant events (either post-4 Ma only or all post-12 Ma, as shown by the second node in the logic tree of Figure 3.2.4-2). For the 1-My assessment, the ages of past events used for weighting are adjusted to reflect the age of the events at 1 My.

MK provided an assessment of the likely values of lithostatic pressure at the location of a hypothetical future event in his region of interest, as illustrated in Figure 3.2.4-4. This assessment was combined with the lithostatic pressure at each point in the region of interest through the Bayesian updating approach described in Section 3.1 and Appendix E to create a spatial density estimate based on lithostatic pressure. Similarly, MK provided an assessment of the likely values of seismic velocity at the location of a hypothetical future event in his region of interest: there is a 90% chance the seismic velocity will be “low” at the location of a future event. “Low” and “high” were defined by MK based on tomography data, and those definitions and the seismic velocities across the region of interest were used to divide the region into areas of low and high velocity. These regions are illustrated in the Elicitation Summary for MK in Appendix D. This assessment was combined with the seismic velocity at each point in the region of interest to create a spatial density estimate based on velocity. The two geologic-data-informed estimates were combined with the kernel density estimate with probabilities of 50% for the kernel density estimate and 25% each for the geology-informed estimates.

For spatial models using kernel density estimation, additional uncertainty exists in the spatial density resulting from fitting the kernel density estimators to the relatively small data sets. As described in Section 3.1 and Appendix E, uncertainty in the spatial density is modeled through a simulation approach known as bootstrapping. This is represented conceptually by the “Uncertainty in Spatial Density” node in the logic tree of Figure 3.2.4-1; in the actual bootstrapping analyses, more than three representations are used.

For conceptual models based on the spatial smoothing approach, two alternative conceptual models were specified for estimating the rate of future events: a homogenous Poisson model and a time-volume model. The rate for the homogenous Poisson models are estimated as described above for the spatial zones model. The mean of the estimated rate based on the most likely event set for events less than 4 Ma is $1.8e-6$ events per year in the region of interest. The mean of the estimated rate based on the most likely event set for events less than 12 Ma is $1.3e-6$ events per year in the region of interest. In the logic tree formulation of Figure 3.2.4-1, uncertainty in the rate is represented by the 5th, 50th, and 95th percentiles of the Gamma distribution with the appropriate parameters as described in Section 3.1.

To develop a rate estimate based on the time-volume model, MK specified three alternative models for estimating the cumulative volume over time, each fit to the estimated volumes of

events from Table 3.2.4-1. The models, the probability for each, and the best fit linear regression functions are given in Table 3.2.4-2.

The 90% confidence interval on the slope of the regression lines is used to represent the uncertainty in the estimated magma generation rate, as described in Section 3.1 and Appendix E.

MK specified that the average volume per event for future events should be estimated based on the mean and variance of the volume of Quaternary events in his region of interest. To incorporate uncertainty in the volume per event for future events, volume per event is modeled with a lognormal distribution with mean and variance matching the mean and variance of the volume of Quaternary events, and the 5th, 50th, and 95th percentiles of that distribution are used in the logic tree. The volume per event differs for different event sets.

Figure 3.2.4-5 illustrates uncertainty in the estimated rate for each of the alternative temporal models specified by MK, based on one specific event set. In all cases, the bar represents the 5th to 95th percentiles of the distribution on rate for the specified model based on the most likely event set from Table 3.2.4-1.

Mean Rate Density and Mean Recurrence Rate

Figure 3.2.4-6 illustrates the mean rate density for igneous events calculated from MK's spatial and temporal models for the 10,000-year assessment. In this figure, one can see the effect of the zones-based spatial model, in the location and shape of the $3e-9$ contour, and the effect of the spatial model based on kernel density estimate, in the location and shape of the $1e-9$ contour. The effect of the consideration of geology data is the relative smoothness of the mean rate density outside of the zone. With finer contouring, differences related to interpretation of the geology data would be visible.

A mean recurrence rate for events in the region of interest can be calculated by summing the mean rate density at each grid point. Based on the mean rate density shown in Figure 3.2.4-6, the mean recurrence rate for events in this region is $2e-6$ events per year, giving recurrence intervals between 16,000 and 1.5 million years (5th to 95th percentile of the distribution on recurrence interval), and a mean recurrence interval of about 500,000 years for events in the region illustrated.

Event Simulation Model

Figure 3.2.4-7 illustrates the key features of an event simulator for MK's PVHA-U model. In this model an *event* is characterized by a combination of dikes, conduits, and sills; the number, locations and dimensions of each of these features define the event.

An event consists of one to six dikes, and may have zero to eight conduits. The distribution on the number of dikes in an event is shown in Figure 3.2.4-8. When multiple dikes exist, they are arranged en echelon, and may overlap or have a gap between the dike tips by as much as 50% of the length of the shorter dike. Dike lengths follow the distribution shown in Figure 3.2.4-9, and dike azimuths follow the distribution shown in Figure 3.2.4-10. Right-stepping en echelon arrangements are more likely than left-stepping (75% versus 25%), and the spacing between

dikes in the direction perpendicular to dike azimuth is drawn from the distribution shown in Figure 3.2.4-11.

The number of conduits in an event is a function of the total length of dikes in that event. MK provided an assessment of the number of conduits associated with events with different total dike lengths. Figure 3.2.4-12 illustrates the simulated number of conduits in an event based on MK's assessment of dike length, the number of dikes, and the number of conduits as a function of total dike length. Conduits are located along dikes, following the distribution shown in Figure 3.2.4-13, and are likely (75%) to be located on the longest dike in an event. For events with more than one conduit, the spacing between conduits is defined by a triangular distribution between 250 m and 1 km, with a most likely spacing of 500 m. Conduit diameter is defined as a function of dike width, which is itself uncertain. Figure 3.2.4-14 shows the simulated distribution of conduit diameter based on MK's assessment of dike width and conduit diameter as a function of dike width. The likelihood that any one conduit is column producing is a function of the number of conduits in an event and of dike length. MK also assessed a 1% chance (for the 10,000-year assessment) that future eruption, given that an eruption occurs, would be hydromagmatic. For the 1-My assessment the chance increases to 3%.

MK's event description includes the potential for sills. Based on his assessment of the likelihood of sill formation, and the probable depth of sill formation and sill thickness, the frequency of a sill at repository depth in an event is 5.45%. If a sill occurs in an event, it is elliptical in shape with an aspect ratio between 1 and 3, and is located along the side of a dike with the long axis of the ellipse either parallel (30%) or perpendicular (70%) to the dike azimuth. The length of the sill ranges from 20 m to 1,000 m with a most likely value of 500 m (defined by a triangular distribution).

Figure 3.2.4-15 illustrates examples of the simulated events, a relatively common type of event in the top panel and a fairly rare type of events (both in terms of the number of features and their placement) in the bottom panel. Table 3.2.4-3 describes the number of dikes and the number of conduits and vents (combined) in an event, and how frequently such events occur in the event simulation. The table indicates, for example, that the most common type of event consists of one dike and one conduit or vent: 14.9% of events are of this type, and an example is shown in the top half of Figure 3.2.4-15. Events with no conduits or vents are possible (e.g., 3.1% of simulated events have 1 dike and no conduits or vents). The most complex event simulated had 6 dikes and 7 conduits. Note that events may also include sills, which are not represented in this table.

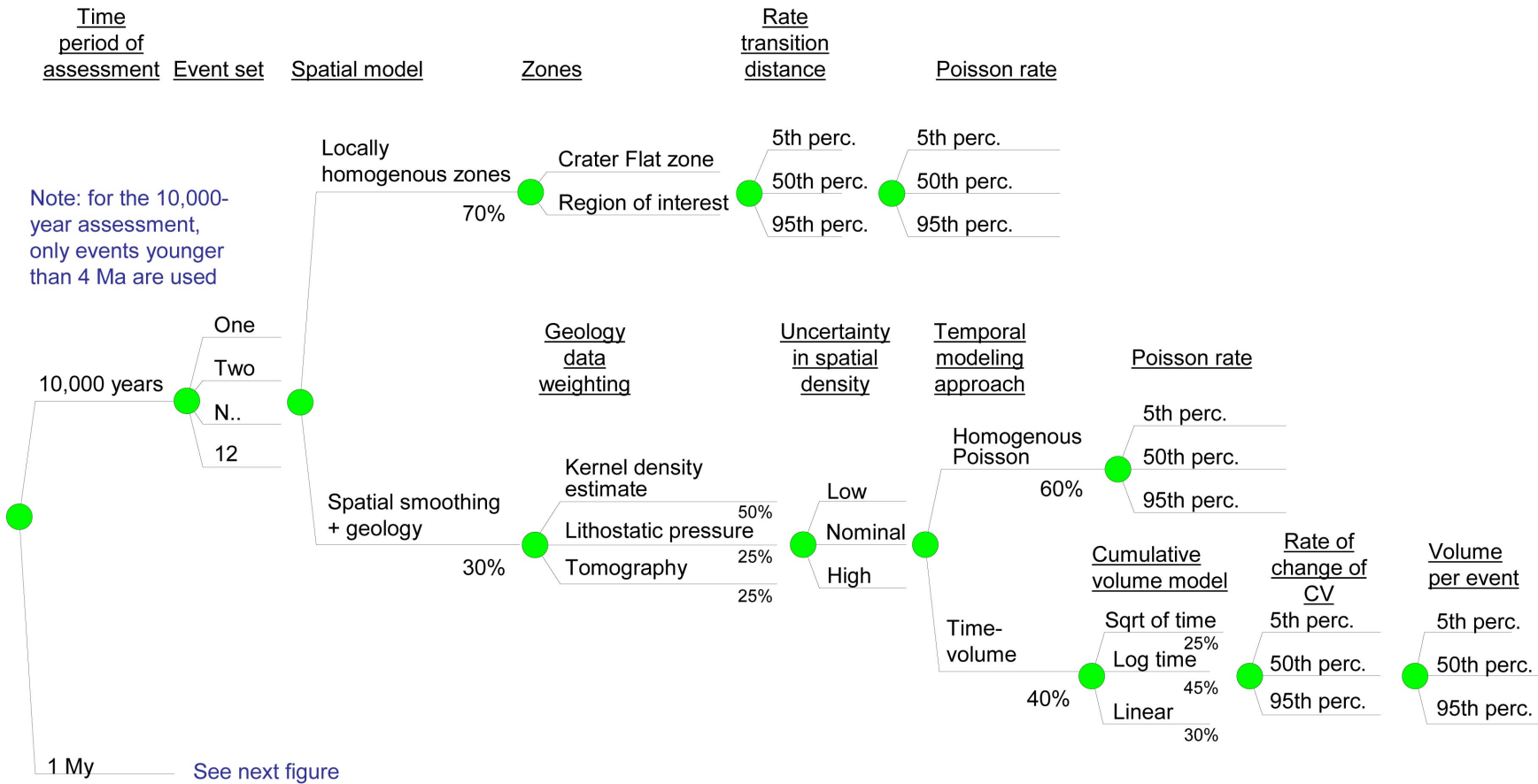
Conditional Probability of Intersection

Figure 3.2.4-16 illustrates the conditional probability of the intersection of any igneous feature with the repository footprint based on MK's event descriptions. For ease of comparison across experts, the same scale is used of the conditional probability of intersection maps across all experts. Due to the potentially large size of some of MK's events, the lower probability contours extend beyond the boundaries of this figure. In addition to illustrating the potential for long event lengths, these contours show the effect of the two azimuth distributions, with the elongation of the contours in the slightly N5W direction and the lesser elongation in the N30E direction.

As described above, MK's events include at least one dike, and may include column-producing conduit(s), vents, and sills. Figure 3.2.4-17 shows the conditional probability of intersection for each of these types of igneous features. The contours for features other than dikes do not show the impact of dike azimuth, but do show the impact of the en echelon geometry of events.

Differences Between the 10,000-year and 1-My Assessments

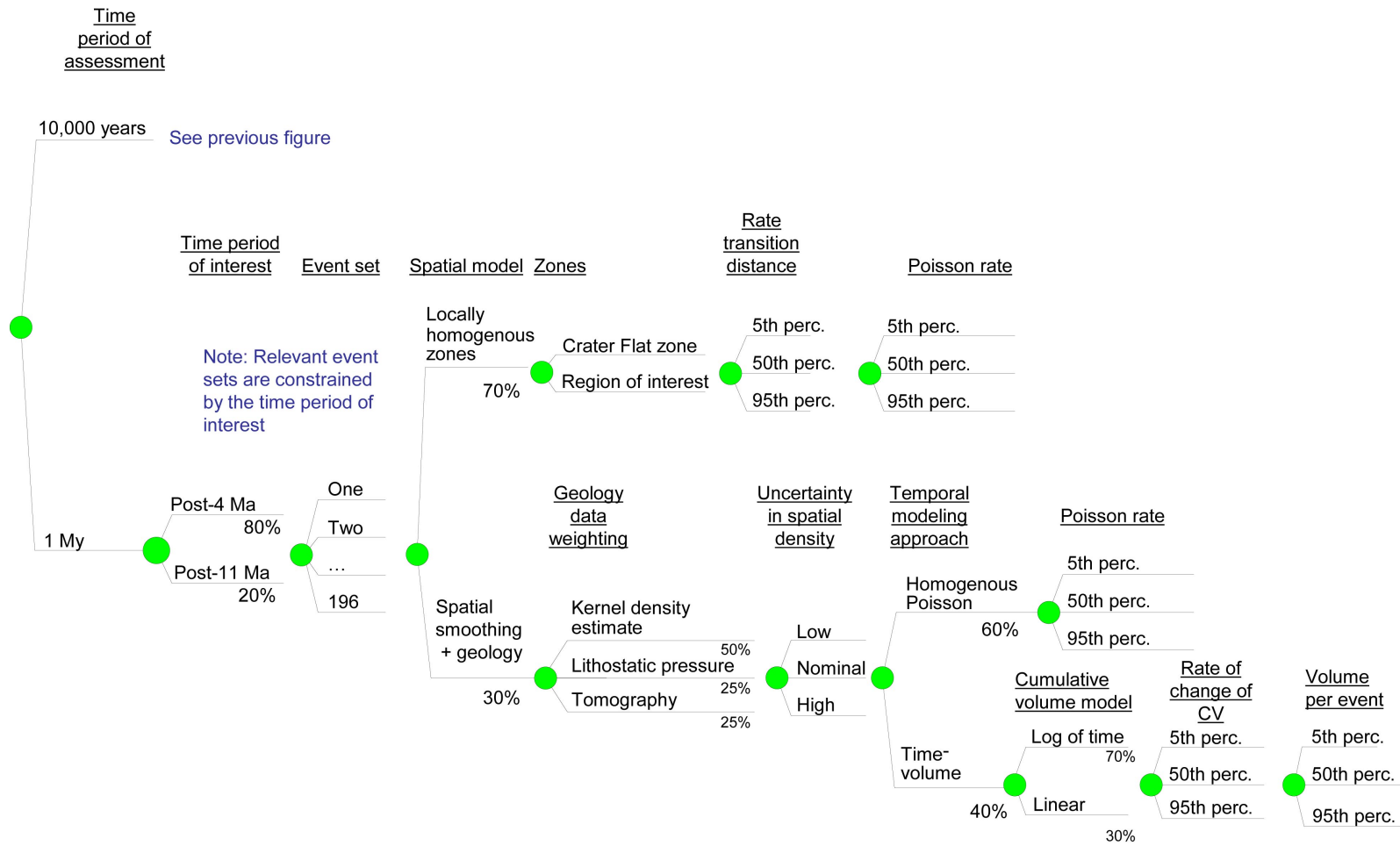
Differences in MK's spatial and temporal models based on the different time periods of assessment are described above. Although models for the 1-My assessment added consideration of additional event sets and additional alternative spatial models, and the spatial model includes weighting of past events by the inverse of their age resulting in slight differences in rate density over time. These changes lead to only a small difference in the mean rate density, and they are assigned relatively low probability. Thus the mean rate density maps for the two assessments (Figure 3.2.4-18) appear very similar.



NOTES: All probabilities shown on the branches are those assigned by the expert. Uncertainty in spatial density, uncertainty in the Poisson rate, and uncertainties associated with the rate of change of cumulative volume (CV) and the volume per event are all modeled based on the approaches described in Section 3.1.5, and the probabilities for those branches are defined by the modeling approach.

A single parameterization of the kernel density estimation approach was specified for spatial density, so no uncertainties relative to those parameters appear in the logic tree.

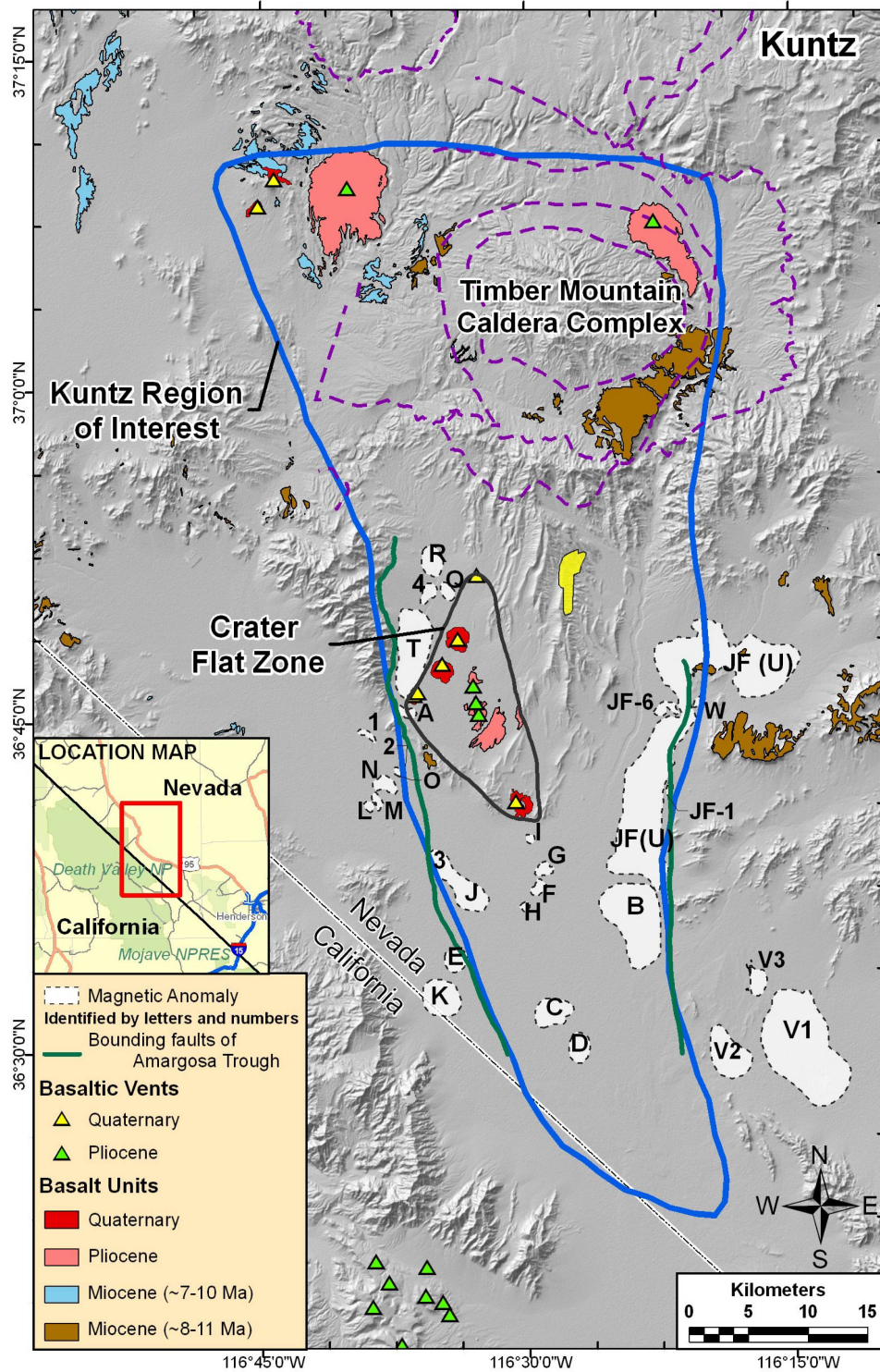
Figure 3.2.4-1. Logic Tree Representing the Spatial and Temporal Components of the PVHA-U Model for the 10,000-Year Assessment Specified by Mel Kuntz



NOTES: All probabilities shown on the branches are those assigned by the expert. Uncertainty in spatial density, uncertainty in the Poisson rate, and uncertainties associated with the rate of change of cumulative volume (CV) and the volume per event are all modeled based on the approaches described in Section 3.1.5, and the probabilities for those branches are defined by the modeling approach.

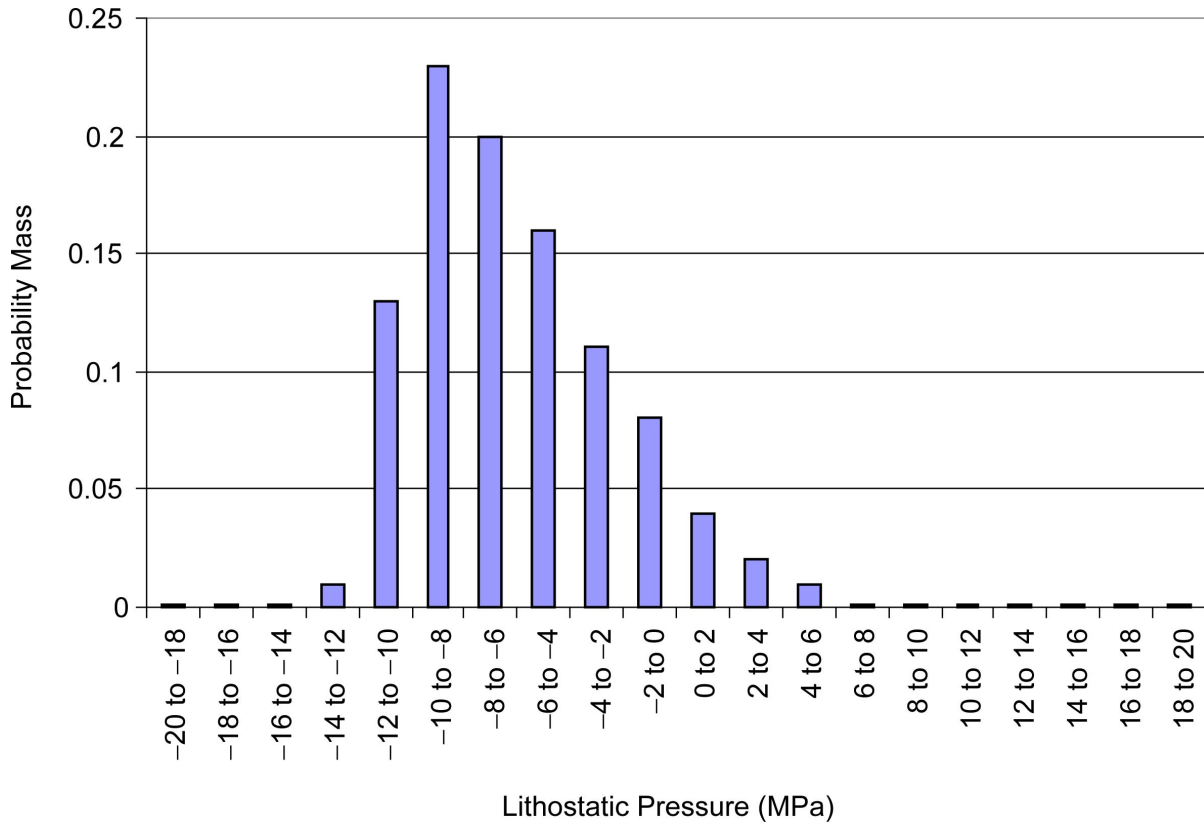
A single parameterization of the kernel density estimation approach was specified for spatial density, so no uncertainties relative to those parameters appear in the logic tree.

Figure 3.2.4-2. Logic Tree Representing the Spatial and Temporal Components of the PVHA-U Model for the 1-My Assessment Specified by Mel Kuntz



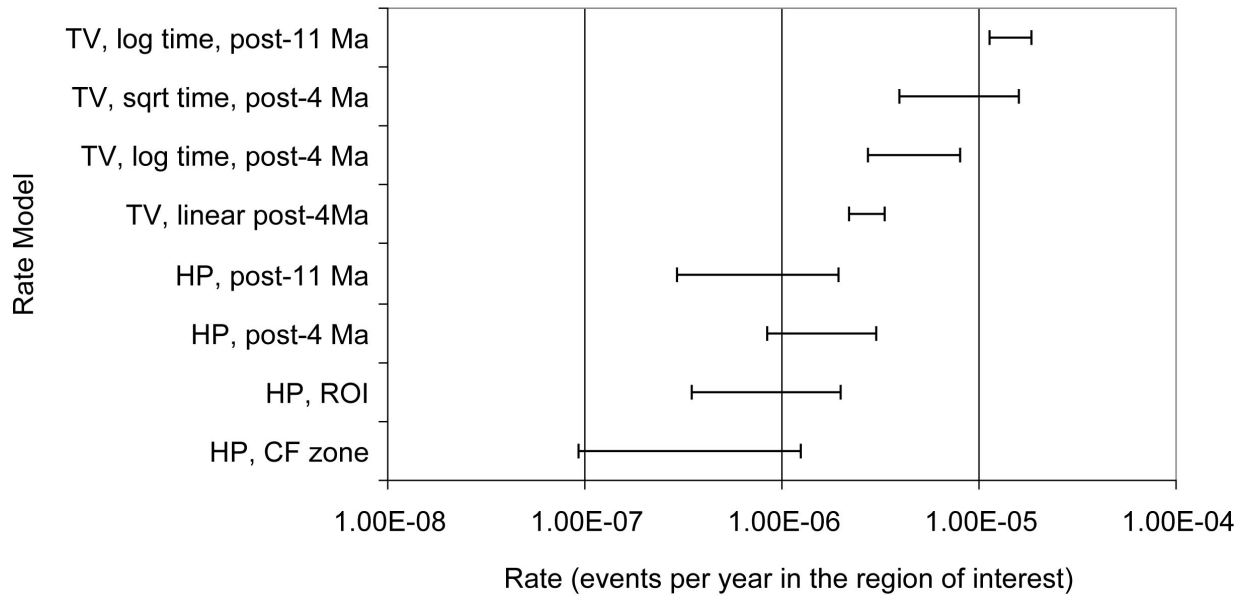
NOTE: The blue line outlines the region of interest. The black line outlines the Crater Flat zone.

Figure 3.2.4-3. Region of Interest and the Crater Flat Zone Boundary as Specified by Mel Kuntz



NOTE: Lithostatic pressure in the YMR is one of the data sets provided to the panel and listed in Appendix B. Lithostatic pressure values were calculated from free-air gravity and reflect gravity (mass) excesses (represented as positive lithostatic pressure values) and deficiencies (represented as negative values) relative to a theoretical gravity value at sea level.

Figure 3.2.4-4. Assessment of Lithostatic Pressure at the Location of a Hypothetical Future Event in the Region of Interest, as Specified by Mel Kuntz

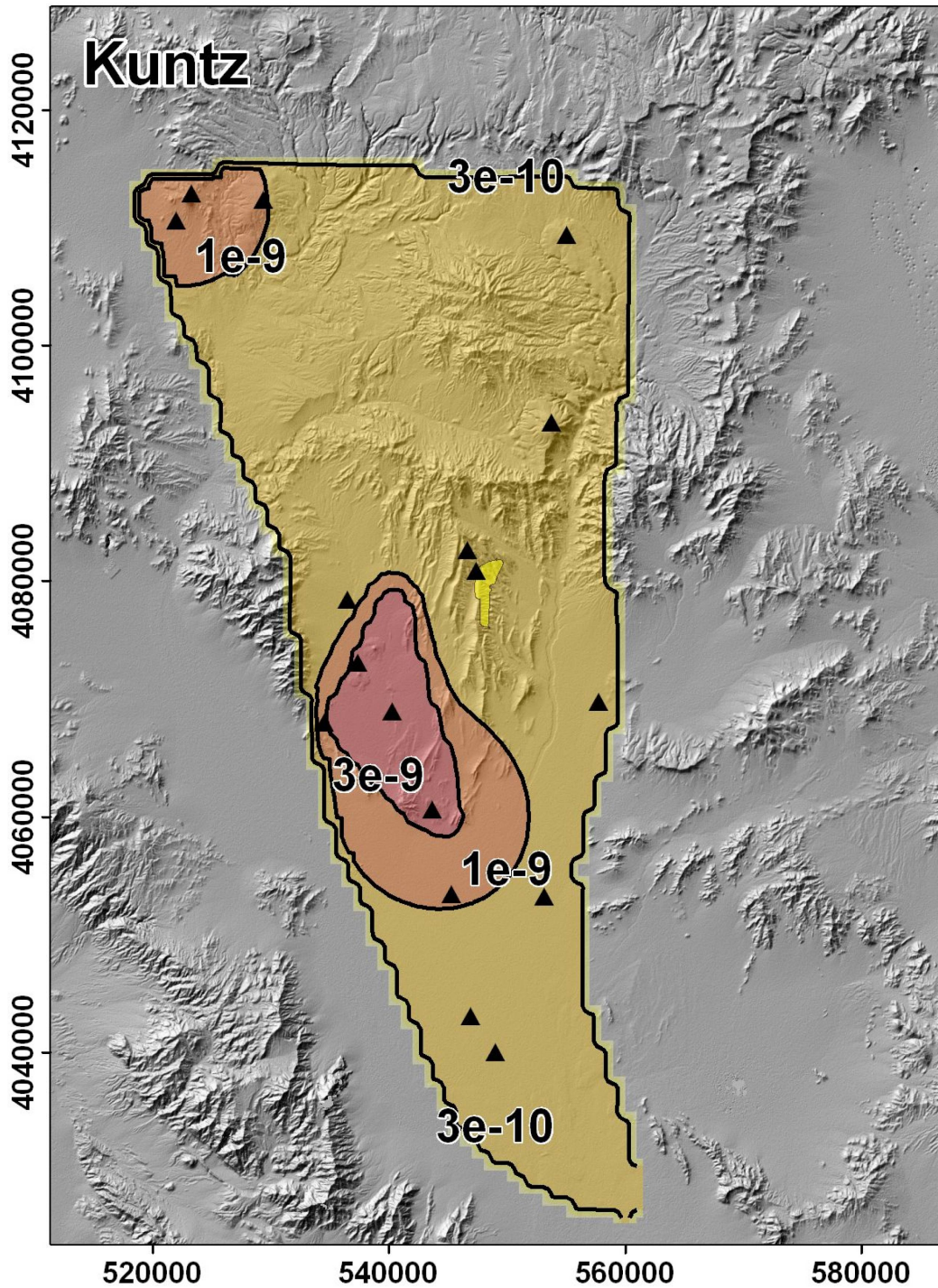


NOTES: Bars represent the 5th to 95th percentile of the uncertainty in the rate for each alternative rate model, for estimates based on the most likely event set identified in Table 3.2.4-1.

HP = homogenous Poisson rate model; TV = time-volume rate model; CF zone = Crater Flat zone; ROI = region of interest

The HP, CF zone model provides the rate estimate for the Crater Flat zone only; the HP, ROI model provides the rate for the region of interested *outside* the Crater Flat zone only; all other rates apply to the entire region of interest.

Figure 3.2.4-5. Example of Uncertainty in Estimated Rate Based on a Single Interpretation of Past Events for Alternative Temporal Models Specified by Mel Kuntz



NOTE: Contours show the mean rate density in events per year per km². Yellow polygon represents the repository footprint; black triangles represent past events (MK's most likely post-12 Ma event set). Map grid ticks are in UTM meters; tick intervals are 20 km.

Figure 3.2.4-6. Mean Rate Density for the 10,000-Year Assessment Based on Models Specified by Mel Kuntz



Figure 3.2.4-7. Components of an Event Simulator Based on the Characteristics of Future Events Described by Mel Kuntz

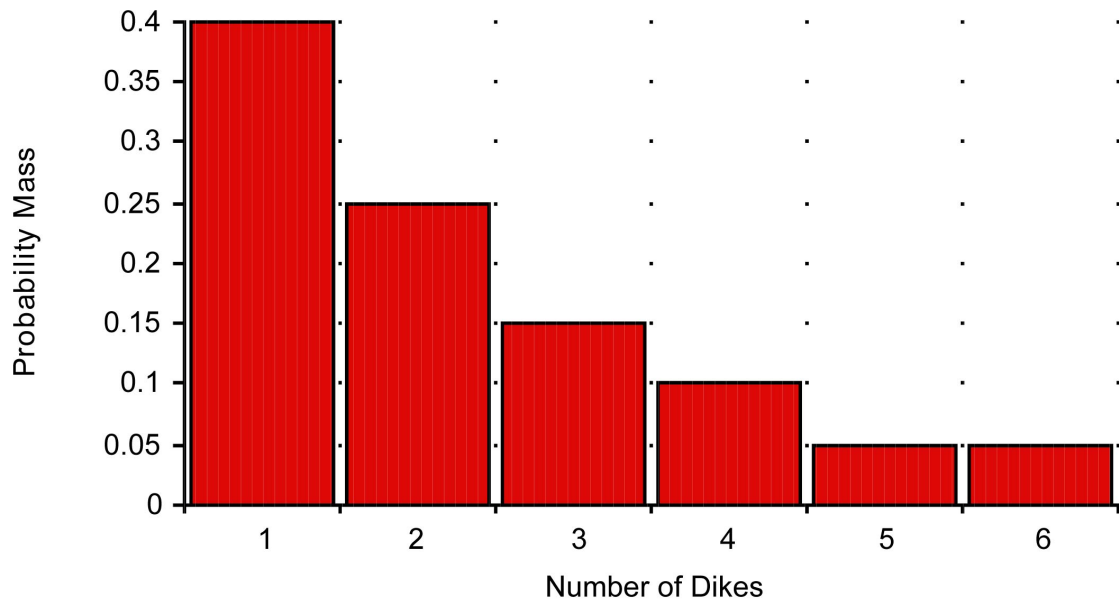
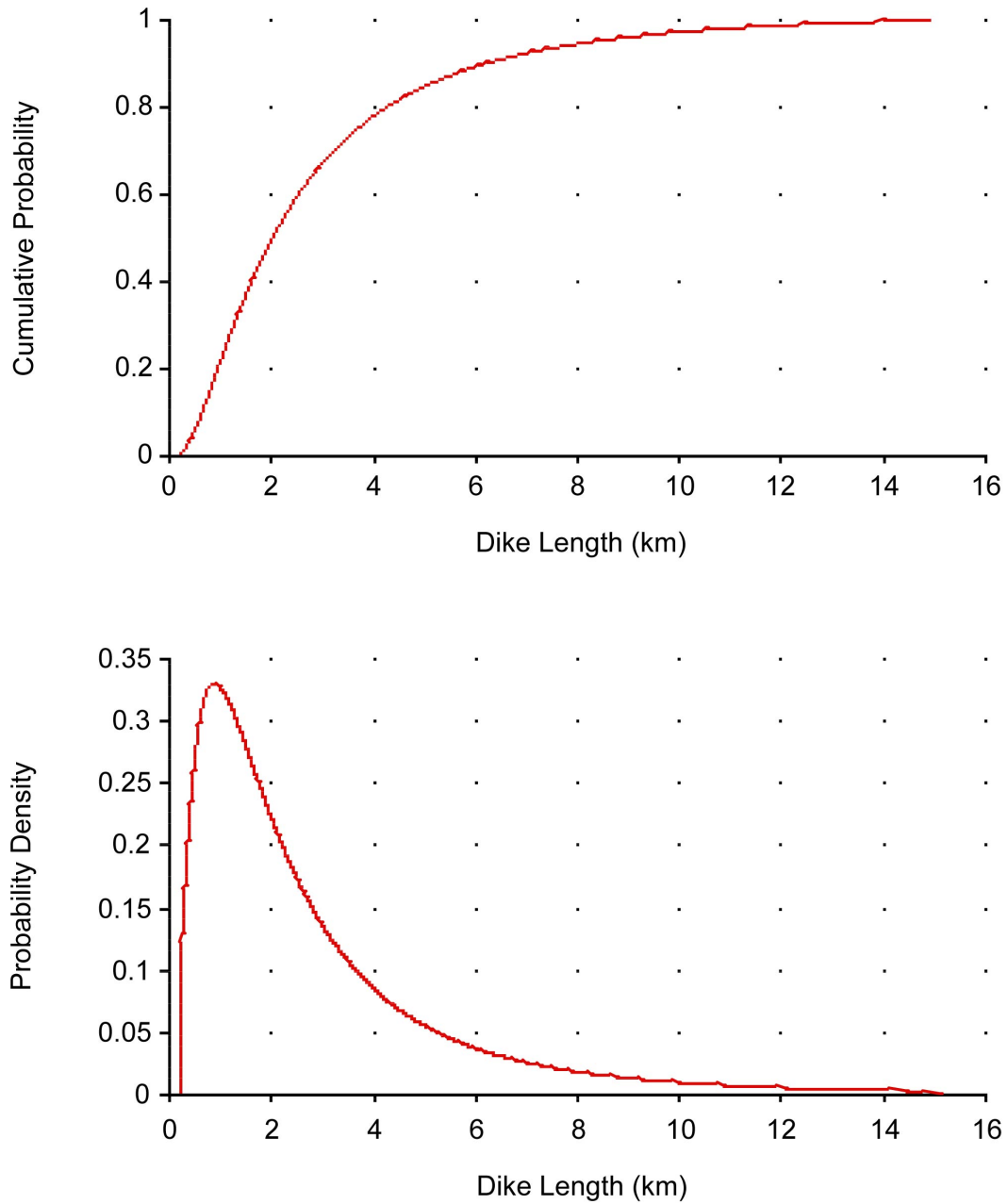
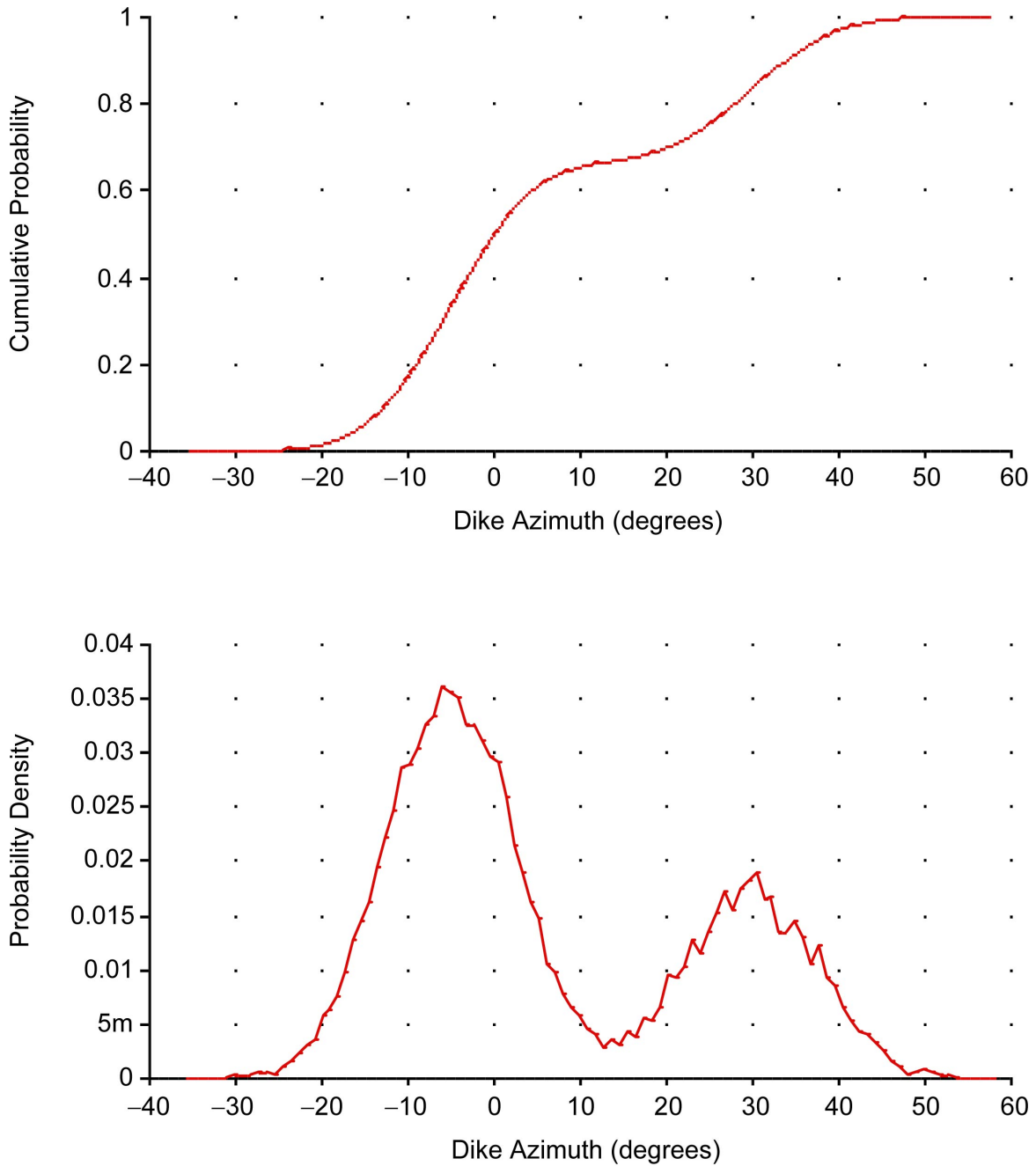


Figure 3.2.4-8. Distribution of the Number of Dikes in an Event as Assessed by Mel Kuntz



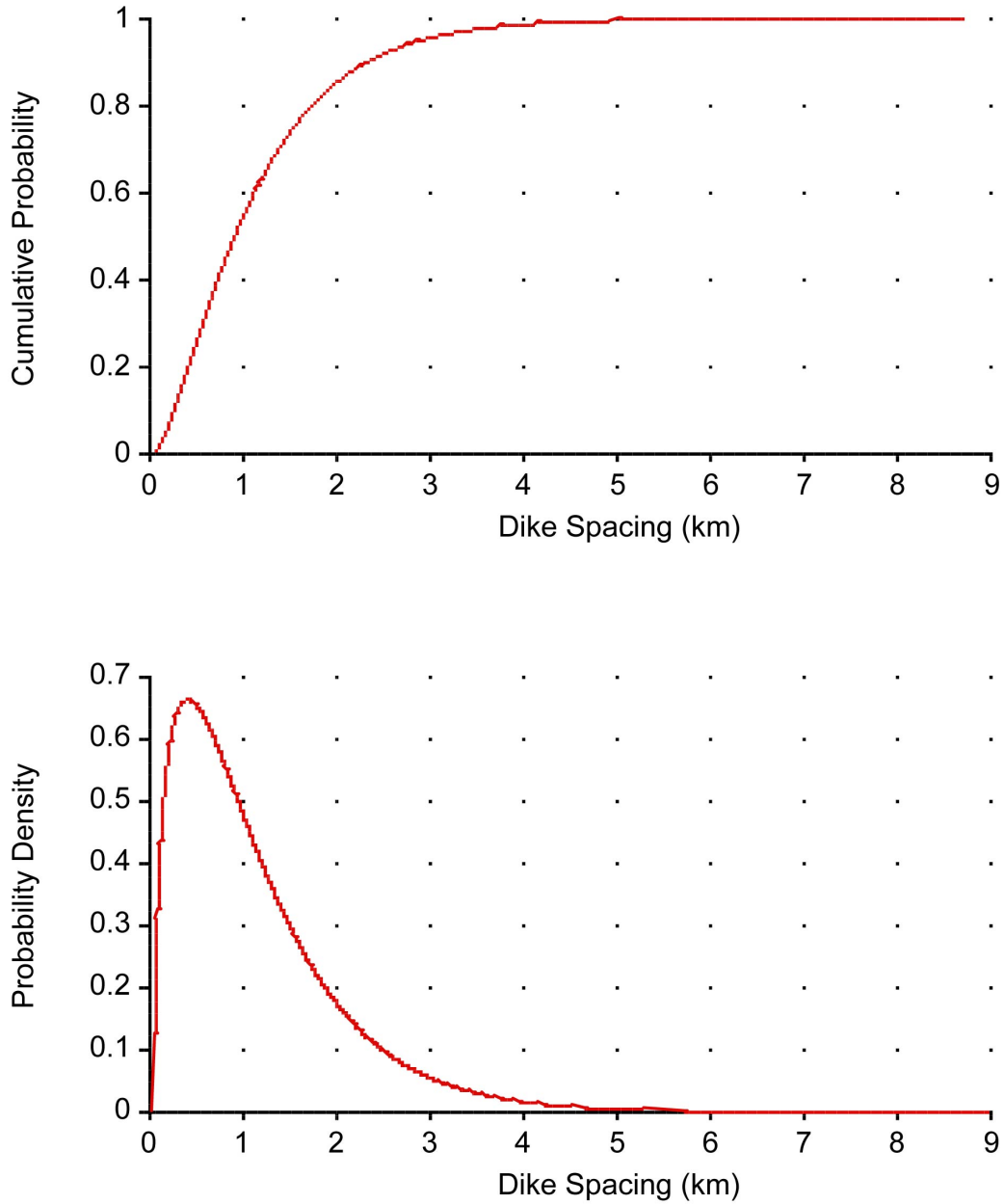
NOTE: Top graph is a cumulative distribution function; bottom graph is a probability density function.

Figure 3.2.4-9. Distribution for Dike Length as Assessed by Mel Kuntz



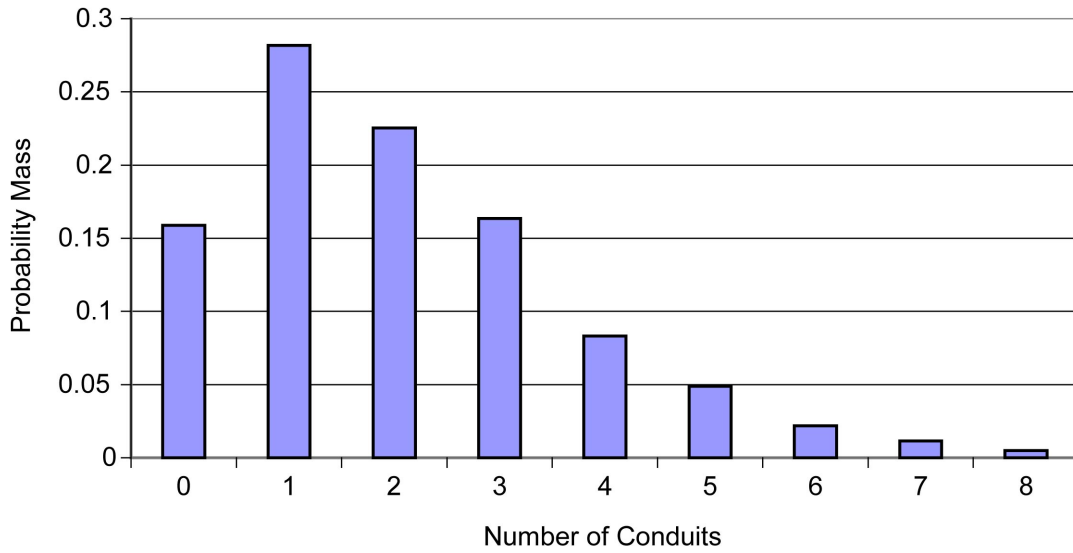
NOTE: Top graph is a cumulative distribution function; bottom graph is a probability density function. For values less than 0.01 on the y-axis, suffix notation is used ($m = 10^{-3}$, so 5m = 0.005). Roughness in the probability density function is a result of simulation from the mixture of two normal distributions. Zero represents North.

Figure 3.2.4-10. Distribution for Dike Azimuth as Assessed by Mel Kuntz



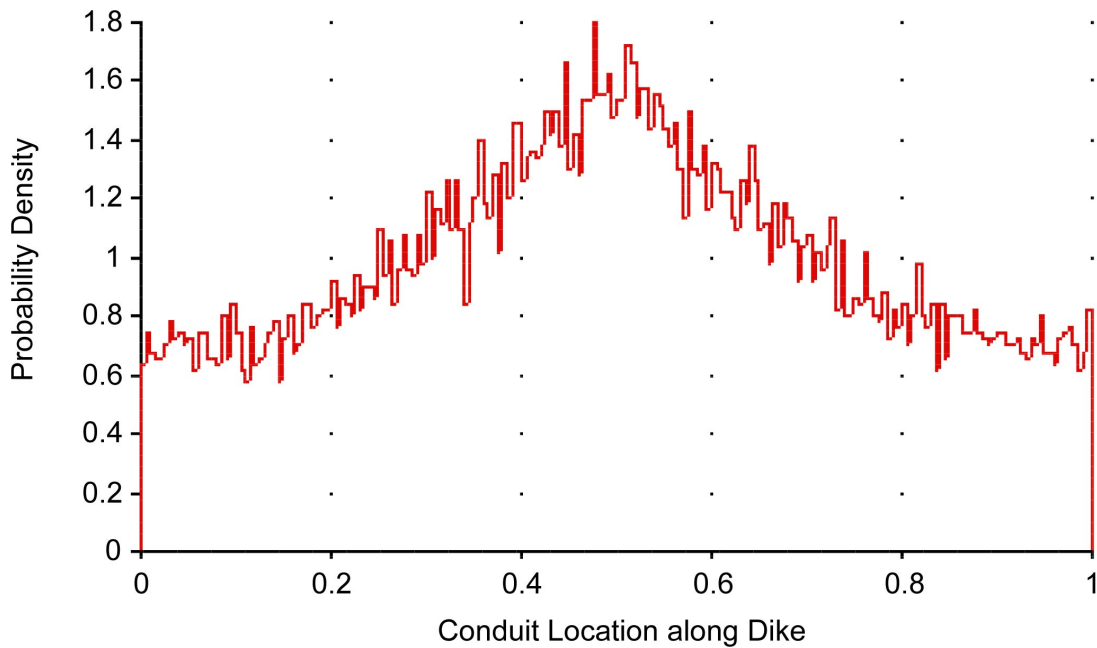
NOTE: Top graph is a cumulative distribution function; bottom graph is a probability density function.

Figure 3.2.4-11. Distribution for the Spacing between Dikes in the Direction Perpendicular to Dike Azimuth as Assessed by Mel Kuntz



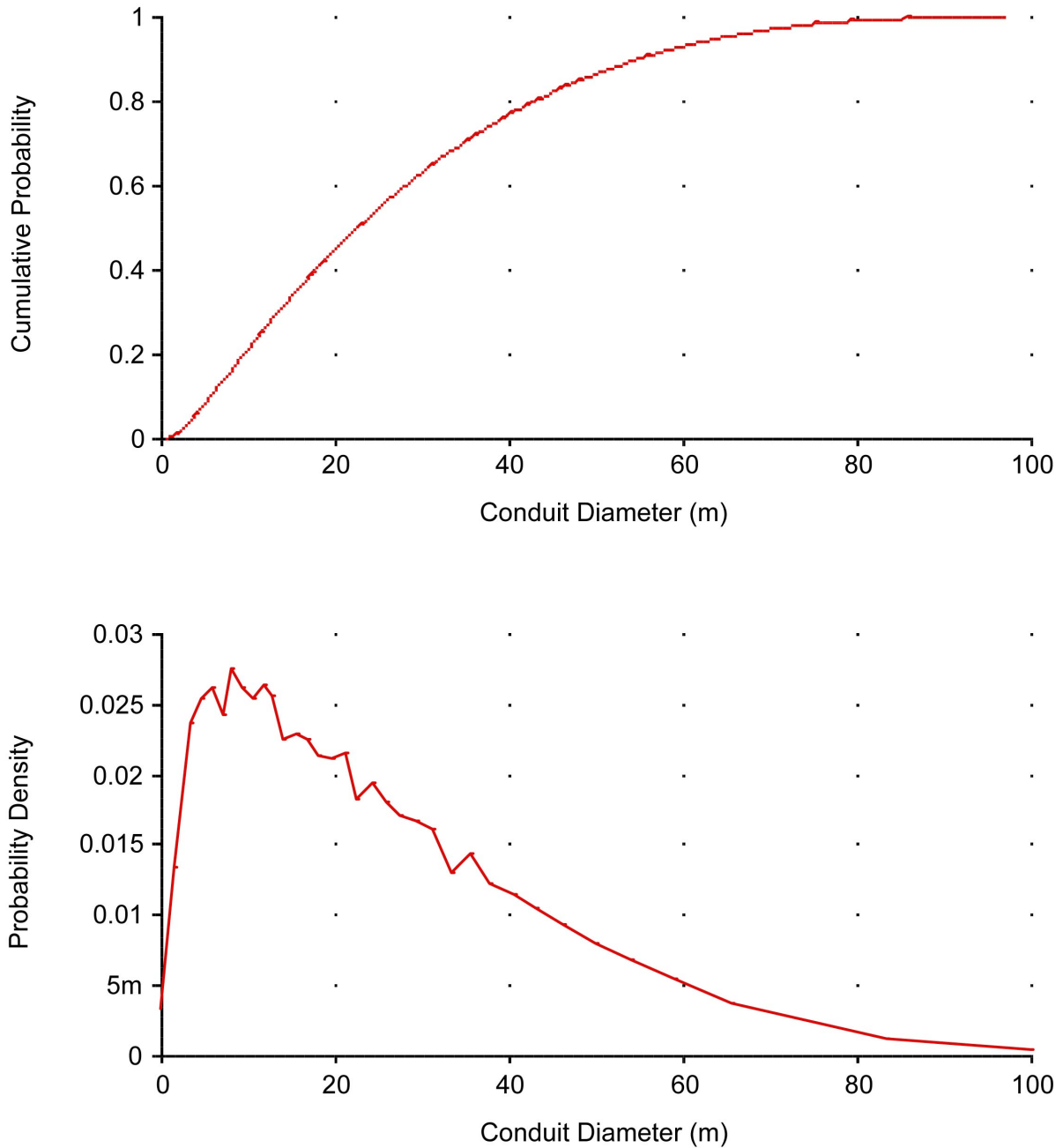
NOTE: Number of conduits is a function of the total length of dikes in an event. Result here is a simulated result based on 30,000 iterations.

Figure 3.2.4-12. Distribution of the Number of Conduits in an Event Based on Assessments of Mel Kuntz



NOTE: Zero and one represent the ends of the dike. Simulation from a mixture of a uniform and normal distribution with 10,000 iterations. Roughness of the distribution is an artifact of simulation.

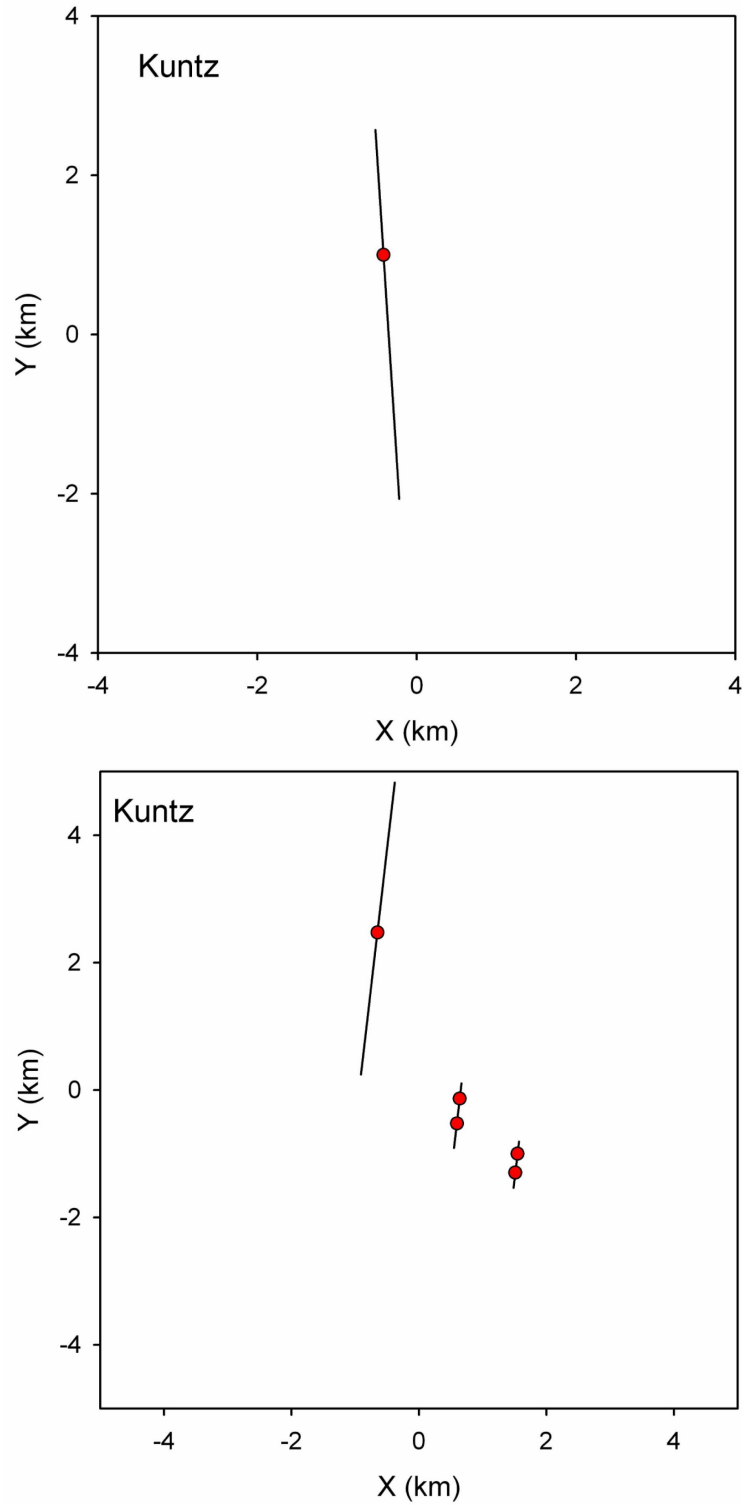
Figure 3.2.4-13. Distribution Describing the Location of a Conduit Along a Dike as Assessed by Mel Kuntz



NOTES: Top graph is a cumulative distribution function, bottom is a probability density function. For values less than 0.01 on the y-axis, suffix notation is used (m = 10^{-3} , so 5m = 0.005)

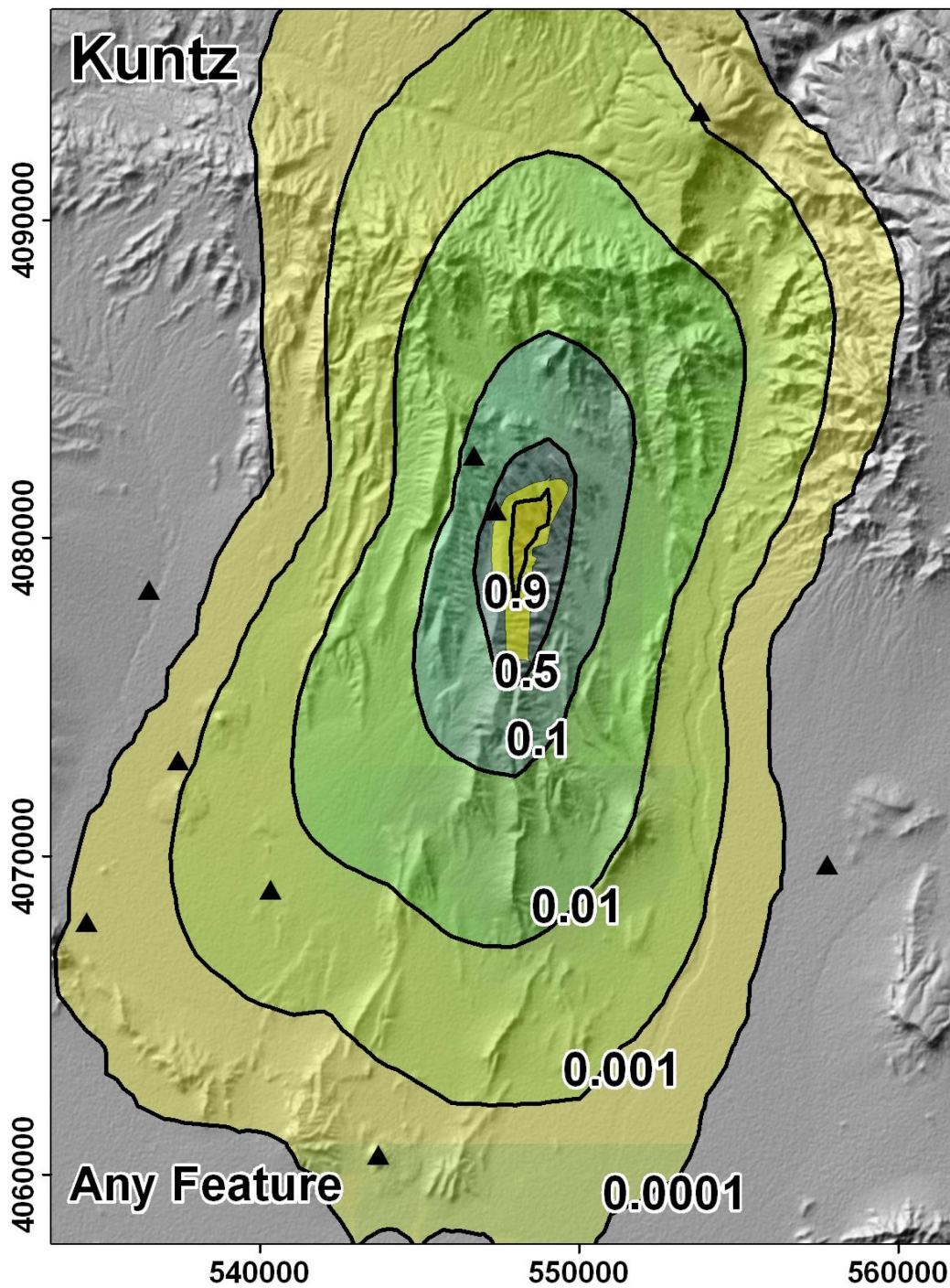
Conduit diameter distribution is bounded by dike width, itself uncertain. Graphs shown are simulation results with 30,000 iterations.

Figure 3.2.4-14. Distribution Describing Conduit Diameter Based on Assessments of Mel Kuntz



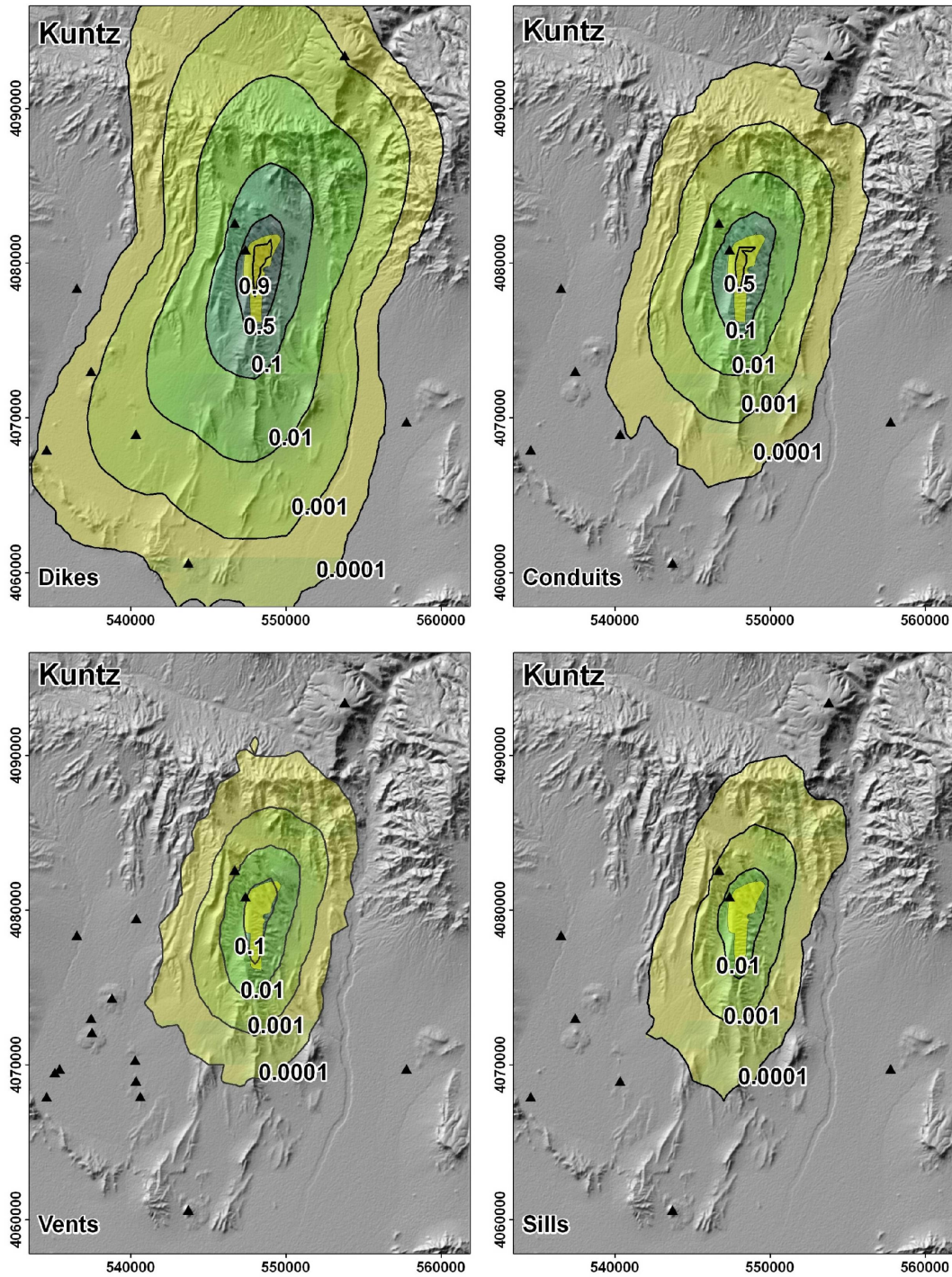
NOTE: Dikes are represented as black lines, their lengths on the figure are the lengths of the simulated dikes. Conduits and vents are represented as small red circles; they are not differentiated and their diameters are not represented. Sills, if they exist, are represented by light yellow ovals or polygons.

Figure 3.2.4-15. Examples of Simulated Events from the PVHA-U Model for Mel Kuntz



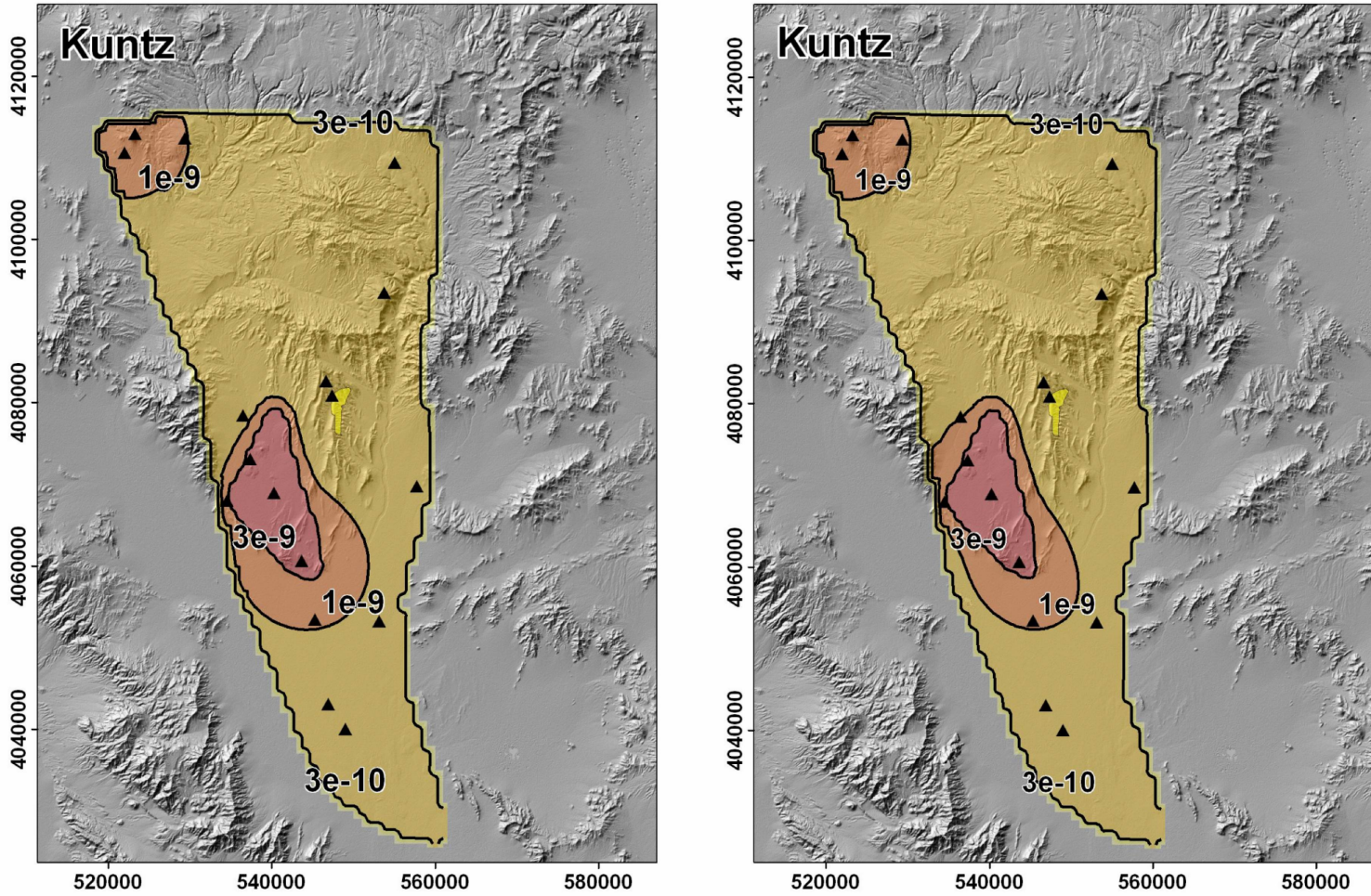
NOTE: Yellow polygon represents the repository footprint. Black triangles represent past events for MK's most likely event set. Map grid ticks are UTM meters; tick intervals are 10 km.

Figure 3.2.4-16. Conditional Probability of Intersection of Any Feature with the Repository Footprint Based on Event Descriptions Developed by Mel Kuntz



NOTE: Yellow polygon represents the repository footprint. Black triangles represent past events for MK's most likely event set. Map grid ticks are UTM meters; tick intervals are 10 km.

Figure 3.2.4-17. Conditional Probability of Intersection of Each Igneous Feature with the Repository Footprint Based on Event Descriptions Developed by Mel Kuntz



NOTE: The left figure is the mean rate density for the 10,000-year assessment, the right figure is the mean rate density for the 1-My assessment. Yellow polygon represents the repository footprint. Black triangles represent past events for MK's most likely event set.

Figure 3.2.4-18. Mean Rate Density for the 10,000-Year Assessment and the 1-My Assessment Based on the Assessments of Mel Kuntz

Table 3.2.4-1. Data Used to Define Spatial Distribution and Event Rates for Future Volcanic Events for Mel Kuntz's PVHA-U Model

Zone	Center	Number of events	Age (Ma)	Volume (km ³)
Crater Flat Zone	Lathrop Wells	1	0.08	0.048
	Quaternary Crater Flat	1 (weight = 0.9)		
	Makani Cone	2 (weight = 0.05)	1.07	0.002
	Black Cone	4 (weight = 0.05)	1.07	0.06
	Red Cone		1.07	0.055
	Little Cones NE		0.78	0.014
	Little Cones SW		0.78	0.02
	Pliocene Basalt of Crater Flat	1 (weight = 0.7) or part of a single event including Anomaly B and Anomalies F, G, and H (weight = 0.3)	3.8	0.585
Region of interest	Sleeping Butte	1 (weight = 0.3)		
	Hidden Cone	or 2 (weight = 0.7)	0.35	0.032
	Little Black Peak		0.35	0.014
	Buckboard Mesa	1	2.87	0.838
	Anomaly B	2 (weight = 0.7) or part of a single event including the Pliocene Basalt of Crater Flat (weight = 0.3)	3.8	1.227
	Anomalies F, G, and H		3.9	0.063
	Thirsty Mountain	1	4.63	2.28 to 2.63
	Dome Mountain	1	10.5	~10
	Anomaly C	1 (weight = 0.5)	4.8	0.117
	Anomaly D	2 (weight = 0.5)	4.8	0.073
	Jackass Flats	1	9.5	4.1
	Western Crater Flat (Anomalies R, Q, 4, and T)	1 (weight = 0.85) 2 (weight = 0.05) 3 (weight = 0.05) 4 (weight = 0.05)	11.2	2.3
	Solitario Canyon	1 (weight = 0.3) 2 (weight = 0.7)	11 (10 or 11.7)	Unknown
	Anomaly A	1	10	0.06

NOTE: Table derived from MK's Elicitation Summary in Appendix D.

Table 3.2.4-2. Alternative Models of Cumulative Volume over Time as Defined by Mel Kuntz

Model	Probability	Equation
<i>Models based on post-4 Ma events</i>		
Cumulative Volume (CV) as a linear function of time, post-2.87 Ma events	0.3	$CV = 2.63 + 0.084 \times (4 + t)$
CV as a function of the log of time, post-4 Ma events	0.45	$CV = 2.24 + 0.65 \times \log(4 + t)$
CV as a function of the square root of time, post-4 Ma events	0.25	$CV = 0.88 + 1.18 \times (4 + t)^{1/2}$
<i>Models based on post-11 Ma events</i>		
CV as a linear function of time, post-2.87 Ma events	0.3	Same as the linear function above
CV as a function of the log of time	0.7	$CV = 7.4 + 5.42 \times \log(12 + t)$

NOTE: In all cases, t is the time at which cumulative volume is to be estimated, in millions of years from the present. So for 2 Ma prior to the present, t = -2, and for 1 My in the future, t = 1.

Table 3.2.4-3. Frequency of Number of Dikes and Conduits or Vents in Simulated Events Based on the Assessments of Mel Kuntz

		Number of Conduits and Vents in an Event								
		0	1	2	3	4	5	6	7	8
Number of Dikes in an Event	1	3.1%	14.9%	9.7%	6.1%	3.0%	1.8%	0.8%	0.4%	0.1%
	2	2.0%	6.5%	6.2%	4.6%	2.6%	1.7%	0.8%	0.4%	0.1%
	3	2.7%	3.2%	3.3%	2.7%	1.6%	0.9%	0.4%	0.2%	0.02%
	4	3.2%	2.1%	1.9%	1.4%	0.8%	0.4%	0.2%	0.1%	0.001%
	5	2.2%	1.0%	0.8%	0.5%	0.3%	0.1%	0.05%	0.02%	0.0%
	6	2.7%	1.1%	0.7%	0.3%	0.1%	0.1%	0.02%	0.01%	0.0%

3.2.5 Alexander McBirney

Spatial and Temporal Models

Figure 3.2.5-1 presents the logic tree describing the basic structure of the spatial and temporal models developed by Alexander McBirney (AM) for PVHA-U. AM specified a spatial zones model, with two zones: a “Crater Flat zone” shown in Figure 3.2.5-2, and a background zone shown in Figure 3.2.5-3. Table 3.2.5-1 lists the past events in each zone judged relevant by AM to his spatial and temporal models. The table includes alternative interpretations of some events, along with the relative probability AM assigned to each interpretation. In combination, 24 unique interpretations of the number of past events in the Crater Flat zone are possible. These are represented conceptually in the second node of the logic tree.

The transition in rate density between the zones is gradual over a distance defined by AM. That transition distance varies around the zone, as shown in Figure 3.2.5-2.

Spatial smoothing using kernel density estimation is used to calculate the conditional spatial density within the Crater Flat zone. AM specified a single parameterization of the kernel density estimator: a symmetric Gaussian kernel function with a bandwidth of 7 km and past events weighted by the inverse of the age of the event (probability 75%) and the volume of the event (probability 25%). Because only one parameterization was specified, no nodes are specified in the logic tree representing the kernel function, the bandwidth, or the event weighting. For the 1-My assessment, the ages of past events used for weighting are adjusted to reflect the age of the events at 1 My. Future events in the background zone are assumed to be spatially homogenous.

For the kernel density estimate within the Crater Flat zone, additional uncertainty exists in the spatial density resulting from fitting the kernel density estimators to the relatively small datasets. As described in Section 3.1 and Appendix E, uncertainty in the spatial density is modeled through a simulation approach known as bootstrapping. This is represented conceptually by the “Uncertainty in Spatial Density” node in the logic tree of Figure 3.2.5-1; in the actual bootstrapping analyses, more than three representations are used.

Two alternative conceptual models were specified for estimating the rate of future events in the Crater Flat zone: a homogenous Poisson model and a time-volume model, as illustrated in the logic tree. For the homogenous Poisson model, two rates were considered: a rate based on the number and ages of Quaternary events in the zone, and one based on the number and ages of post-4.7 Ma events in the zone.

The rate for the homogenous Poisson model was estimated based on the number of events in the relevant region and the age of the oldest such relevant event using the approach described in Section 3.1. The mean of the estimated rate based on Quaternary events is $4.7e-6$ events per year in the Crater Flat zone; the mean of the estimated rate based on post-4.7 Ma events for the most likely event set is $3.1e-6$ events per year in the Crater Flat zone. Uncertainty in the rate is calculated using the approach described in Section 3.1 and is represented by the 5th, 50th, and 95th percentiles of the distribution on rate, as shown in the “Poisson rate” node in the logic tree.

To develop a rate estimate based on the time-volume model, AM specified that a model of cumulative volume as a function of time should be fit to the events he specified in Table 3.2.5-1,

and that the model should be consistent with a conductive heat loss model. Two alternative functions were fit to his data: cumulative volume as a function of the square-root of time, as suggested by Rick Carlson in the 1996 PVHA study (CRWMS M&O 1996, and presentations at Workshop 2), and cumulative volume as a function of the natural log of time. The latter model provided a better statistical fit to the data and is used here. The best-fit linear regression was:

$$CV(t) = 1.87 + 0.282 \times \ln(3.91 + t) \quad (\text{Eq. 3.2.5-1})$$

In all cases, t is the time at which CV is to be estimated, in millions of years from the present. So for 2 Ma prior to the present, $t = -2$, and for 1 My in the future, $t = 1$.

The 90% confidence interval on the slope of the regression lines is used to represent the uncertainty in the estimated magma generation rate, as described in Section 3.1 and Appendix E.

The volume per event for future events is estimated based on the mean and variance of the volume of Quaternary events. To incorporate uncertainty in the volume per event for future events, volume per event is modeled with a lognormal distribution with mean and variance matching the mean and variance of the volume of relevant events, and the 5th, 50th, and 95th percentiles of that distribution are used in the logic tree. The volume per event differs for different event sets.

For the background zone, a homogenous Poisson model is used. Based on the method described in Section 3.1, the mean of the estimated rate based on Quaternary events is $5.1\text{e-}6$ events per year in the background zone; the mean rate estimate based on post 4.7-Ma events is $8.7\text{e-}7$ events per year in the background zone.

Figure 3.2.5-4 illustrates uncertainty in the estimated rate based on the most likely event set from Table 3.2.5-1, for each of the alternative temporal modeling approaches specified by AM. Each bar represents the 5th to 95th percentiles of the distribution on rate for the specified model, events set, and zone or region.

Mean Rate Density and Mean Recurrence Rate

Figure 3.2.5-5 illustrates the mean rate density for igneous events calculated from AM's spatial and temporal models for the 10,000-year assessment. The primary effect seen in this figure is the zone boundary and transition distance, but the effect of kernel density estimation within the zone, with inverse-age weighting of past events, is also evident. The color-shaded area represents the model domain, which includes both the CF-AD zone and a portion of the "background zone." The model domain was chosen for modeling convenience but was constrained to be at least as large as the area where an event could potentially intersect the repository footprint, as discussed below.

A mean recurrence rate for events in the region of interest can be calculated by summing the mean rate density at each grid point. Based on the mean rate density shown in Figure 3.2.3-6, the mean recurrence rate for events in this region is $4.3\text{e-}6$ events per year, giving recurrence intervals between 12,000 and 697,000 years (5th to 95th percentile of the distribution on recurrence interval), with a mean recurrence interval of about 233,000 years for events in the region illustrated.

Event Simulation Model

Figure 3.2.5-6 illustrates the key features of an event simulator for AM's PVHA-U model. In this model an *event* is characterized by a combination of dikes, conduits, and sills; the locations and dimensions of each of these features define the event.

An event may have from one to 10 individual dikes, with probability as illustrated in Figure 3.2.5-7. All dikes in an event have the same azimuth, with the distribution as illustrated in Figure 3.2.5-8. Individual dikes in an event are arranged in a right-stepping en echelon pattern, with the overlap between dikes in the direction of dike azimuth ranging from 0 (no overlap) to 20% of the length of the shorter of the overlapping segments. The length of individual dikes is calculated by dividing the assessment of the total length of dikes in the event (Figure 3.2.5-9) randomly between dikes. The spacing between dikes in the direction perpendicular to the azimuth is shown in Figure 3.2.5-10.

AM assessed the number of conduits in an event as a function of total dike length. Figure 3.2.5-11 shows the simulated distribution of the number of conduits in an event based on those assessments. Conduits are located along dikes, following the distribution shown in Figure 3.2.5-12. For events with multiple conduits, the second and subsequent conduits are placed so as to honor specified conduit spacing constraints: a minimum of 500 m and a maximum of 1 km between conduits. Conduit diameter is defined as a function of dike width, which is itself uncertain. Figure 3.2.5-13 shows the simulated distribution of conduit diameter based on those assessments. Each conduit in an event has a probability of 0.85 of being column-producing.

A sill can occur in an event, with a probability from 0 to 10%. If a sill occurs, it is located along a dike following the same distribution defined for conduit location (see Figure 3.2.5-12). Sills are elliptical, with the long dimension following the dike azimuth and an aspect ratio of two. The assessment of sill length is a triangular distribution with minimum of 0, maximum of 1 km, and a mode of 500 m. AM specified that sill formation would be possible only for dikes that do not intersect the repository drifts.

Figure 3.2.5-14 illustrates examples of the simulated events, and Table 3.2.5-2 describes the number of dikes and the number of conduits and vents (combined) in an event, and how frequently such events occur in the event simulation. The table indicates, for example, that the most common type of event consists of one dike and one conduit or vent – about 20% of all simulated events are of this type (as shown by the bolded number in the table). The top half of Figure 3.2.5-14 illustrates an example of a one-dike, one-conduit event. Although rare, events could contain as many as 10 dikes and 30 conduits. Note that events may also include sills, which are not represented in this table.

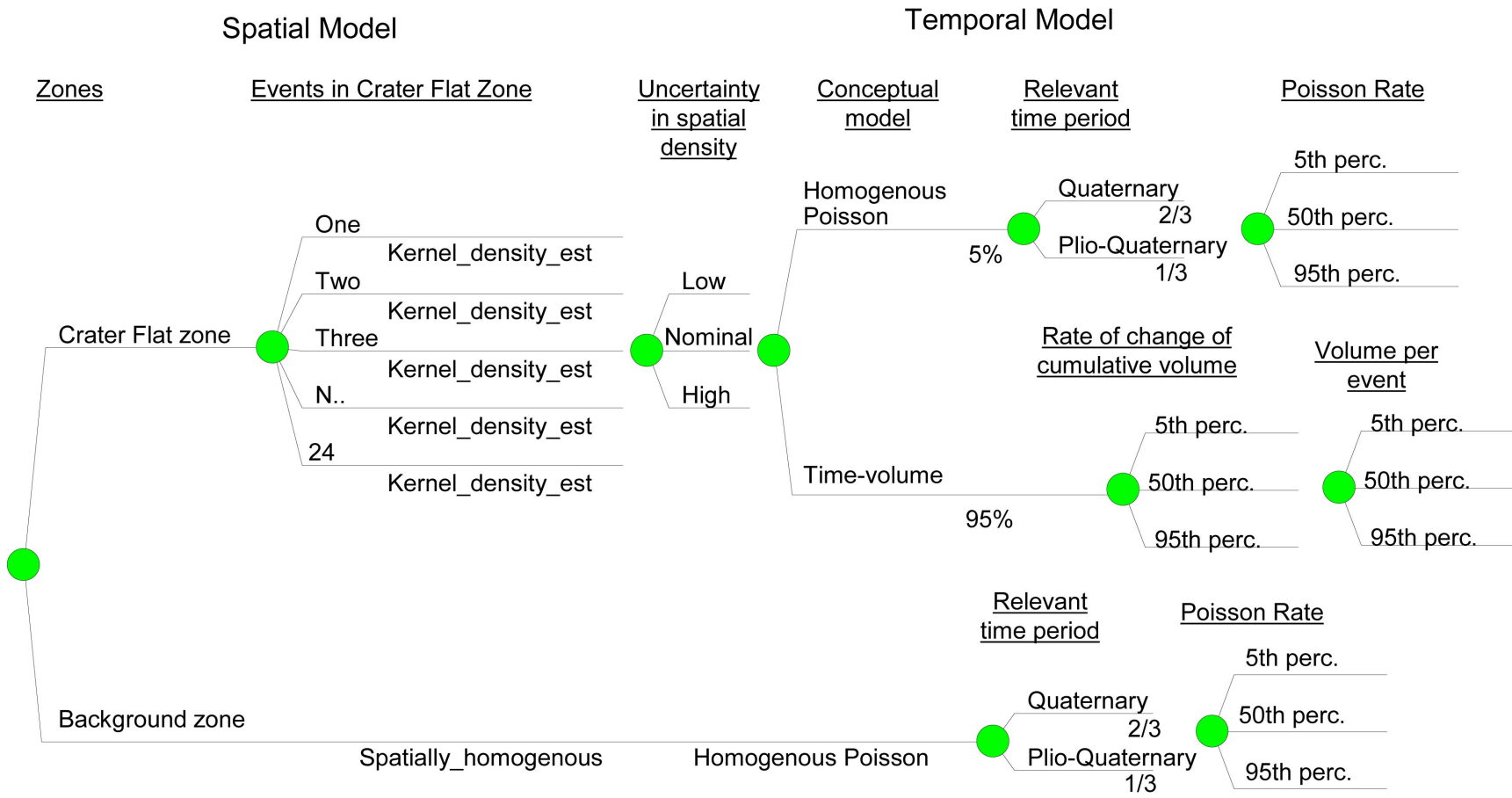
Conditional Probability of Intersection

Figure 3.2.5-15 illustrates the conditional probability of the intersection of any igneous feature with the repository footprint based on AM's event descriptions. The size of the contours is indicative of the relatively small overall size of AM's events, driven by the distribution on total dike length. The north-south orientation of the contours reflects the dike azimuth distribution.

As described above, AM's events include at least one dike, and may include column-producing conduit(s), vents, and sills. Figure 3.2.5-16 shows the conditional probability of intersection for each of these types of igneous features. These maps reflect the same spatial distribution of features as the intersection of any feature, indicating that no particular clustering of features within an event occurs. The conditional probability of intersection for conduits and vents is lower than for dikes for an event at any given location due to their smaller size and their distribution along a dike. Sills occur rarely, as reflected in the low probability contours.

Differences Between the 10,000-year and 1-My Assessments

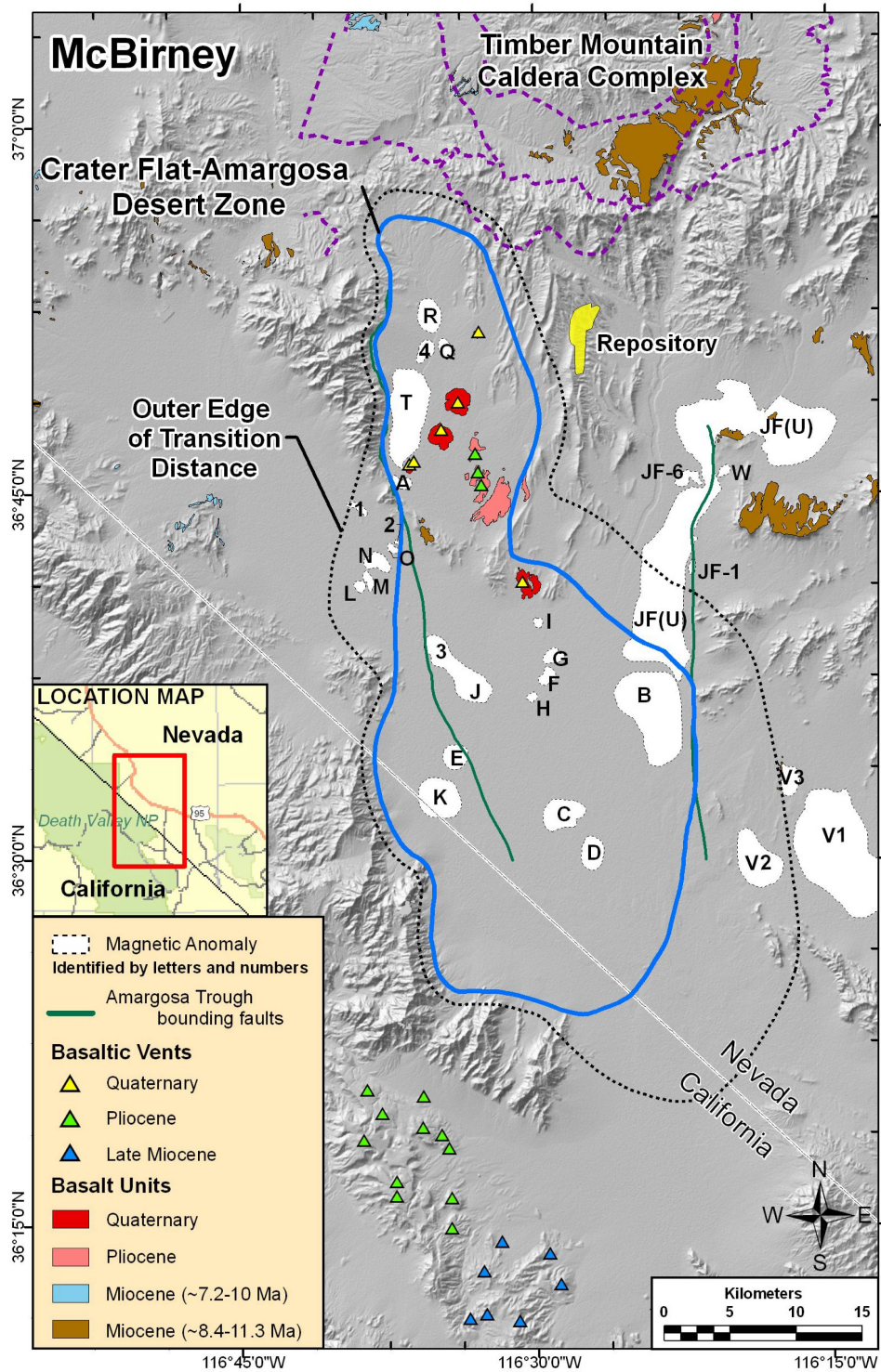
No structural differences exist in AM's spatial model, temporal model, or event characteristics based on the different assessment periods. However, the spatial model includes weighting of past events by the inverse of their age, so the rate density will be different when evaluated at different times. Similarly, the use of the time-volume rate model results in a rate estimate that varies over time. Figure 3.2.5-17 shows the mean rate density for the 10,000-year assessment (on the left), which uses the current ages for all past events, and the mean rate density for the 1-My assessment (on the right), which uses events assumed to be 1 My older than the current estimated ages. The contours on this figure show the decreased influence of Lathrop Wells (the youngest event) on mean rate density when it (and all other events) is assumed to be 1 My older than it is today. Lathrop Wells is the black triangle enclosed by the $1e-8$ contour on the 10,000-year assessment plot.



NOTES: All probabilities shown on the branches are those assigned by the expert. Uncertainty in spatial density, uncertainty in the Poisson rate and uncertainties in the rate of change of cumulative volume and the volume per event are modeled based on the approaches described in Section 3.1.5, and the probabilities for those branches are defined by the modeling approach.

A single parameterization of the kernel density estimation approach was specified for spatial density within the Crater Flat zone, so no uncertainties relative to those parameters appear in the logic tree.

Figure 3.2.5-1. Logic Tree Representing the Spatial and Temporal Components of the PVHA-U Model Specified by Alexander McBirney



NOTE: The blue line represents the zone boundary; black dashed line represents the outer boundary of the rate transition distance.

Figure 3.2.5-2. Crater Flat Zone as Specified by Alexander McBirney

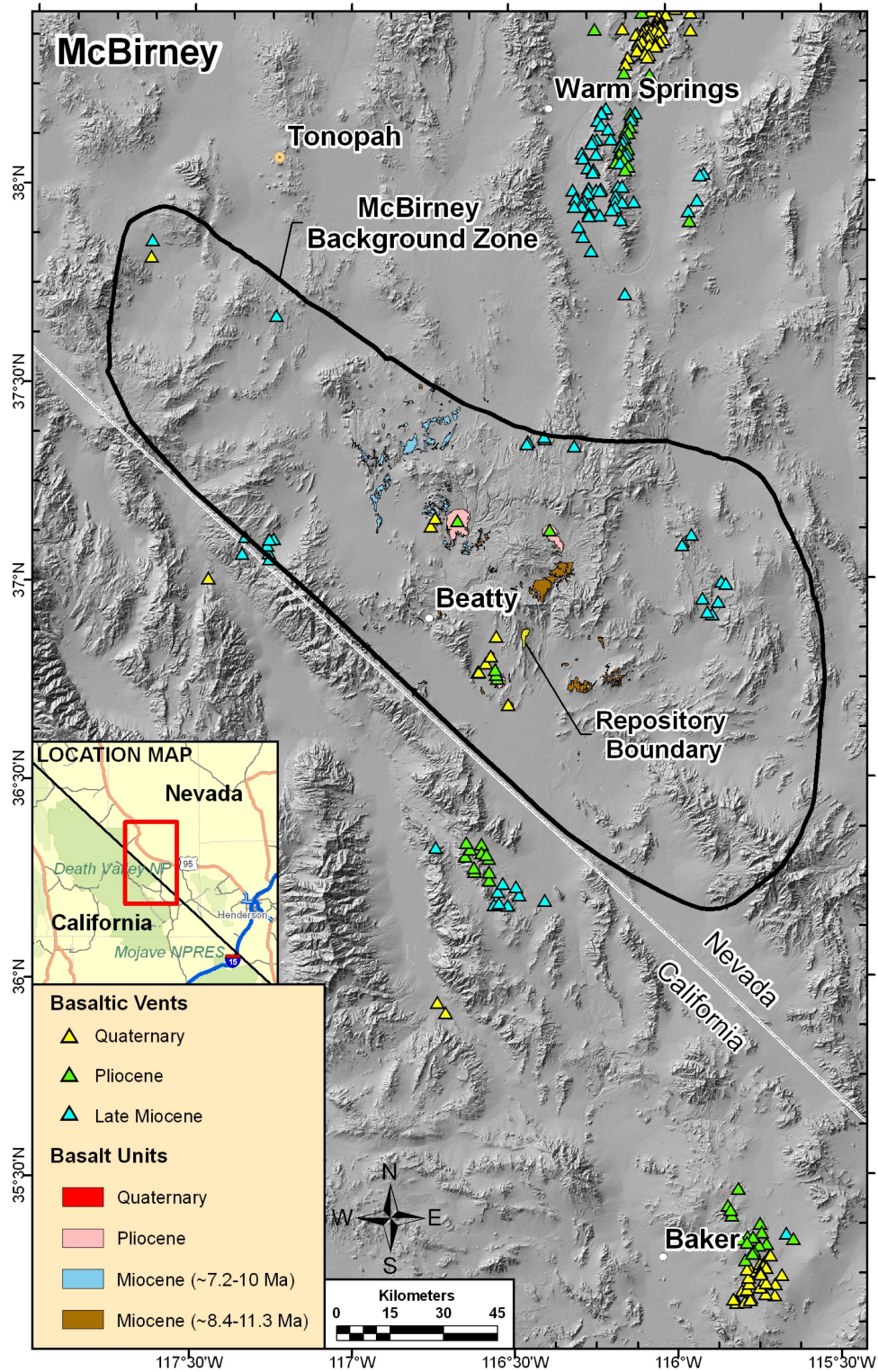
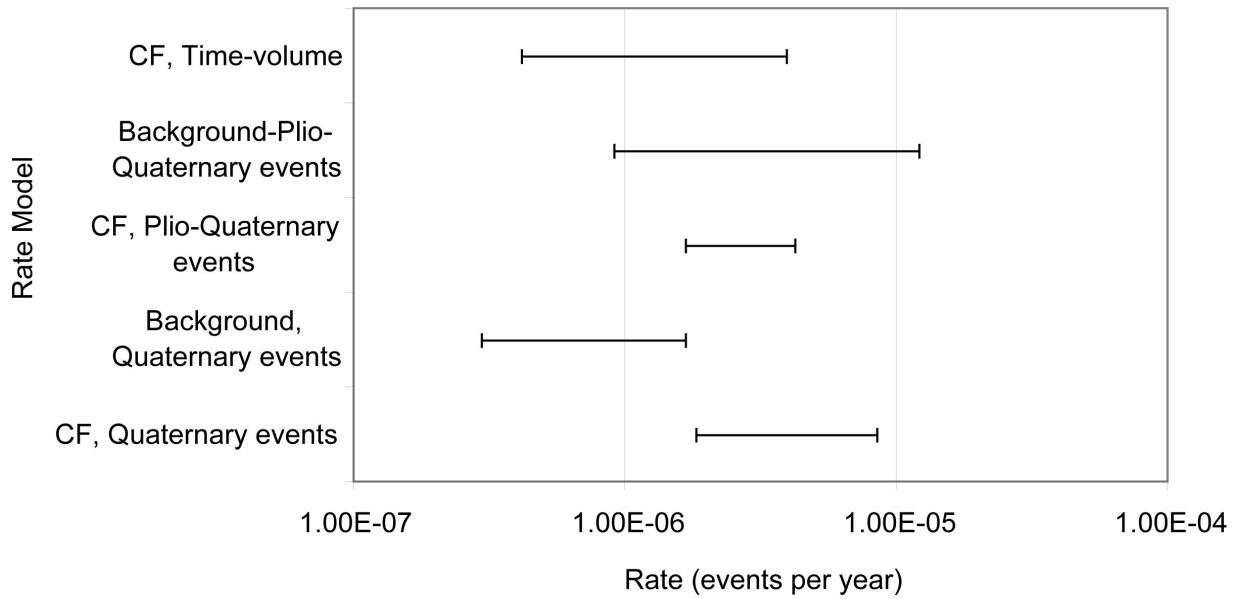


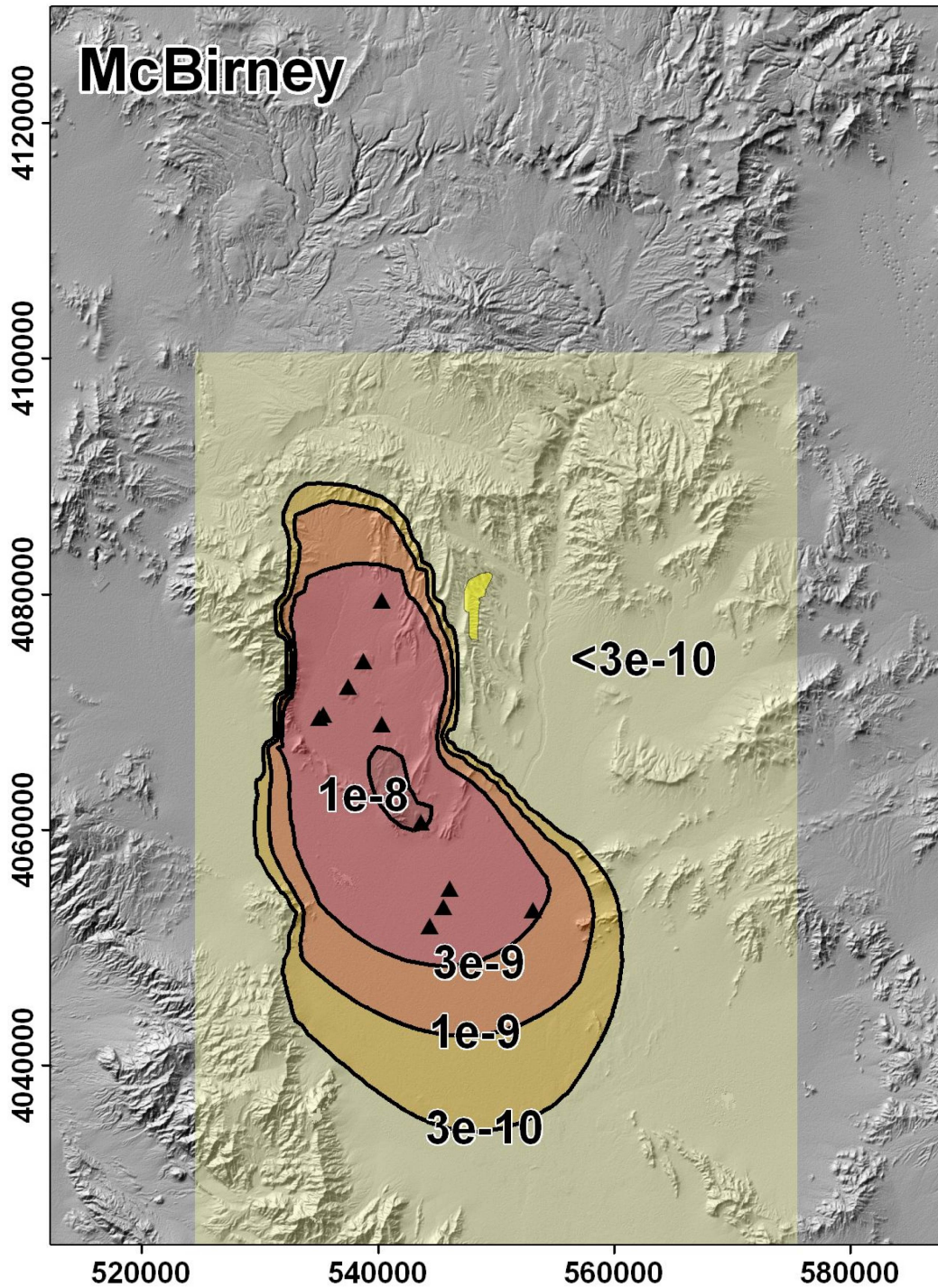
Figure 3.2.5-3. Background Zone as Specified by Alexander McBirney



NOTES: Bars represent the 5th to 95th percentile of the uncertainty in the rate for each alternative rate model, for estimates based on the most likely event set identified in Table 3.2.5-1.

Caution is recommended in comparing these rate distributions. Note that for each model, the estimated rate applies to the specific zone (CF = the Crater Flat zone, Background = background zone), the areas of which vary, implying different rate densities. In addition, the rate is spatially varying (as described in the text of the report).

Figure 3.2.5-4. Example of Uncertainty in Estimated Rate Based on a Single Interpretation of Past Events for Alternative Temporal Models Specified by Alexander McBirney



NOTE: Contours show the mean rate density in events per year per km². Yellow polygon represents the repository footprint; black triangles represent past events (AM's most likely event set). Map grid ticks are UTM meters; tick intervals are 20 km.

Figure 3.2.5-5 Mean Rate Density for the 10,000-Year Assessment Based on Models Specified by Alexander McBirney



Figure 3.2.5-6. Components of an Event Simulator Based on the Characteristics of Future Events Described by Alexander McBirney

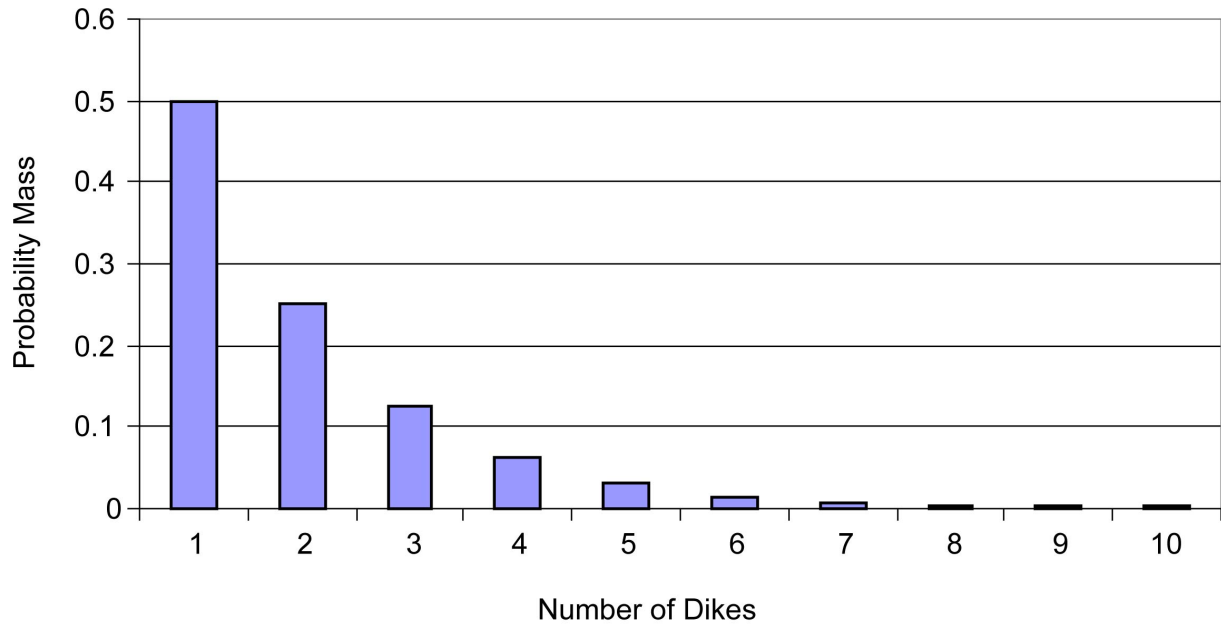
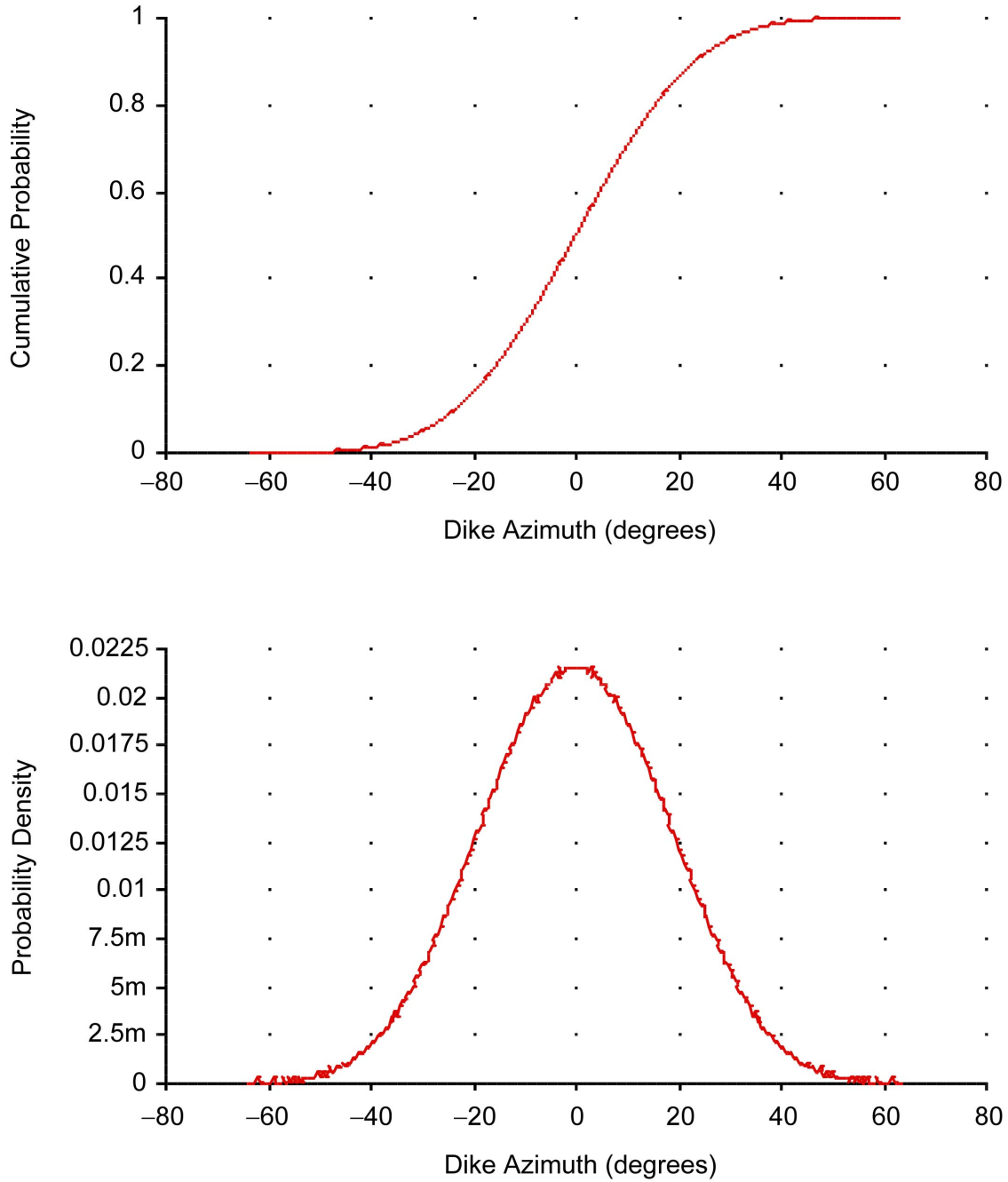


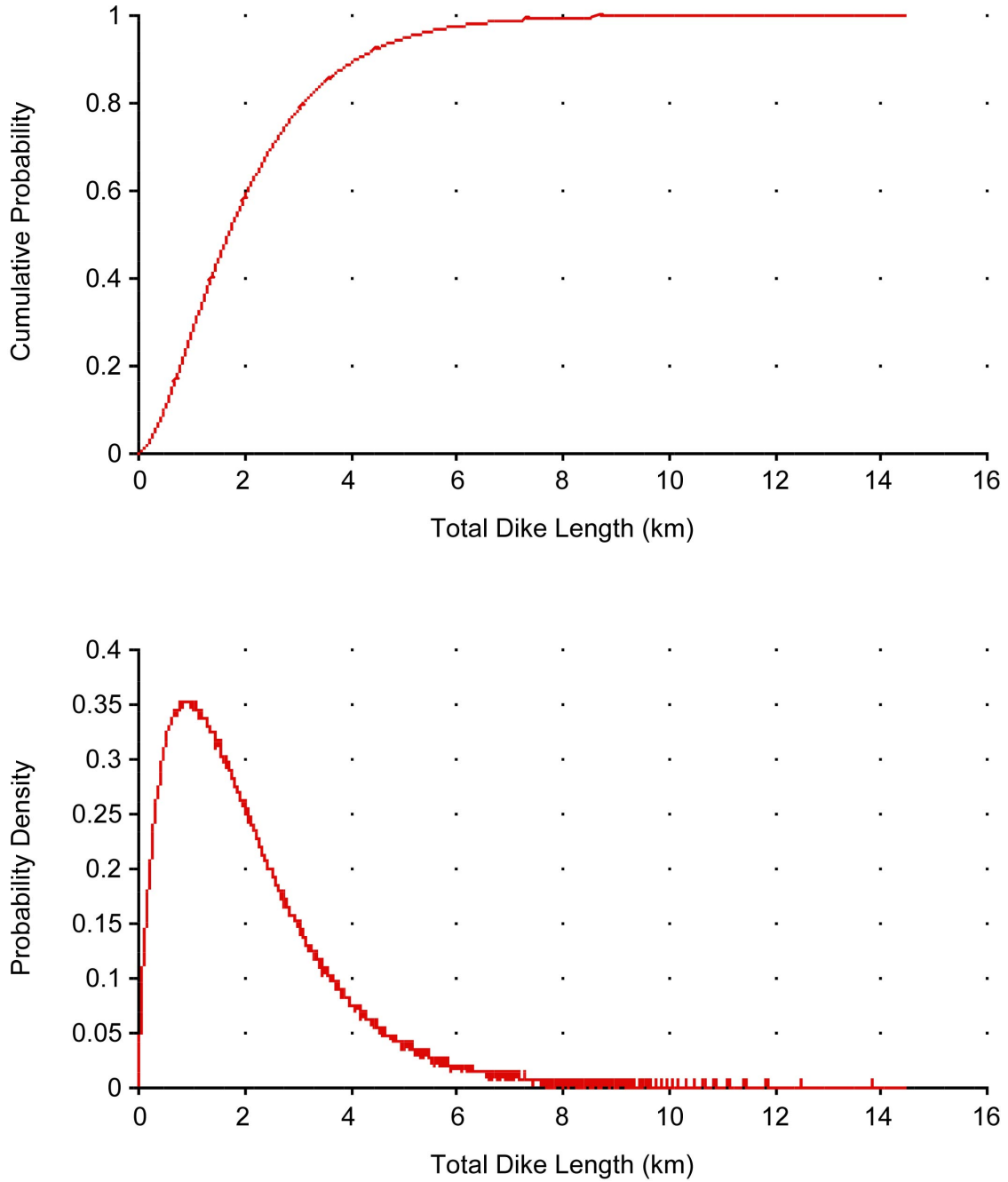
Figure 3.2.5-7. Distribution of the Number of Individual Dikes in an Event as Assessed by Alexander McBirney



NOTES: Top graph is a cumulative distribution function; bottom graph is a probability density function. For values less than 0.01 on the y-axis, suffix notation is used ($m = 10^{-3}$, so 5m = 0.005).

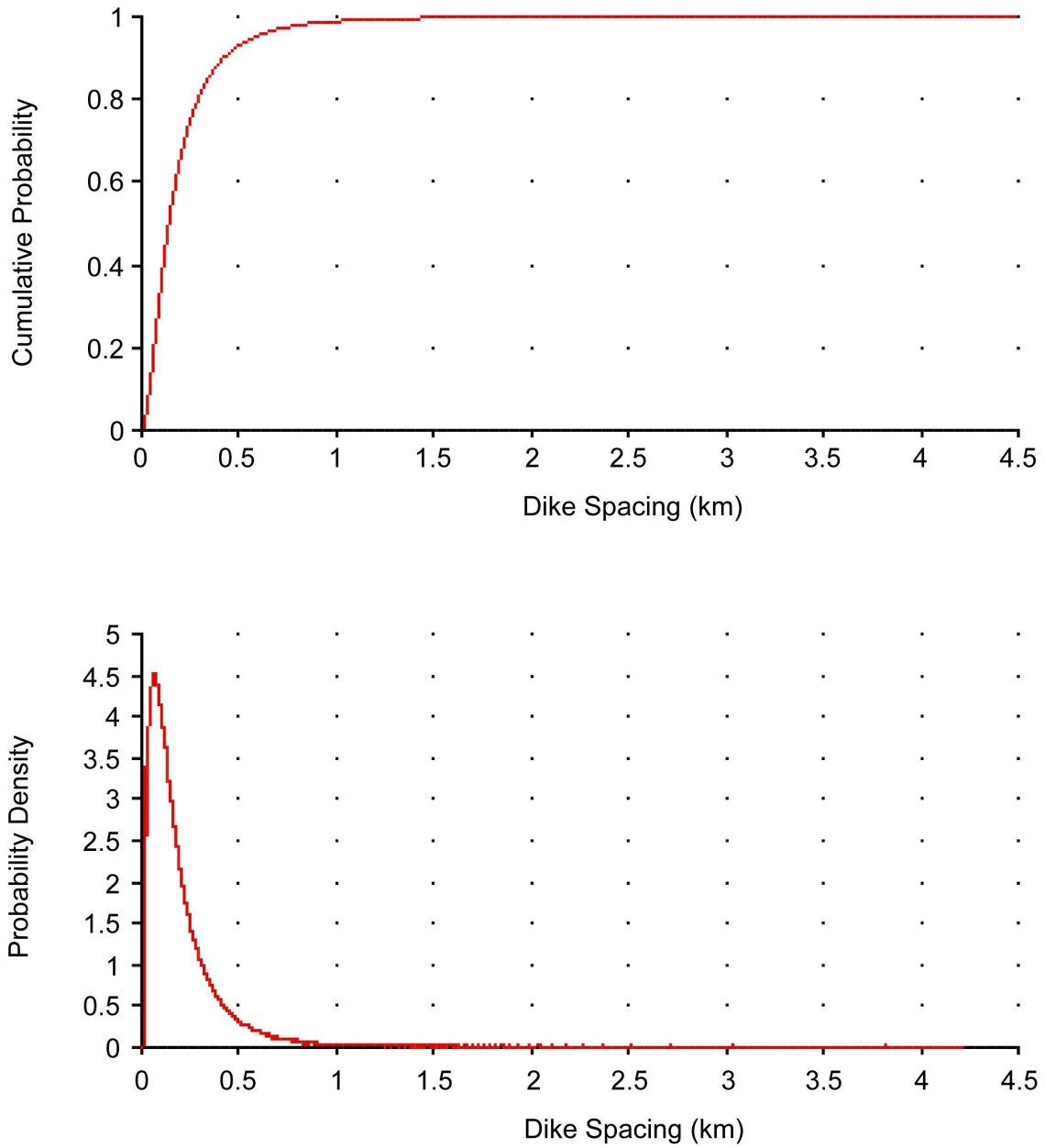
Zero represents North

Figure 3.2.5-8. Distribution for Dike Azimuth as Assessed by Alexander McBirney



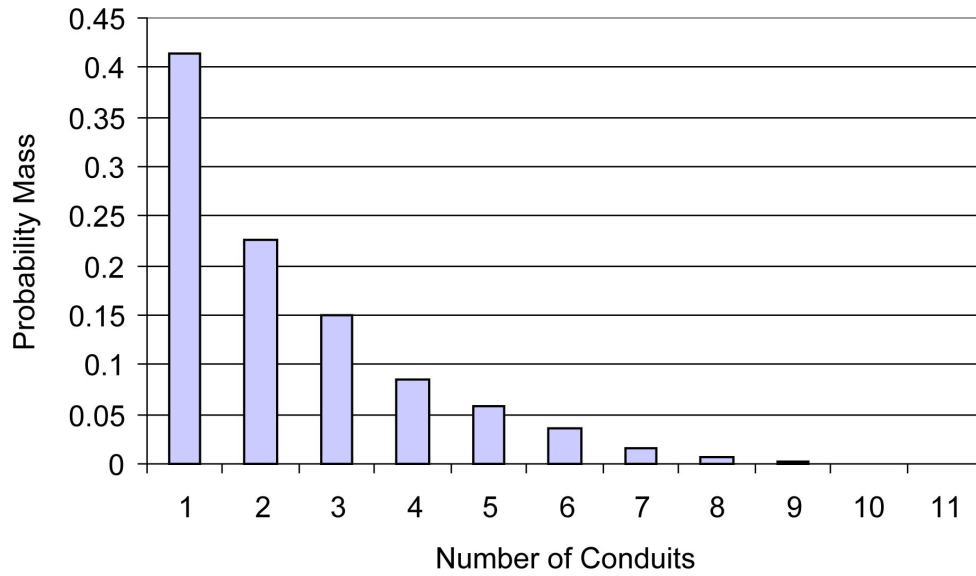
NOTE: Top graph is a cumulative distribution function; bottom graph is a probability density function.

Figure 3.2.5-9. Distribution for the Total Length of Dikes in an Event as Assessed by Alexander McBirney



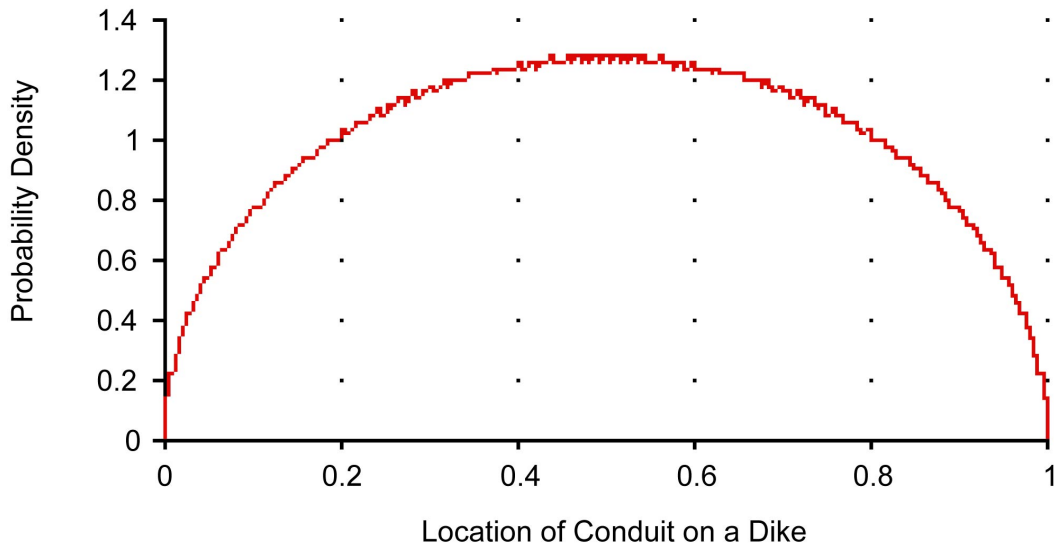
NOTE: Top graph is a cumulative distribution function; bottom graph is a probability density function.

Figure 3.2.5-10. Distribution for the Spacing between Dikes in the Direction Perpendicular to Dike Azimuth as Assessed by Alexander McBirney



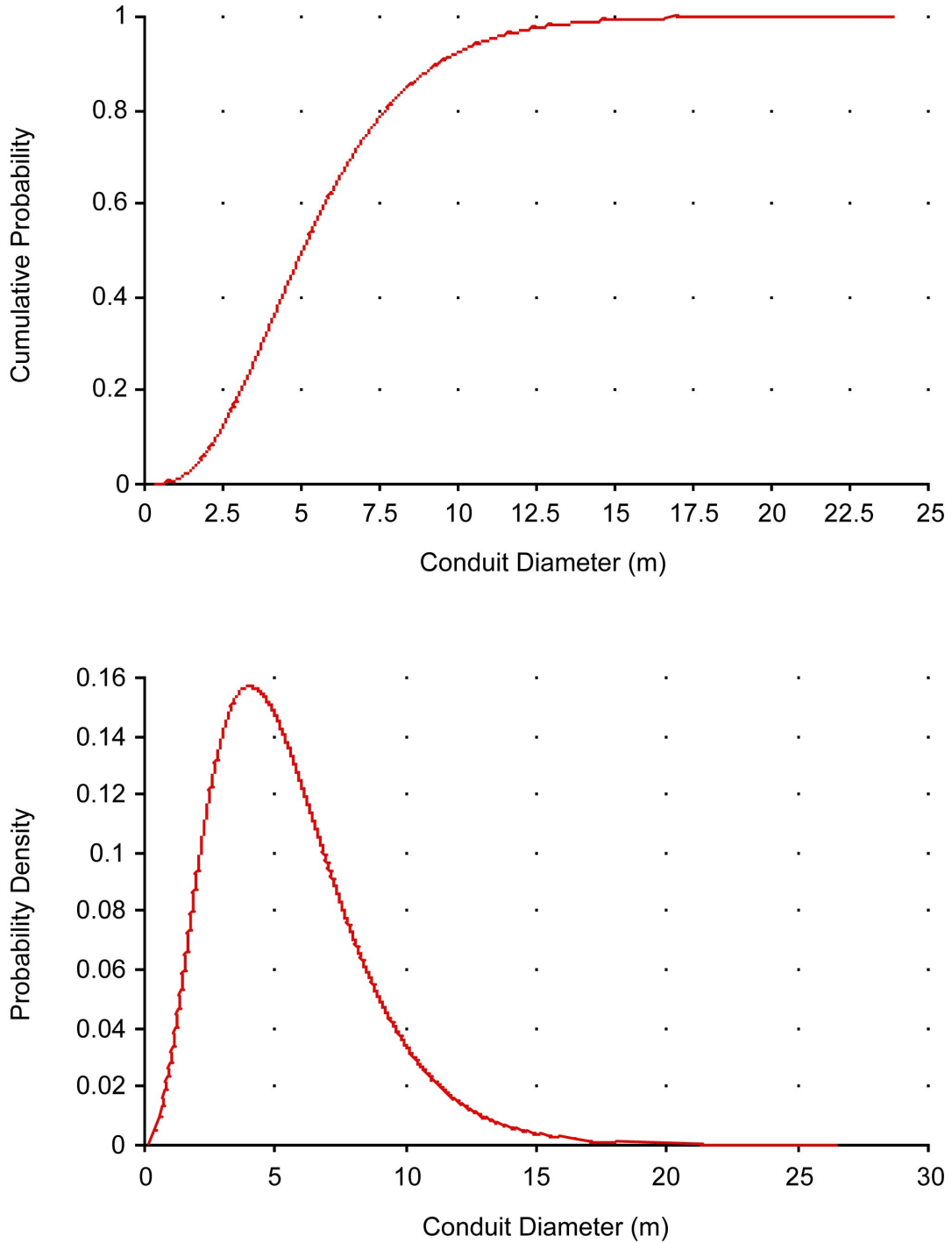
NOTE: Number of conduits is a function of the total dike length and the minimum allowable spacing between conduits. Graph shows the result of 100,000 iterations of the event simulator, combining uncertainty in the total dike length with the expert assessment of the number of conduits as a function of total dike length. Probability of 8, 9, 10, or 11 conduits in an event is less than 0.5%.

Figure 3.2.5-11. Number of Conduits in an Event Based on Assessments of Alexander McBirney



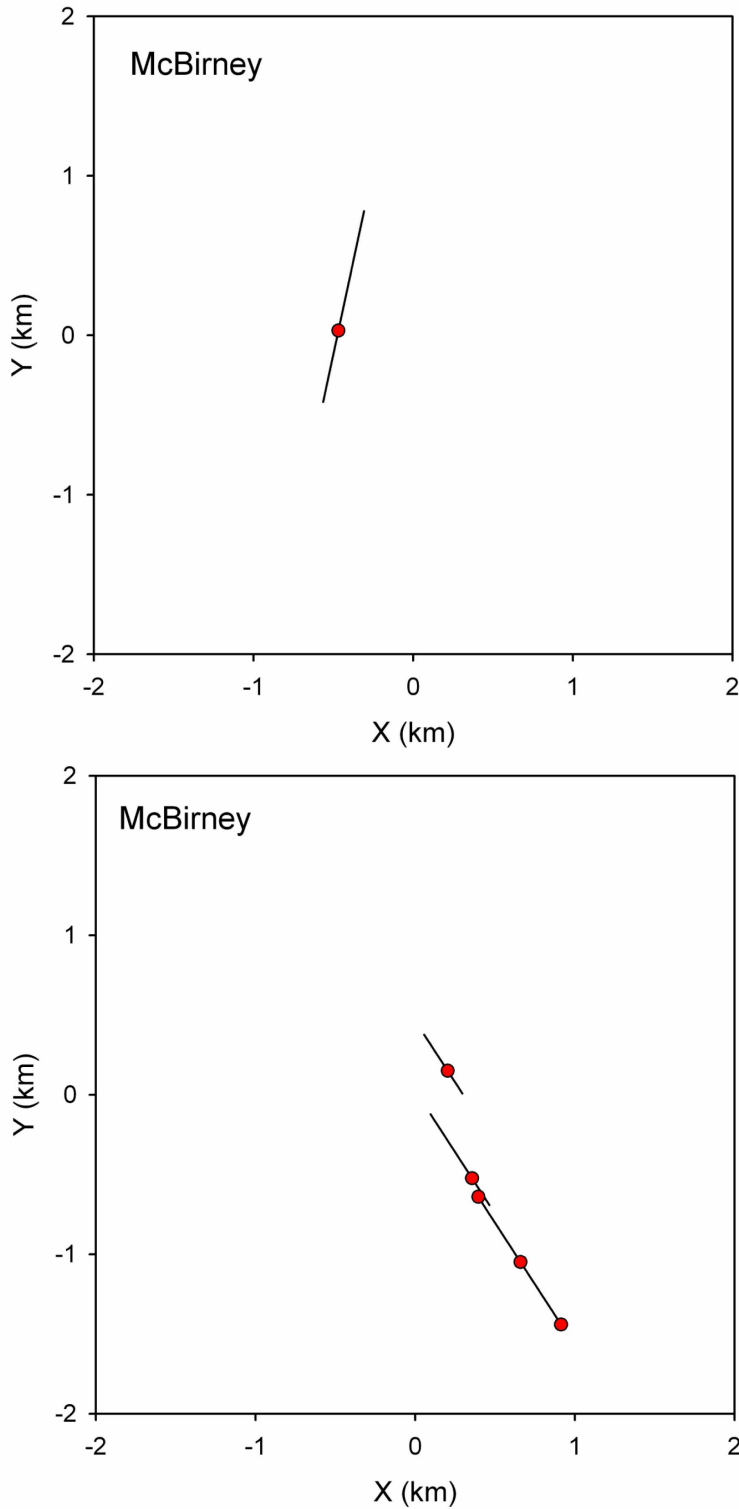
NOTE: Graph shows the relatively likelihood of a conduit being located at any position along the dike length, with zero and one representing the ends of the dike.

Figure 3.2.5-12. Distribution for the Location of a Conduit along the Length of a Dike as Assessed by Alexander McBirney



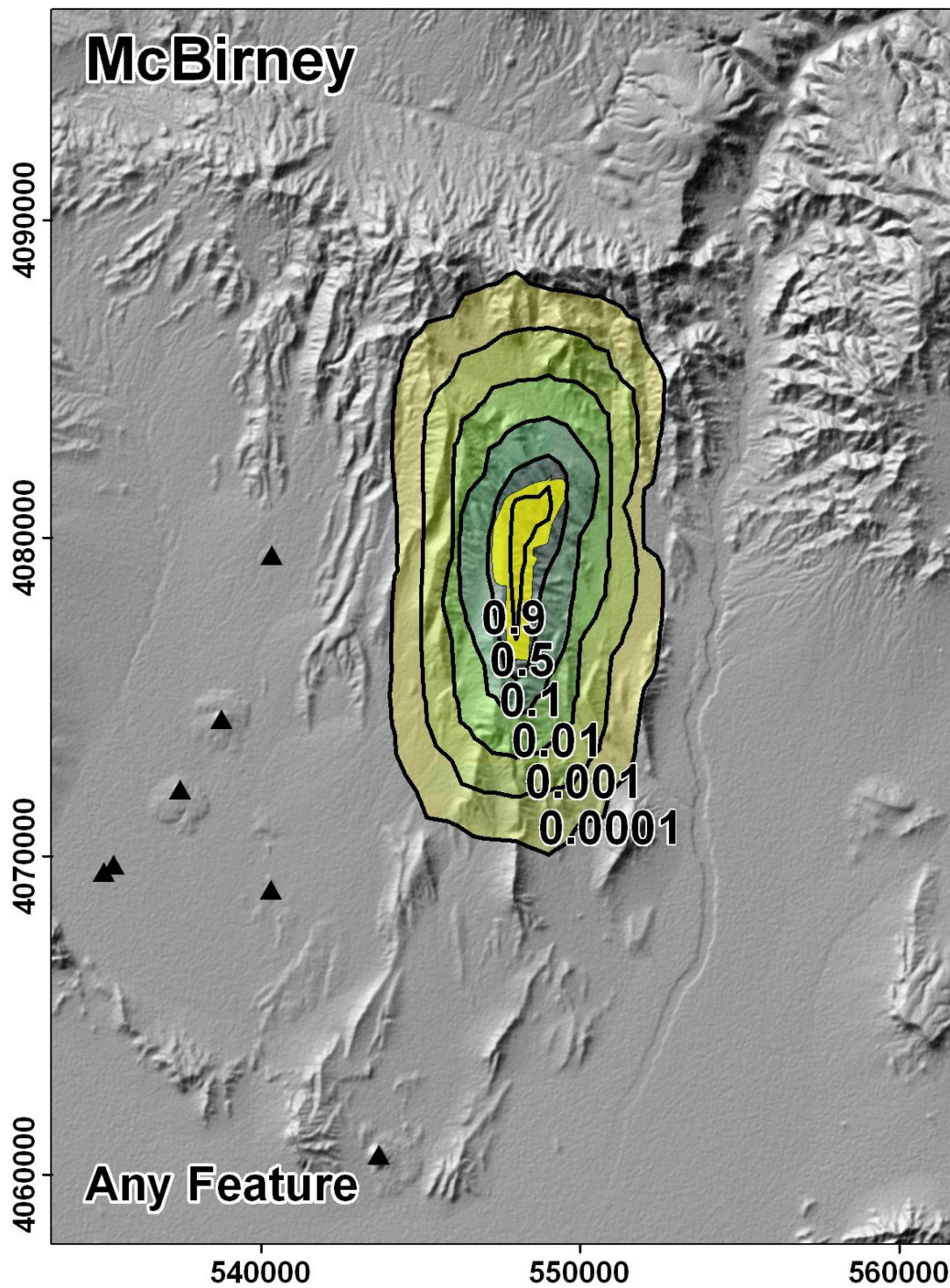
NOTES: Top graph is a cumulative distribution function; bottom graph is a probability density function.
 Results of 10,000 iterations of the event simulator; minimum conduit diameter constrained by dike width, which is itself uncertain.

Figure 3.2.5-13. Distribution for Conduit Diameter Based on Assessments of Alexander McBirney



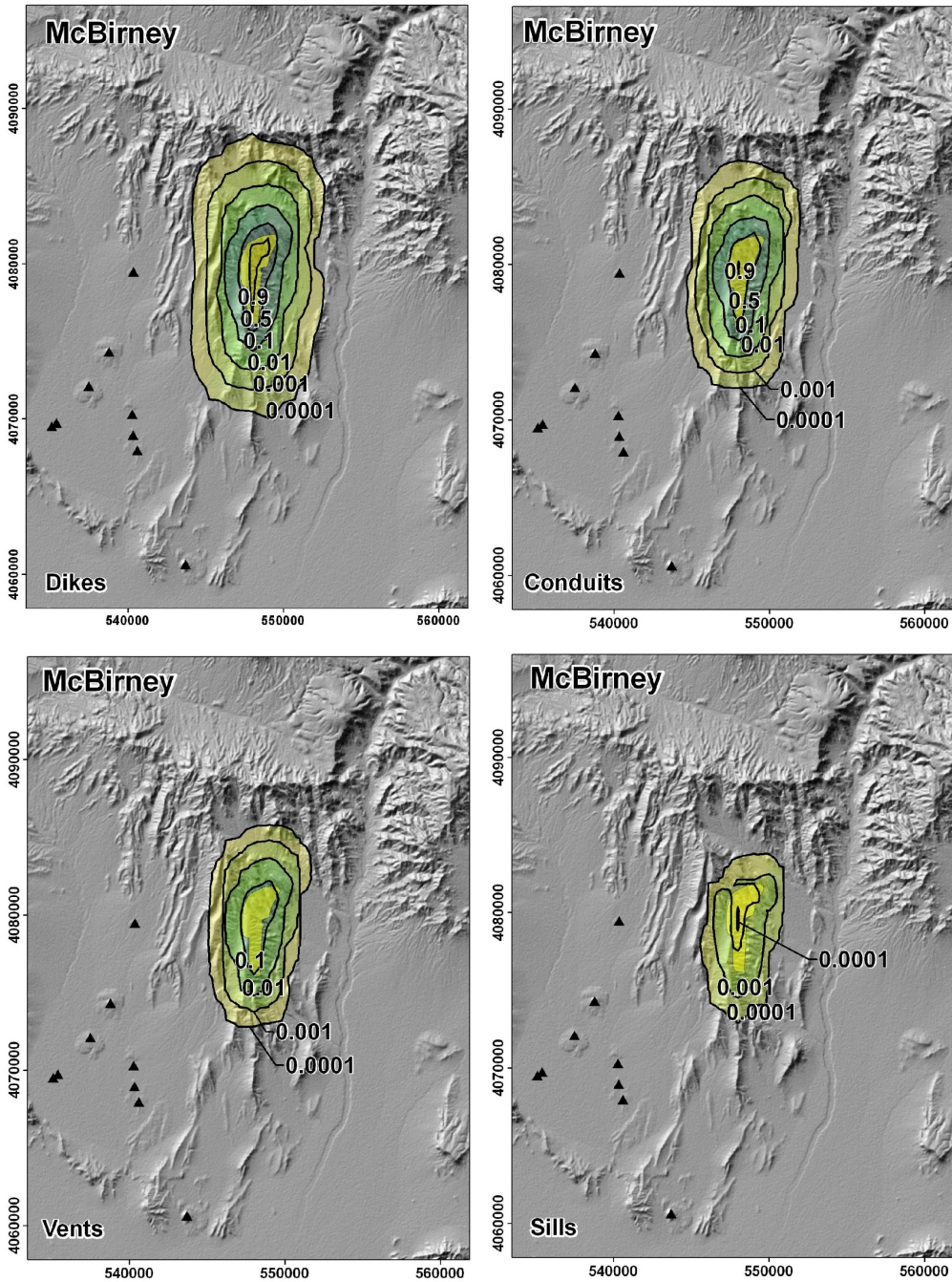
NOTE: Dikes are represented as black lines; their lengths on the figure are the lengths of the simulated dikes. Conduits and vents are represented as small red circles; they are not differentiated and their diameters are not represented. Sills, if they exist, are represented by light yellow ovals or polygons.

Figure 3.2.5-14. Examples of Simulated Events from the PVHA-U Model for Alexander McBirney



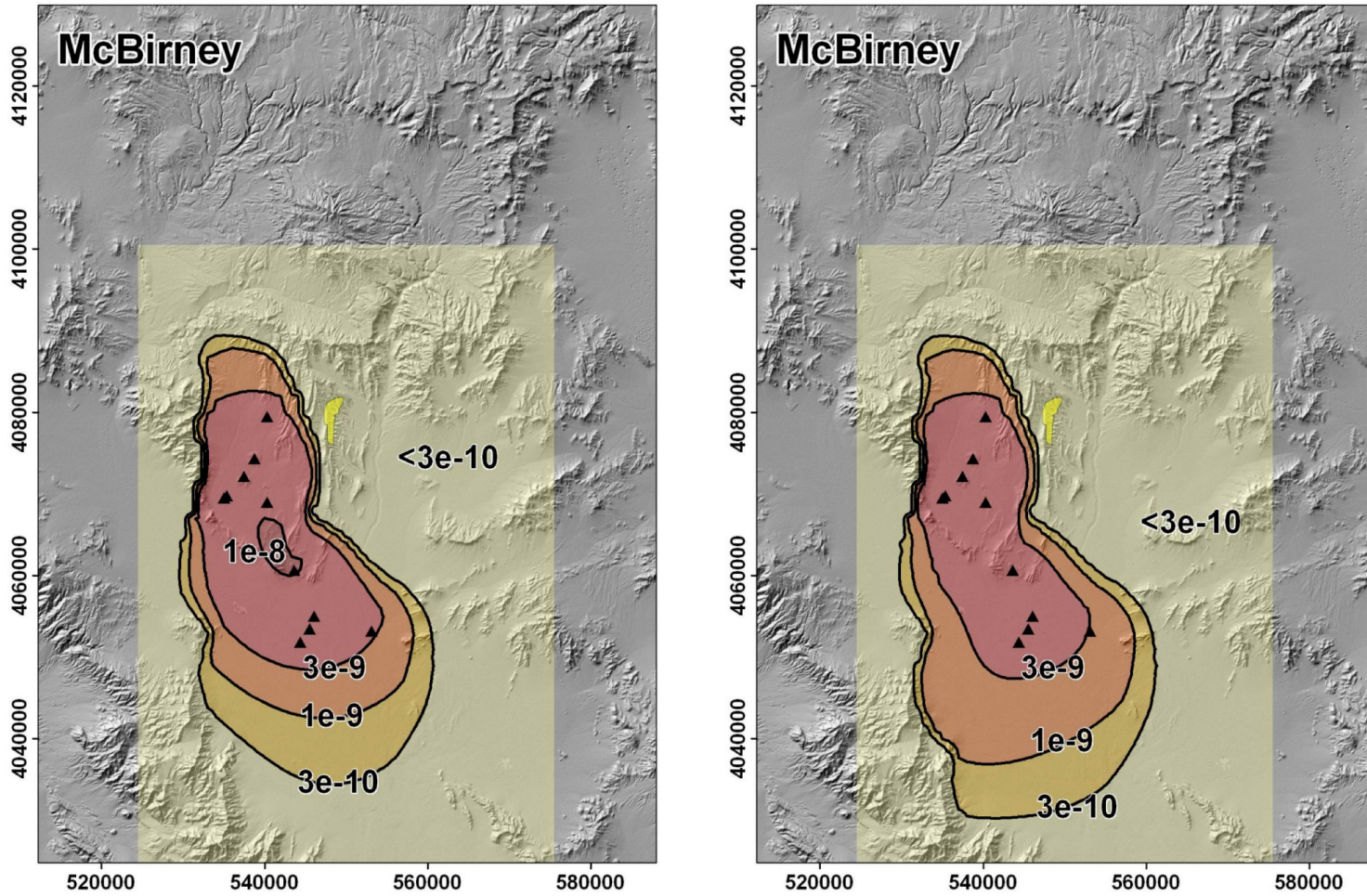
NOTE: Yellow polygon represents the repository footprint. Black triangles represent past events (AM's most likely event set). Map grid ticks are UTM meters; tick intervals are 10 km.

Figure 3.2.5-15. Conditional Probability of Intersection of Any Feature with the Repository Footprint Based on Event Descriptions Developed by Alexander McBirney



NOTE: Yellow polygon represents the repository footprint. Black triangles represent past events (AM's most likely event set). Map grid ticks are UTM meters; tick intervals are 10 km.

Figure 3.2.5-16. Conditional Probability of Intersection of Each Igneous Feature with the Repository Footprint Based on Event Descriptions Developed by Alexander McBirney



NOTE: The left figure is the mean rate density for the 10,000-year assessment; the right figure is the mean rate density for the 1-My assessment. Yellow polygon represents the repository footprint. Black triangles represent past events (AM's most likely event set). Map grid ticks are UTM meters; tick intervals are 20 km.

Figure 3.2.5-17. Mean Rate Density for the 10,000-Year Assessment and the 1-My Assessment Based on the Assessments of Alexander McBirney

Table 3.2.5-1. Data Used to Define Spatial Distribution and Event Rates for Future Volcanic Events for Alexander McBirney's PVHA-U Model

Zone	Name	Number of Events (weight)	Age (Ma)	Volume (km ³)
Crater Flat Zone	Lathrop Wells	1	0.08	0.048
	Makani Cone	1	1.07	0.002
	Black Cone	1	1.07	0.06
	Red Cone	1	1.07	0.055
	Little Cones NE	1	1.07	0.014
	Little Cones SW	1	1.07	0.02
	Anomalies G, F, and H	1 (0.25) 2 (0.33), or 3 (0.42)	3.9	0.028 0.029 0.006
	Pliocene Crater Flat	3	3.8	0.585 (total)
	Anomaly B	1	3.85	1.227
	Anomalies C and D	0 (0.60) 2 (0.40)	3.8 to 5.8	0.117 0.073
	Anomaly E	0 (0.7) 1 (0.3)	Unknown ^a	Unknown ^b
	Anomaly K	0 (0.7) 1 (0.3)	Unknown ^a	Unknown ^b
	Background Zone	Sleeping Butte: Hidden Cone	1	0.35
Sleeping Butte: Little Black Peak		1	0.35	
Buckboard Mesa		1	2.9	
Thirsty Mesa		1	4.6	
Clayton Valley Cone		1	0.39	

^a For events of "unknown" age, the weighting of the number of events takes into account the possibility that the events are older than 4.7 Ma, and therefore not relevant to AM's spatial or temporal models. For any event set that includes these as relevant events, their ages are therefore assumed to be younger than 4.7 Ma for the purposes of rate estimation.

^b Events of "unknown" volume are not used in developing an estimate of the rate based on the time-volume temporal model.

NOTES: Table derived from AM's Elicitation Summary in Appendix D.

Volumes of events outside the Crater Flat zone are irrelevant for the model and are not included.

Table 3.2.5-2. Frequency of Number of Dikes and Conduits or Vents in Simulated Events Based on the Assessments of Alexander McBirney

		Number of Conduits and Vents in an Event										
		1	2	3	4	5	6	7	8	9	10	11
Number of Dikes in an Event	1	20.7%	11.3%	7.6%	4.3%	2.8%	1.8%	0.8%	0.4%	0.2%	0.04%	0.02%
	2	10.3%	5.7%	3.8%	2.1%	1.5%	0.9%	0.4%	0.2%	0.1%	0.03%	0.01%
	3	5.3%	2.9%	1.9%	1.1%	0.8%	0.5%	0.2%	0.1%	0.05%	0.01%	0.01%
	4	2.6%	1.4%	1.0%	0.6%	0.4%	0.2%	0.1%	0.1%	0.03%	0.01%	0.00%
	5	1.3%	0.7%	0.5%	0.3%	0.2%	0.1%	0.05%	0.03%	0.01%	0.00%	0.00%
	6	0.7%	0.4%	0.2%	0.1%	0.1%	0.1%	0.02%	0.01%	0.00%	0.00%	0.00%
	7	0.4%	0.2%	0.1%	0.1%	0.0%	0.0%	0.01%	0.00%	0.00%	0.00%	0.00%
	8	0.2%	0.1%	0.1%	0.0%	0.0%	0.0%	0.00%	0.00%	0.00%	0.00%	0.00%
	9	0.1%	0.0%	0.0%	0.0%	0.0%	0.0%	0.00%	0.00%	0.00%	0.00%	0.00%
	10	0.0%	0.0%	0.0%	0.0%	0.0%	0.0%	0.00%	0.00%	0.00%	0.00%	0.00%

3.2.6 Michael Sheridan

Spatial and Temporal Models

Figure 3.2.6-1 presents the logic tree describing the basic structure of the spatial and temporal models developed by Michael Sheridan (MS) for PVHA-U. MS specified several alternative characterizations of past events, and his spatial and temporal models are dependent on those alternative event sets. Table 3.2.6-1 lists the past events in the region of interest judged relevant by MS to his spatial and temporal models. Figure 3.2.6-2 illustrates the region in the vicinity of the repository, the location of past events, and an extension of the western boundary of the Amargosa Trough (the green line) defined by MS as the western boundary of his region of interest: that is, events to the west of this boundary were not considered relevant to hazard calculation. The table includes alternative interpretations of some events, along with the relative probability MS assigned to each interpretation. In combination, 162 unique interpretations of the number of past events in the region of interest are identified from the assessments in the table. These are represented schematically in the first node of the logic tree: separate spatial and temporal models are fit to each of these alternative event sets. The probability for each event set is calculated from the probabilities given to different interpretations as summarized in Table 3.2.6-1.

Two alternative approaches to modeling the spatial distribution of future events were specified: (1) a bivariate Gaussian field shape approach and (2) an estimate that combines the bivariate Gaussian estimate with a spatial density estimate based on lithostatic pressure. The two models are assigned probabilities of 1/3 for the bivariate Gaussian alone, and 2/3 for the bivariate Gaussian combined with lithostatic pressure, as shown in the second node in the logic tree of Figure 3.2.6-1.

For the bivariate Gaussian estimate of conditional spatial density, MS specified that all events in his region of interest are considered part of a single volcanic field. For each event set, a bivariate Gaussian model was fit to the events.

Additional uncertainty is present in the spatial density resulting from fitting the bivariate Gaussian distribution to the relatively small number of past events. As described in Section 3.1, uncertainty in the spatial density is modeled by explicitly including the uncertainty in the fit of each of the five estimators derived from the event locations. This uncertainty is represented schematically by the “Uncertainty in Spatial Density” node in the logic tree of Figure 3.2.6-1; in actual modeling more than three branches are included.

For the second spatial model, MS provided an assessment of the likely values of lithostatic pressure at the location of a hypothetical future event in his region of interest, as illustrated in Figure 3.2.6-3. This assessment was combined with the lithostatic pressure at each point in the region of interest through the Bayesian updating approach described in Section 3.1 and Appendix E to create a spatial density estimate based on lithostatic pressure. This spatial density estimate was then combined with the conditional spatial density estimate from the bivariate Gaussian approach with probabilities of 0.25 (lithostatic pressure) and 0.75 (bivariate Gaussian) as specified in the logic tree.

Two event rates are required for MS's temporal mode: a field rate and a rate for events within the region of interest but outside the influence of the Crater Flat field. The latter is implemented as a "background rate," based on a background region specified by MS (Figure 3.2.6-4) and the identification of 5 events within that region in the past 1.5 Ma that are not considered part of the Crater Flat field. Events in the background region are modeled as a homogenous Poisson process and the rate is estimated based on the number of events and the age of those events as described in Section 3.1. The mean rate in the background zone is about $2.7e-6$ events per year.

In the Crater Flat volcanic field, two alternative models are used to estimate the rate, as shown in the logic tree: (1) a homogenous Poisson model and (2) a temporal clustering model. For the homogenous Poisson model, the mean rate for the most likely event set from Table 3.2.6-1 is $2.8e-6$ events per year in the Crater Flat field. Uncertainty in that rate is calculated as described in Section 3.1 and is illustrated in Figure 3.2.6-5.

As described in Section 3.1, temporal clustering is modeled with two Poisson processes: clusters occur as a Poisson process with one arrival rate (λ_c), and events occur within clusters as a Poisson process with a different rate (λ_w). MS identified four temporal clusters in the Crater Flat field, the oldest at approximately 4.8 Ma. This leads to a mean cluster arrival rate of $6.2e-7$ clusters per year in the Crater Flat field. The within-cluster arrival rate depends on the number of past events within clusters, the duration of clusters (assessed by MS as being from 0 to 300,000 years), and whether the present time is considered to be within a cluster (assessed by MS as having a 0.8 probability). For the highest total event count and the assumption that the present time is within a cluster, the mean within-cluster arrival rate at the present time is $2e-5$ events per year in the Crater Flat field. The rate from the temporal cluster model varies over time.

Figure 3.2.6-5 illustrates uncertainty in the estimated rate based on the most likely event set from Table 3.2.6-1 for the various rate models used by MS. Each bar represents the 5th to 95th percentile for the rate estimated using the specified model in either the field or the background, as indicated.

Mean Rate Density and Mean Recurrence Interval

Figure 3.2.6-6 illustrates the mean rate density for igneous events calculated from MS's spatial and temporal models for the 10,000-year assessment. The effect of the two alternative spatial models can be seen in this map: the elliptical contours centered on the Quaternary Crater Flat events result from the bivariate Gaussian field shape spatial model, and the irregular shaped contours in the northwest of the modeled region result from the additional consideration of lithostatic pressure. The color-shaded area represents the model domain. The model domain was defined by MS's specification of the Amargosa Trough bounding fault on the west as a truncation boundary for the influence of the field rate. Other boundaries were chosen such that the encompassed no more than the area for which the specified geology data were available and no less than the entire region for which the conditional probability of intersection of an event is non-zero (discussed below).

A mean recurrence rate for events in the region of interest can be calculated by summing the mean rate density at each grid point. Based on the mean rate density shown in Figure 3.2.6-6,

the mean recurrence rate for events in this region for the 10,000 year assessment is $6.3e-6$ events per year, giving recurrence intervals between 8,100 and 476,000 years (5th to 95th percentile of the distribution on recurrence interval), with a mean recurrence interval of about 159,000 years for events in the region shown in Figure 3.2.6-6. Note that this rate is a combination of the field rate and the background rate.

Event Simulation Model

Figure 3.2.6-7 illustrates the key features of an event simulator for MS's PVHA-U model. In this model an *event* is characterized by a combination of dikes, conduits, and sills; the number, locations, and dimensions of each of these features define the event.

The number of conduits in an event is given by the distribution shown in Figure 3.2.6-8. The number of dikes depends in part on the number of conduits: Figure 3.2.6-9 show the distribution of the number of dikes in an event based on simulations using MS's assessments of the number of conduits and the number of dikes conditioned on the number of conduits. Figure 3.2.6-10 illustrates the total length of dikes in an event. In events with multiple dikes, the length of any individual dike is random, with the constraint that the total length must be drawn from the distribution shown and the longest dike is no more than four times the length of the shortest dike. The distribution for dike azimuth is shown in Figure 3.2.6-11. In events with multiple dikes, dikes are right-stepping en echelon, with the spacing between any two dikes as shown in Figure 3.2.6-12. Dikes may overlap or underlap (gap) by as much as 10% of the length of the shorter dike.

Conduits can be located anywhere along the length of a dike, and are preferentially located on longer dikes. The minimum spacing between conduits on a dike is 400 m. Conduit diameter is defined as a function of dike length. Figure 3.2.6-13 illustrates a distribution on conduit diameter based on simulations from MS's assessments of dike length and the relationship between dike length and conduit diameter. Any conduit has a 70% chance of being a column-producing conduit.

For each dike in an event, there is a 5% chance of a sill forming on that dike. Figure 3.2.6-14 illustrates the number of sills in an event, based on simulations from MS's assessment of the number of dikes in an event and the frequency of sill formation on a dike. If a sill occurs, it is modeled as having an oval shape, with an aspect ratio between 1 and 2. A sill can occur anywhere along the length of a dike, the length of the sill is parallel to the dike azimuth, and the length is described by the distribution shown in Figure 3.2.6-15.

Figure 3.2.6-16 illustrates two examples of the simulated events: a relatively common event in the top panel and a less common event (both in terms of the number of features and the total dike length) in the bottom panel. Table 3.2.6-2 describes the number of dikes and the number of conduits and vents (combined) in an event, and how frequently such events occur in the event simulation. The table indicates, for example, that the most common type of event (65.2% of simulated events) consists of one dike with one conduit or vent. Events may contain as many as 6 dikes and 3 conduits or vents, although such events occur much less frequently. Events may also consist solely of a single conduit or vent, without an associated dike at repository depth

(0.8% of simulated events are of this type). Note that events may also include sills, which are not represented in this table.

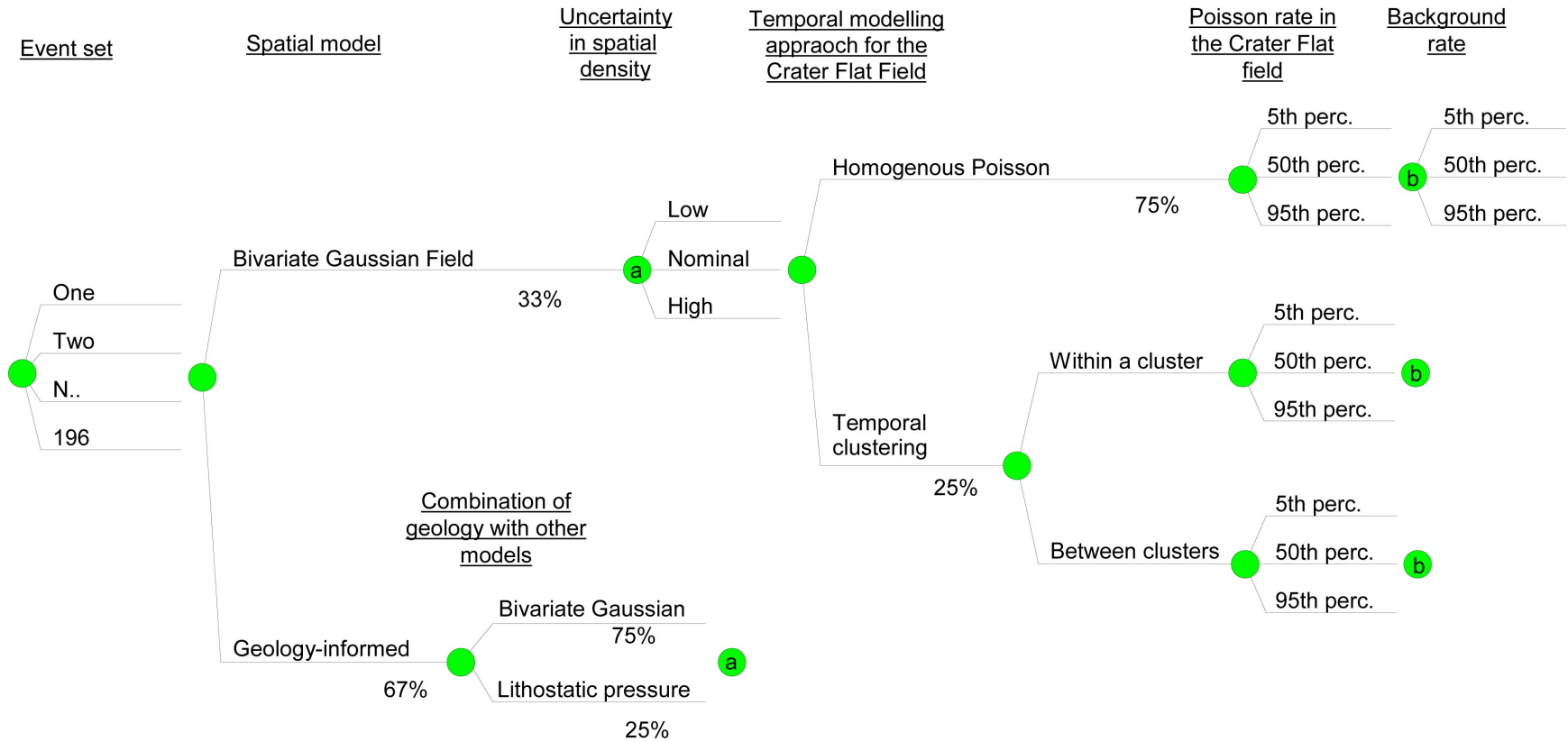
Conditional Probability of Intersection

Figure 3.2.6-17 illustrates the conditional probability of the intersection of any igneous feature with the repository footprint based on MS's event descriptions. The relatively short average dike length, the potentially wide spacing between dikes, and the broad azimuth distribution all contribute to the shape of these contours.

As described above, MS's events include at least one conduit or vent, usually include a dike, and may include sills. Figure 3.2.6-18 shows the conditional probability of intersection for each of these types of igneous features. These maps reflect the same spatial distribution of features as the intersection of any feature, indicating that there is no particular clustering of features within an event. The conditional probability of intersection for conduits and vents is lower than for dikes for an event at any given location due to their smaller size and their distribution along a dike. Sills occur rarely, as reflected in the low probability contours.

Differences Between the 10,000-year and 1-My Assessments

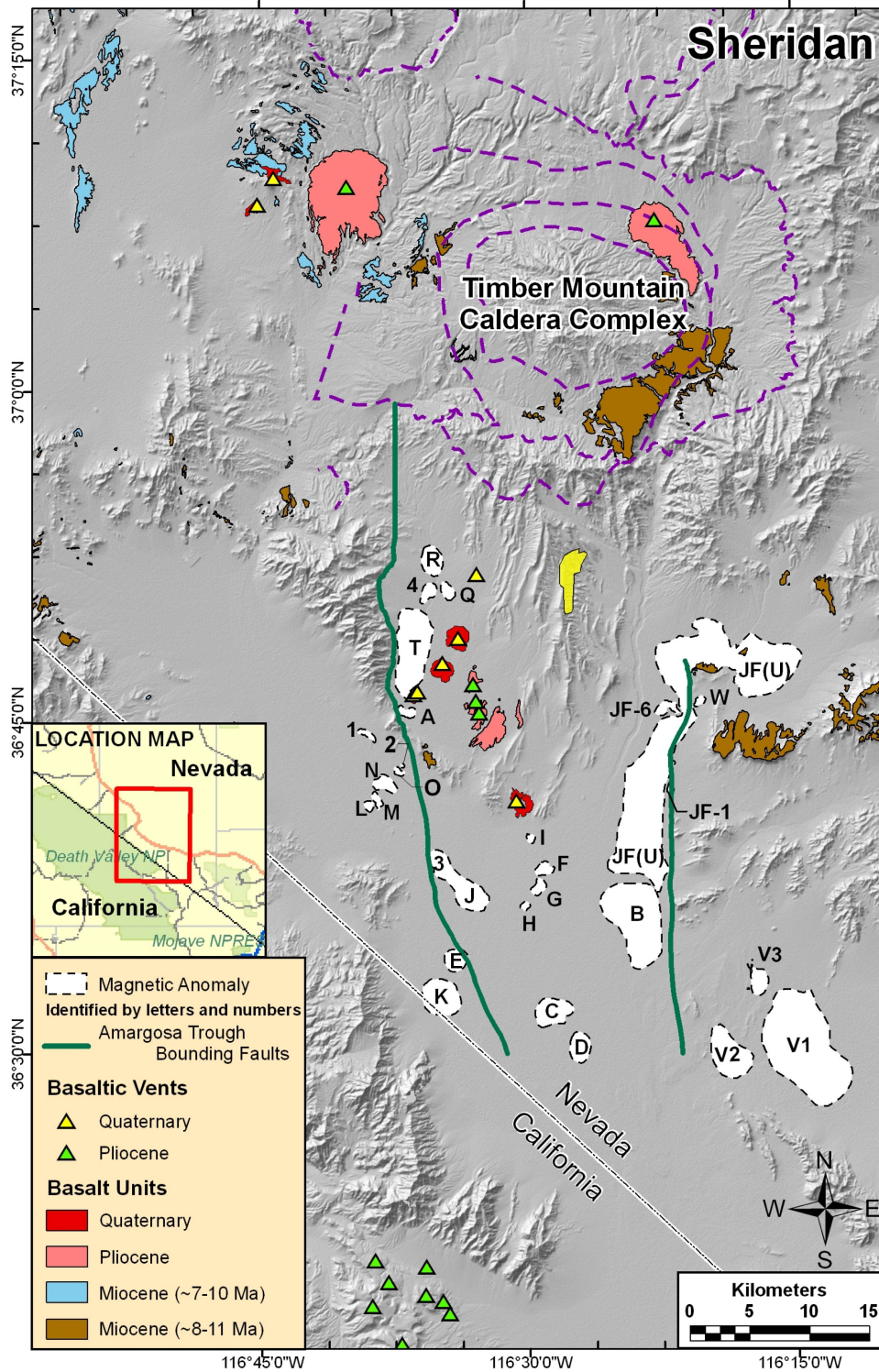
No differences exist in MS's spatial model or event assessments based on the different assessment periods. The temporal clustering model results in a time-dependent rate estimate, and thus different mean rate density estimates for the two compliance periods. Figure 3.2.6-19 shows a comparison of the mean rate density map for the 10,000-year assessment and the mean rate density map for the 1-My assessment based on the recurrence rate calculated at 1 My. As shown, the basic result at 1 My is a reduction in the mean rate density across the region. This reduction in mean rate density comes directly from the reduction in estimated rate, which in turn is a result of the fact that at 1 My there is no chance that the "current" temporal cluster is still active.



NOTES: All probabilities shown on the branches are those assigned by the expert. The lettered nodes along the top branch of the tree indicates that the subtree starting at that node is repeated at subsequent nodes with the same letter.

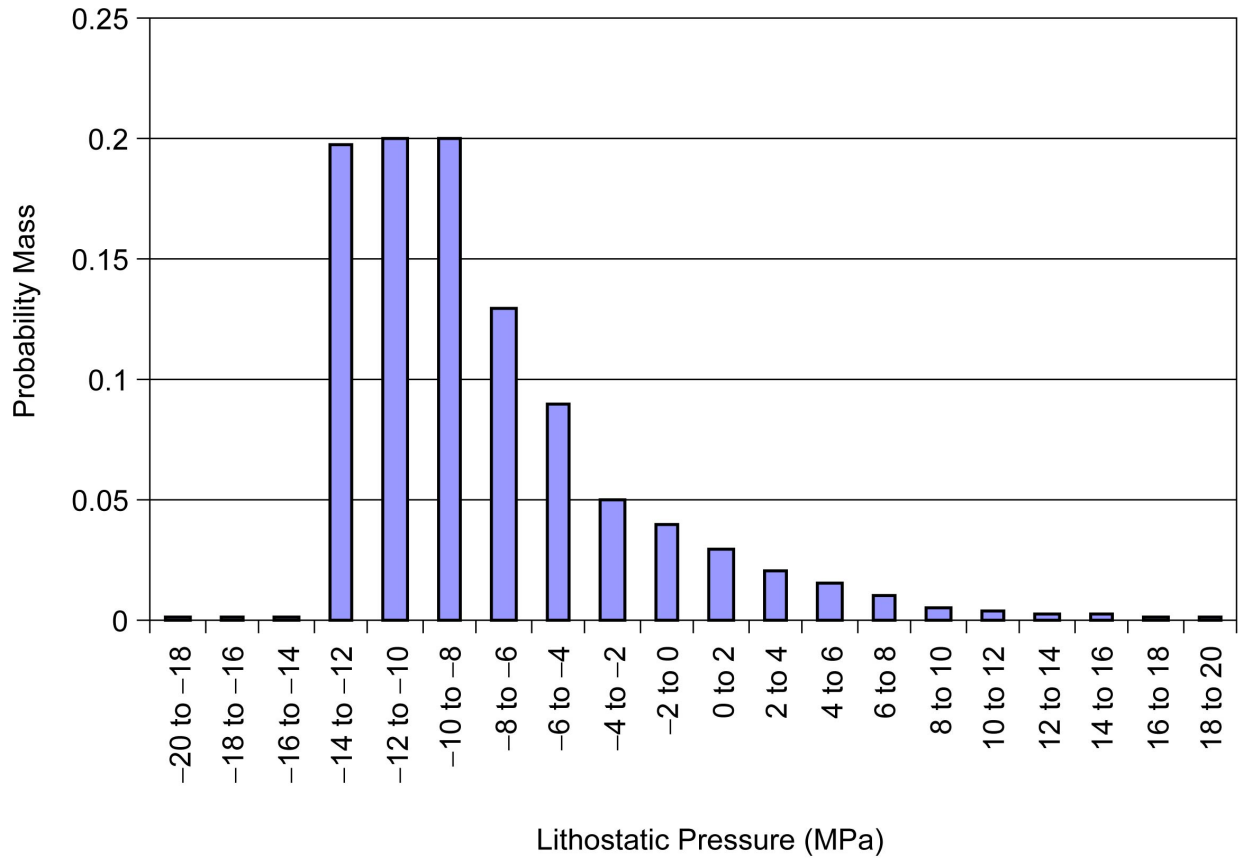
Uncertainty in spatial density and uncertainty in the rates are modeled based on the approaches described in Section 3.1.5, and the probabilities for those branches are defined by the modeling approach.

Figure 3.2.6-1. Logic Tree Representing the Spatial and Temporal Components of the PVHA-U Model Specified by Michael Sheridan



NOTE: Repository footprint is represented by the yellow polygon.

Figure 3.2.6-2. Yucca Mountain Region and the Location of Bounding Faults Identified as Relevant for the Spatial Model by Michael Sheridan



NOTE: Lithostatic pressure in the YMR is one of the data sets provided to the panel and listed in Appendix B. Lithostatic pressure values were calculated from free-air gravity and reflect gravity (mass) excesses (represented as positive lithostatic pressure values) and deficiencies (represented as negative values) relative to a theoretical gravity value at sea level.

Figure 3.2.6-3. Assessment of Lithostatic Pressure at the Location of a Hypothetical Future Event in the Region of Interest, as Specified by Michael Sheridan

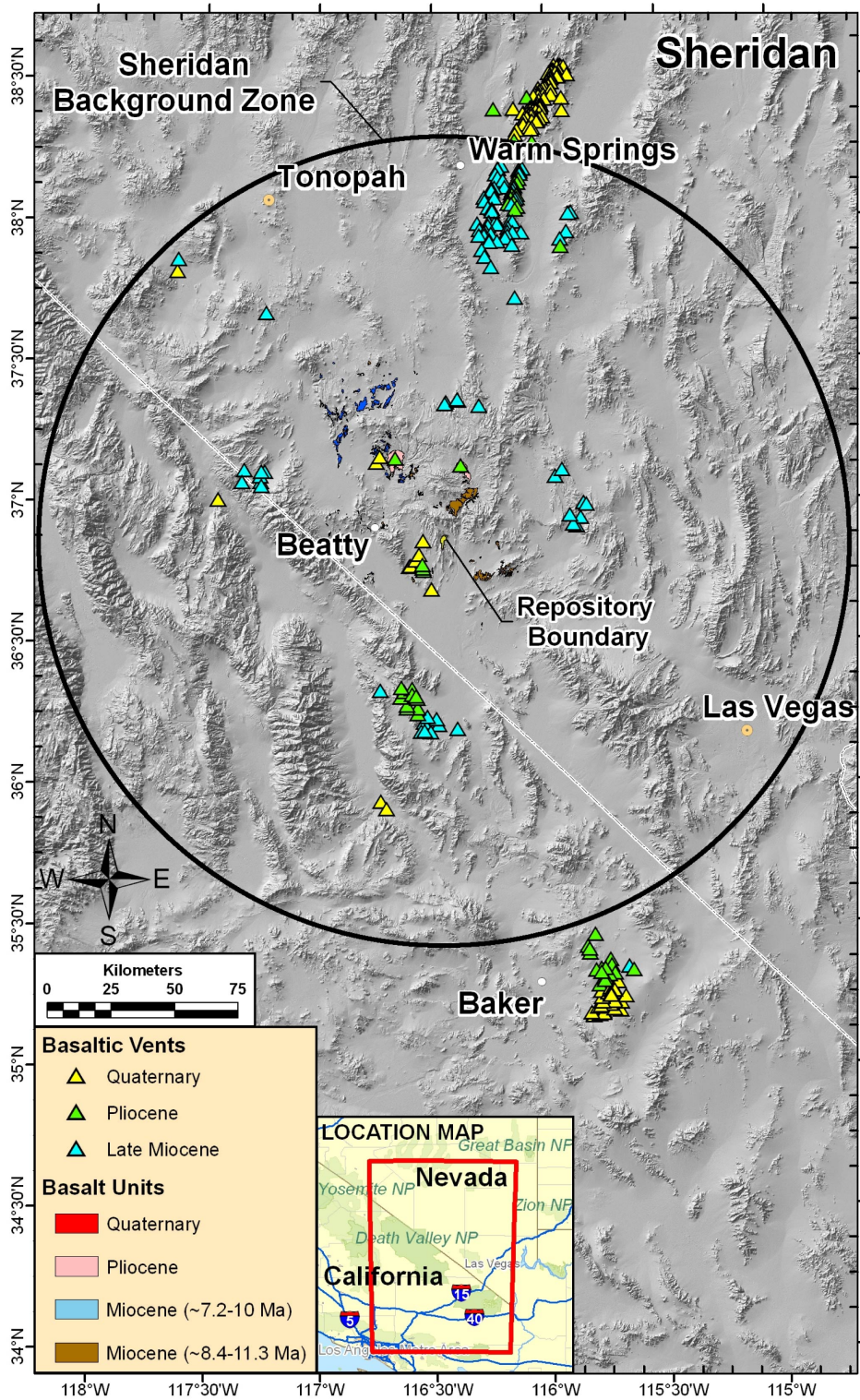
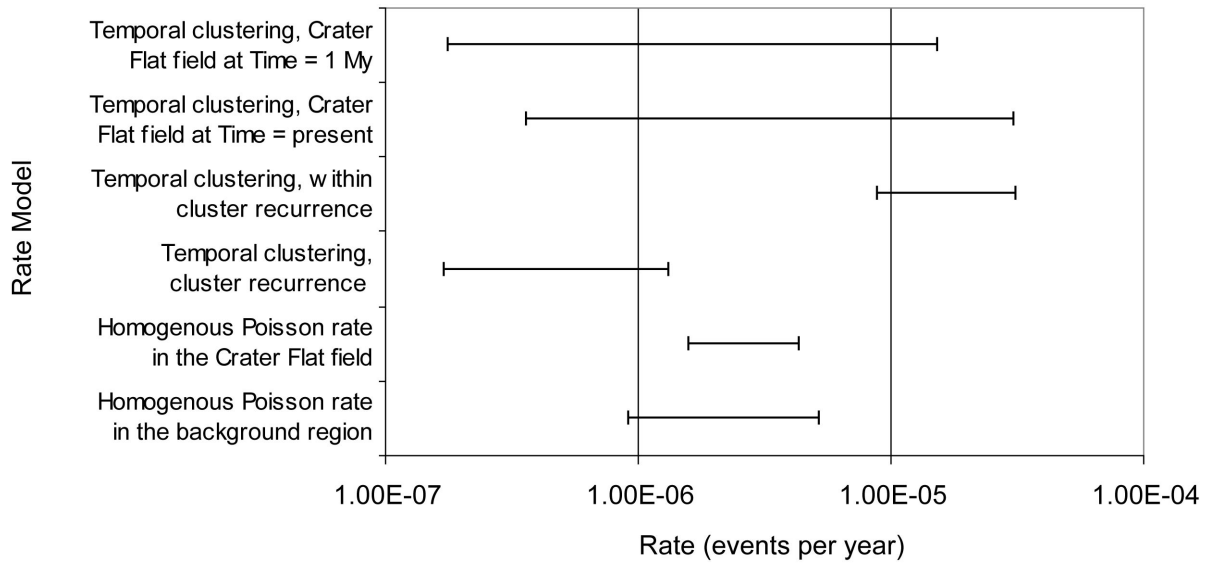


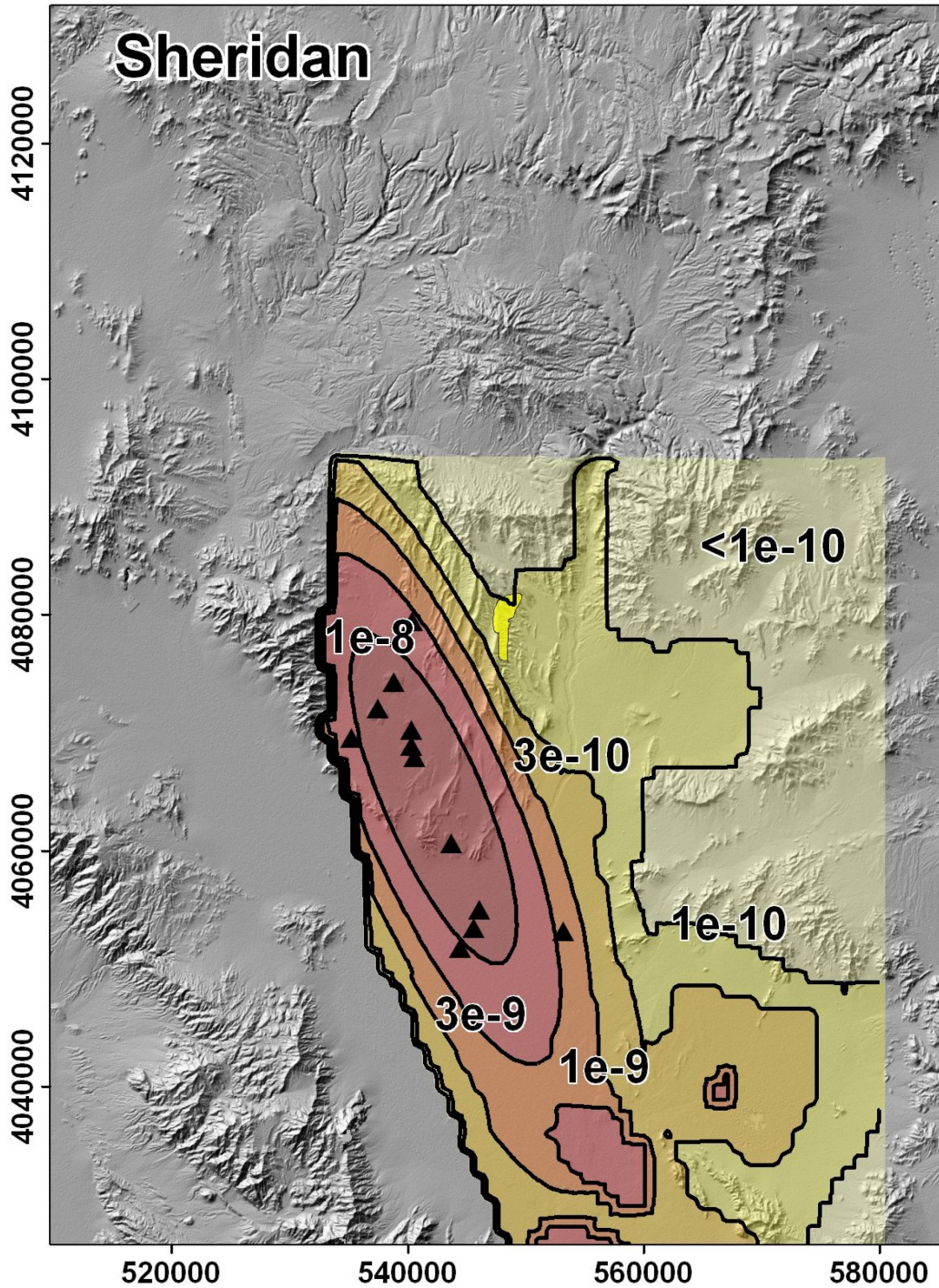
Figure 3.2.6-4. Background Region as Specified by Michael Sheridan



NOTES: Bars represent the 5th to 95th percentile of the uncertainty in the rate for each alternative rate model, for estimates based on the most likely event set identified in Table 3.2.6-1.

Rates under the temporal clustering model are bimodal; the distribution is not symmetric across the range shown here.

Figure 3.2.6-5. Example of Uncertainty in Estimated Rate Based on a Single Interpretation of Past Events for Alternative Temporal Models Specified by Michael Sheridan



NOTE: Contours show the mean rate density in events per year per km². Yellow polygon represents the repository footprint; black triangles represent past events (MS's most likely event set). Map grid ticks are UTM meters; tick intervals are 20 km.

Figure 3.2.6-6. Mean Rate Density for the 10,000-Year Assessment Based on Models Specified by Michael Sheridan



Figure 3.2.6-7. Components of an Event Simulator Based on the Characteristics of Future Events Described by Michael Sheridan

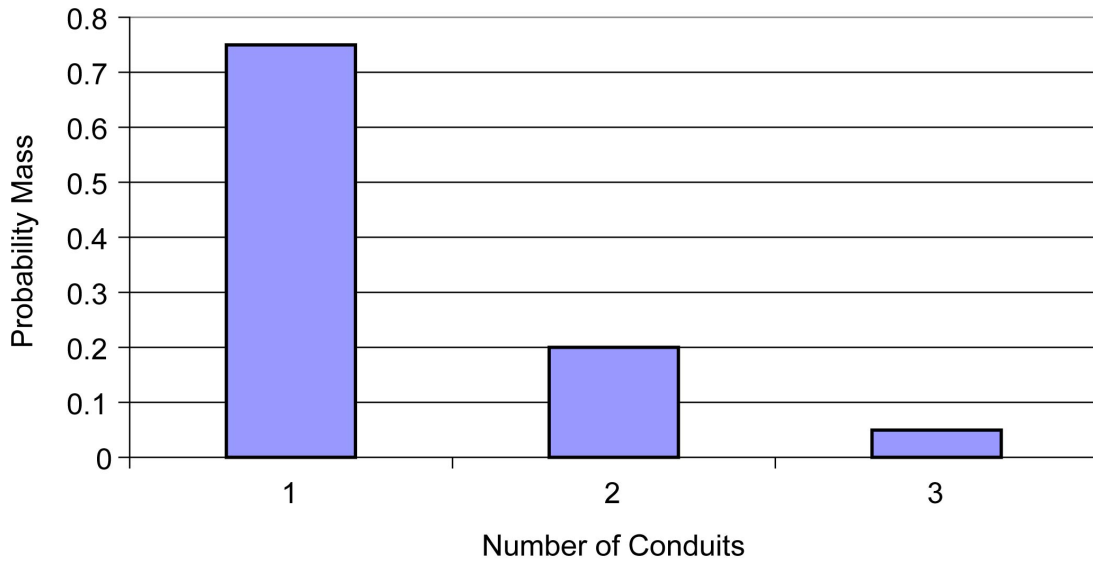
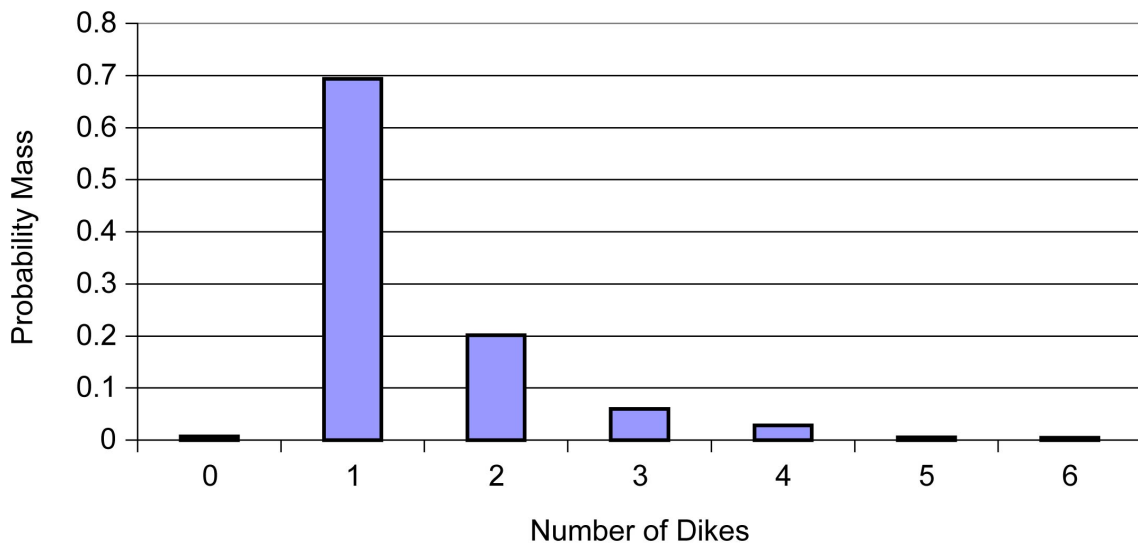
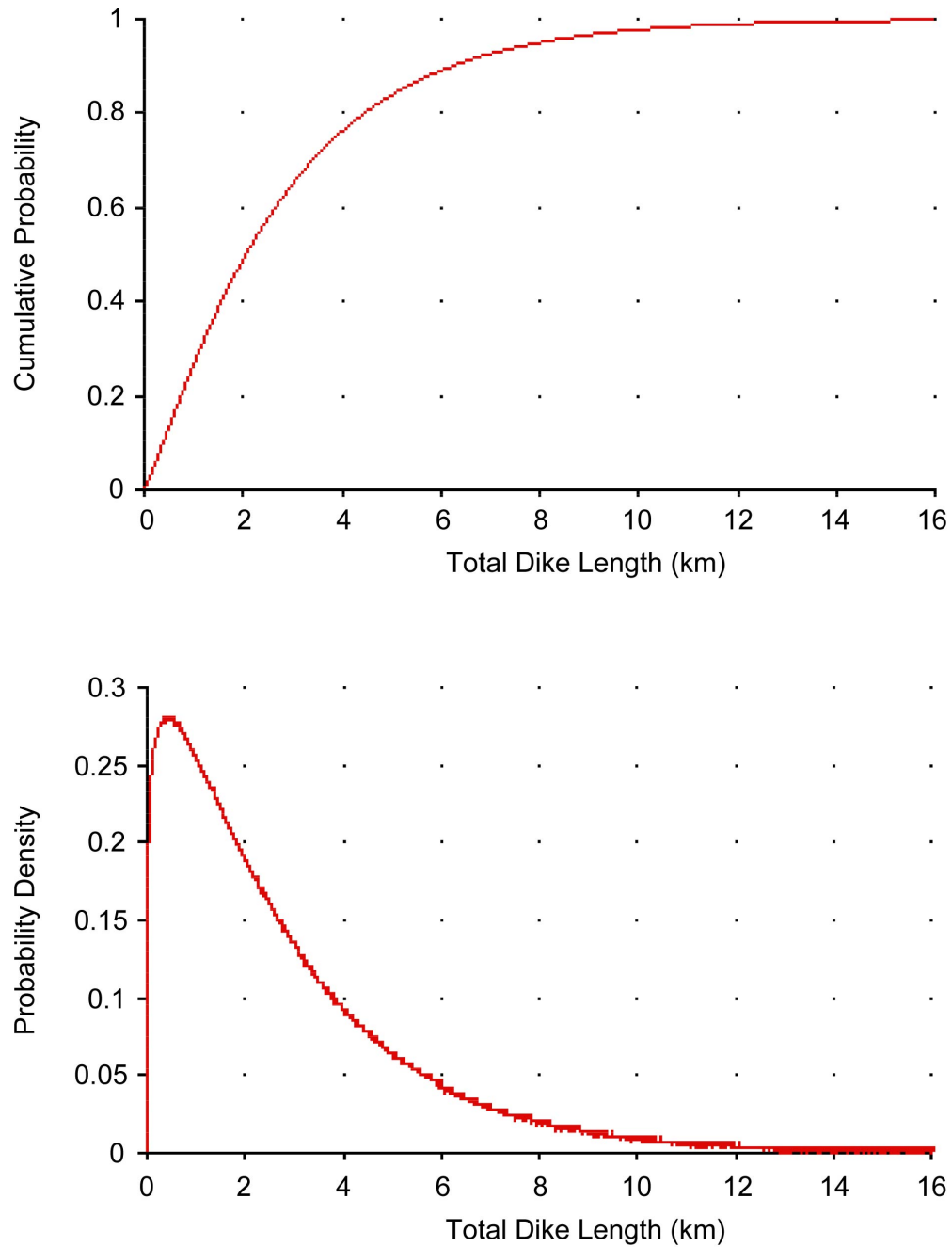


Figure 3.2.6-8. Distribution for the Number of Conduits in an Event as Assessed by Michael Sheridan



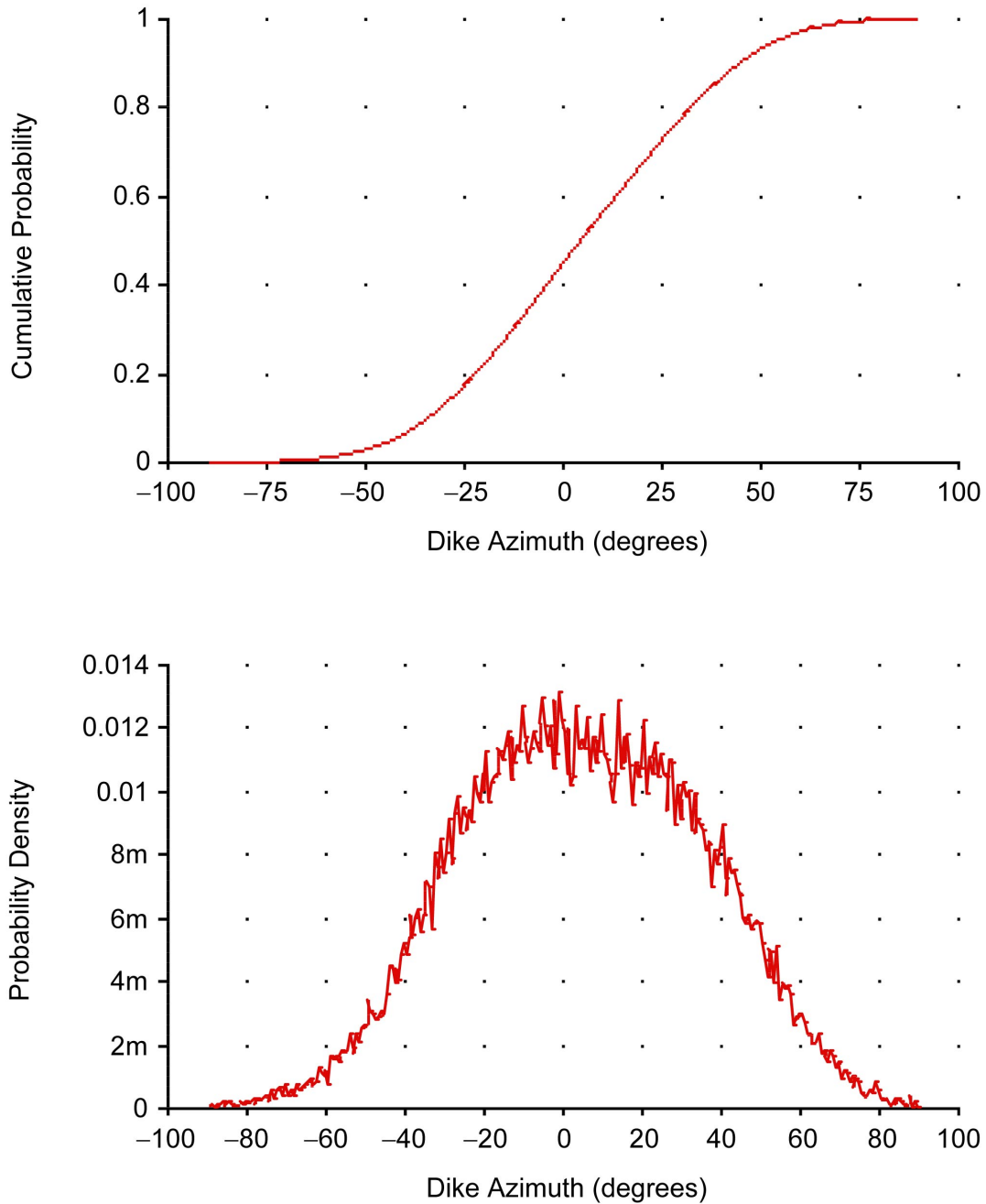
NOTE: Number of dikes is simulated based on the assessments of the number of conduits and the number of dikes as a function of number of conduits. This graph is based on 30,000 simulations. The probability of 0, 5, or 6 dikes in an event is less than 1%.

Figure 3.2.6-9. Distribution of the Number of Dikes in an Event, Based on Assessments of Michael Sheridan



NOTE: Top graph is a cumulative distribution function; bottom graph is a probability density function.

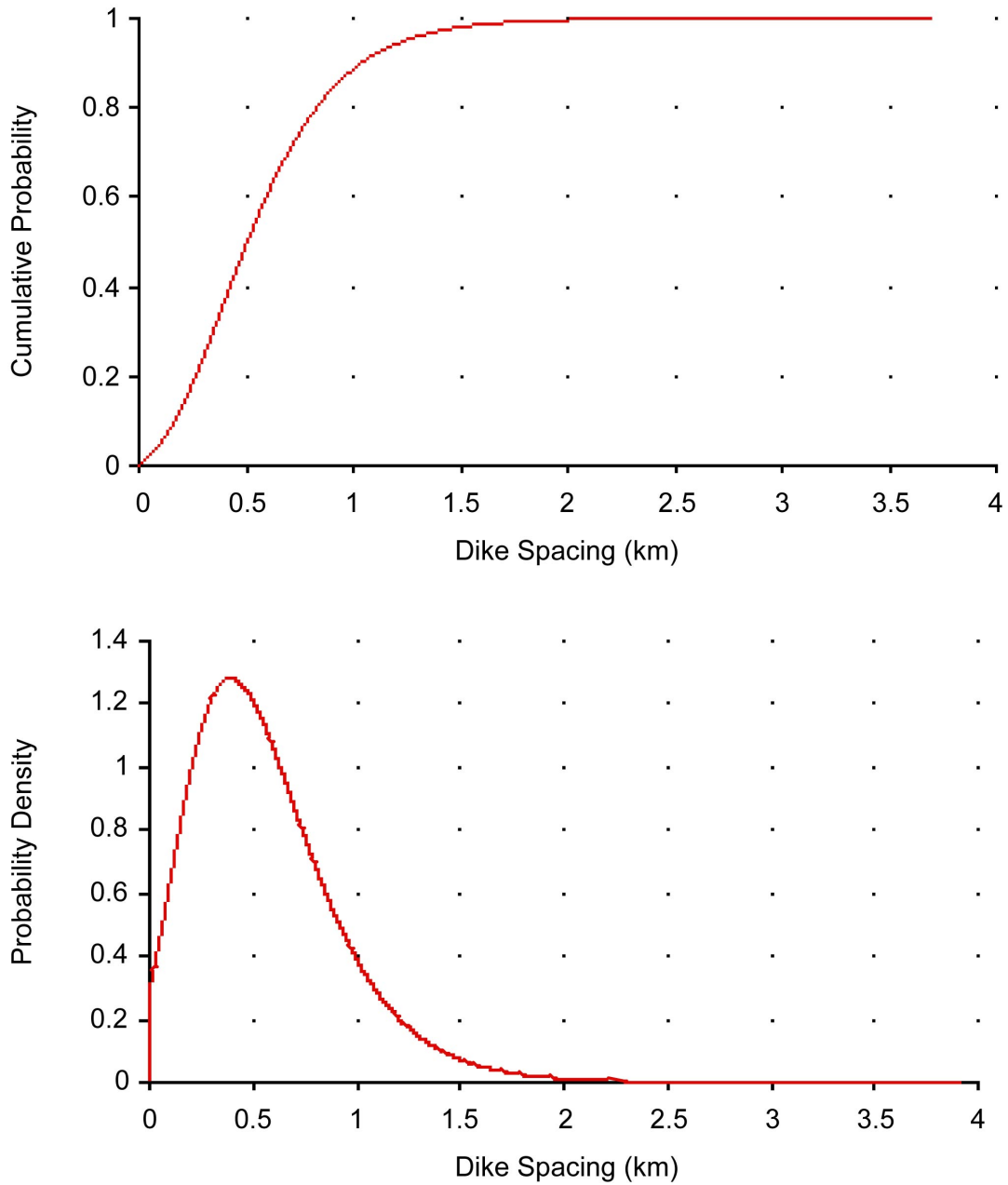
Figure 3.2.6-10. Distribution for the Total Length of Dikes in an Event as Assessed by Michael Sheridan



NOTES: Top graph is a cumulative distribution function; bottom graph is a probability density function. For values less than 0.01 on the y-axis, suffix notation is used ($m = 10^{-3}$, so 8m = 0.008, etc.). Graph shows results of 30,000 iterations from a mixture of three normal distributions. Roughness in the probability density is an artifact of simulation.

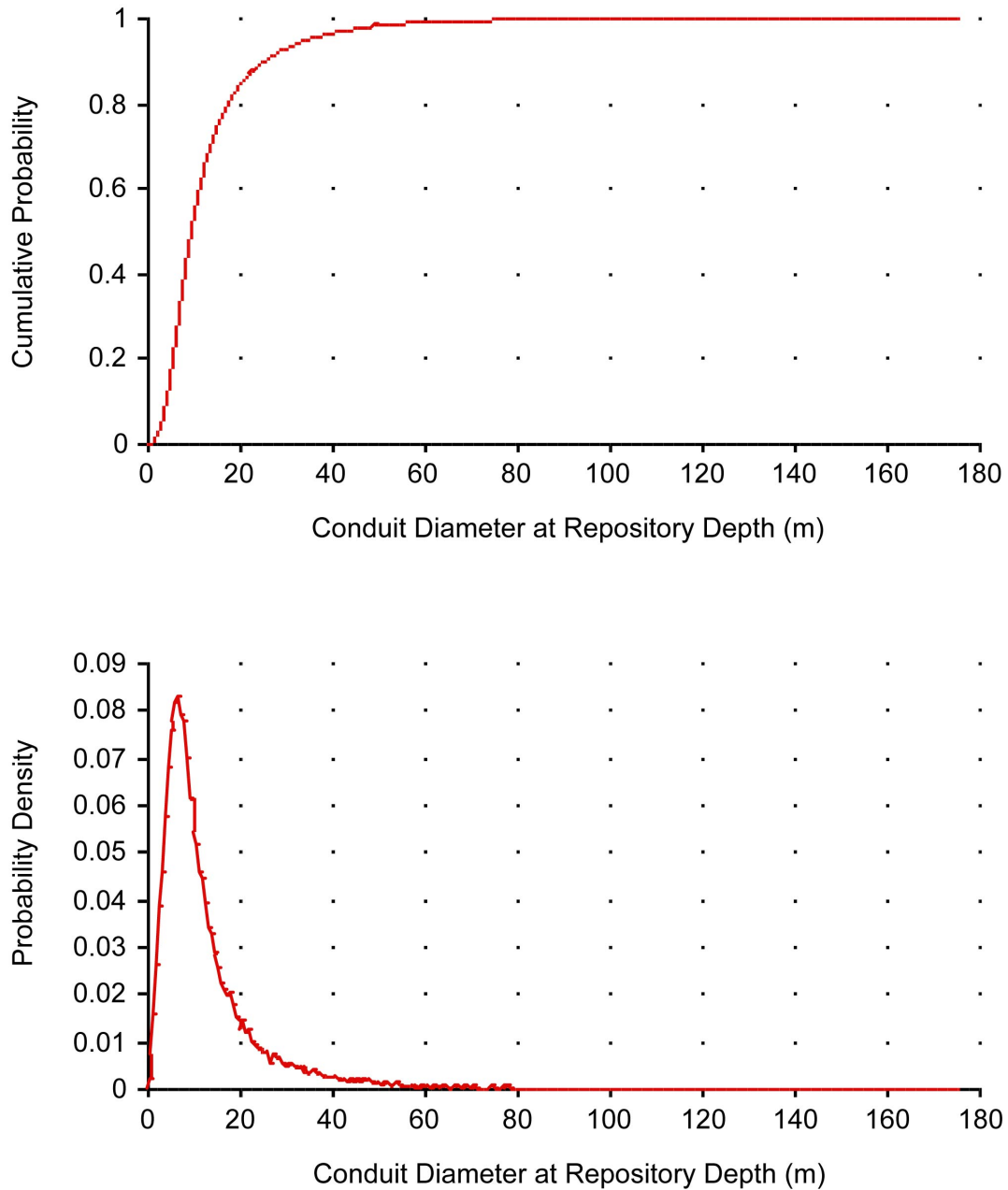
Zero represents North.

Figure 3.2.6-11. Distribution for Dike Azimuth as Assessed by Michael Sheridan



NOTE: Top graph is a cumulative distribution function; bottom graph is a probability density function.

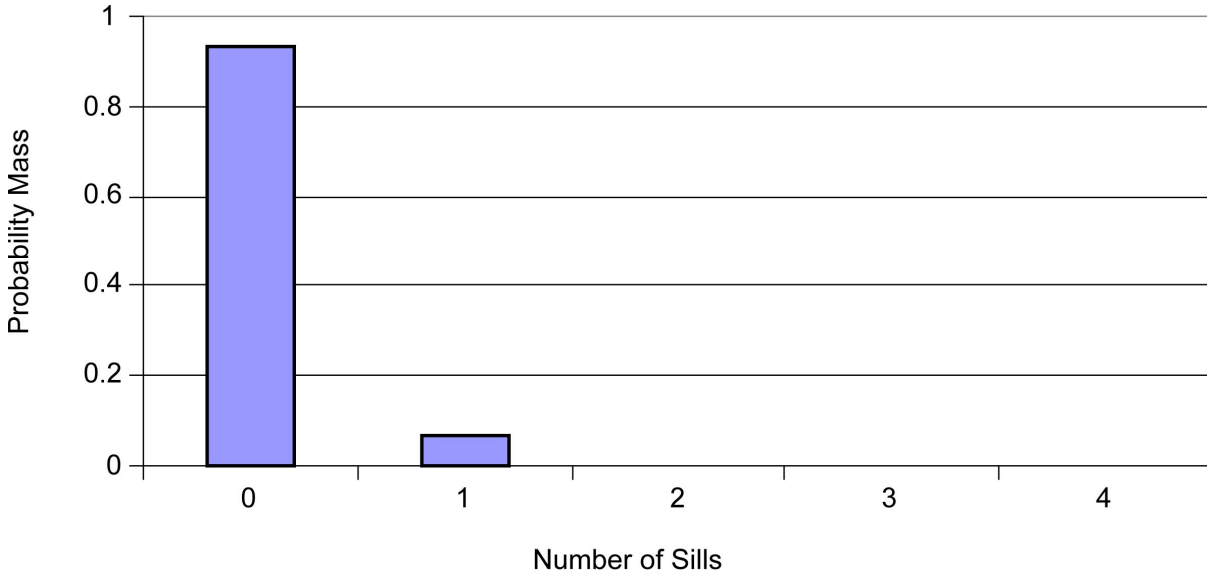
Figure 3.2.6-12. Distribution for the Distance between Dikes in the Direction Perpendicular to Dike Azimuth as Assessed by Michael Sheridan



NOTES: Top graph is a cumulative distribution function; bottom graph is a probability density function.

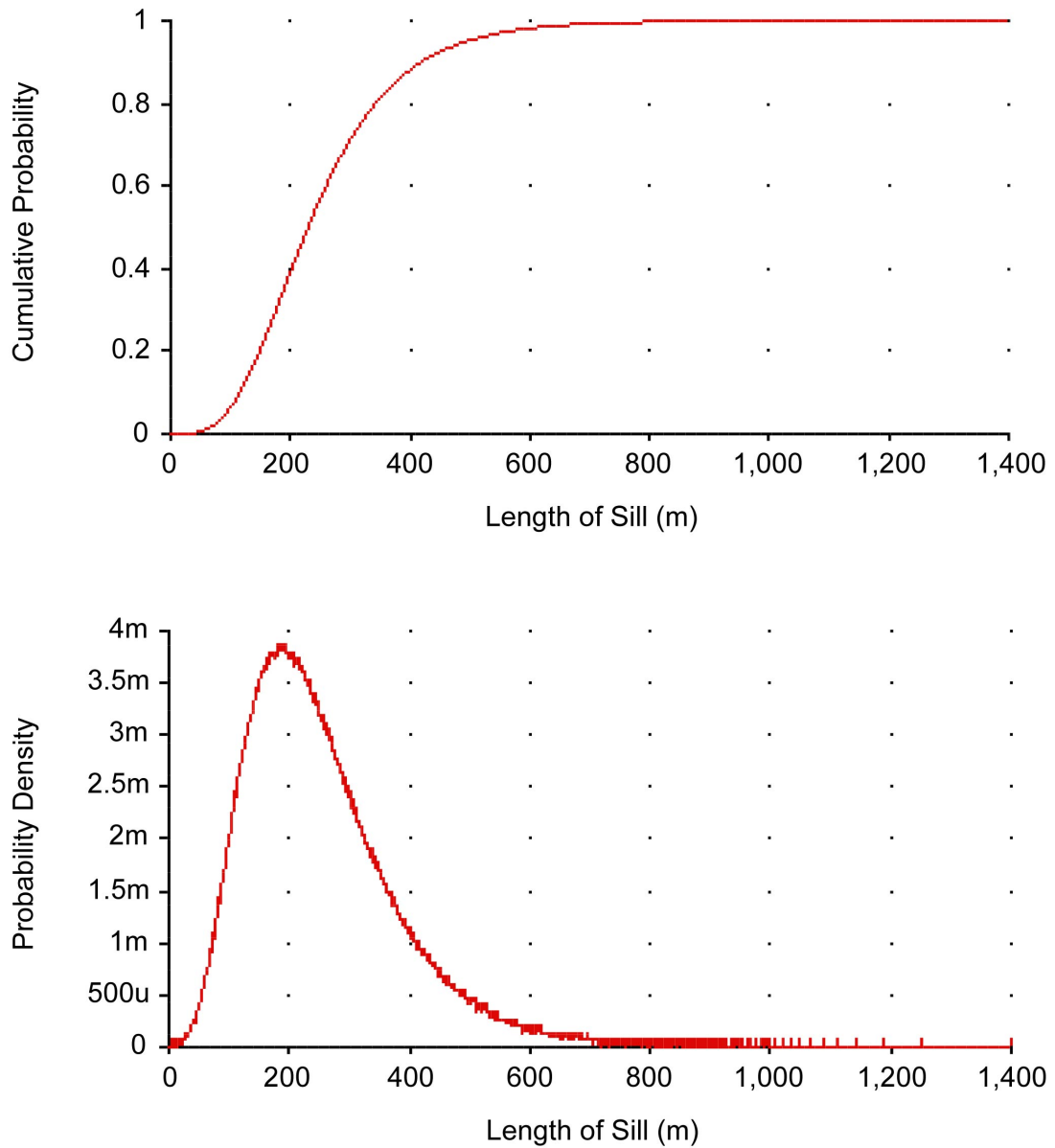
Distributions shown are simulated results with 30,000 iterations based on assessment of dike length and the relationship between dike length and conduit diameter.

Figure 3.2.6-13. Simulated Distribution for Conduit Diameter in an Event Based on Assessments of Michael Sheridan



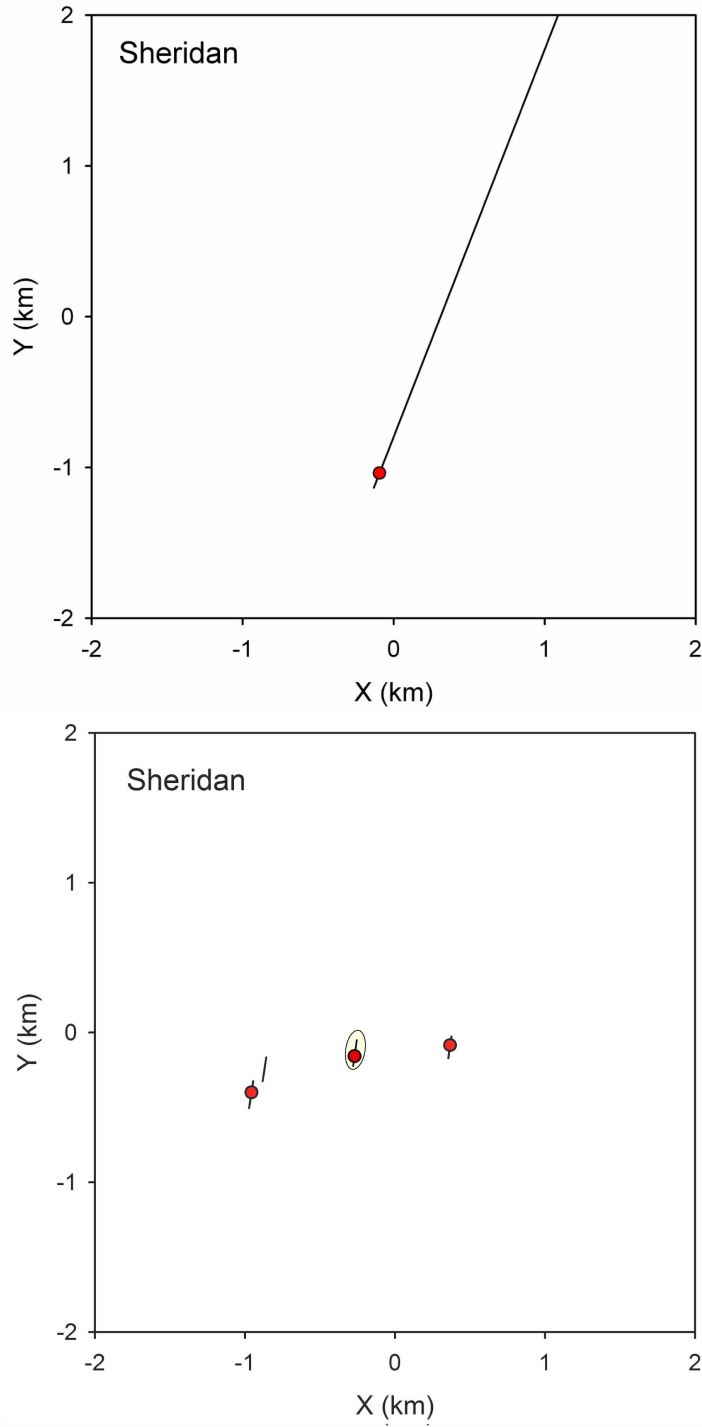
NOTE: Distribution is simulated from the assessment of the number of dikes and the probability of sill formation on a dike. This result is based on 30,000 iterations. Probability of 2 sills is 0.15%; probability of 3 sills is 0.003%.

Figure 3.2.6-14. Simulated Distribution for the Number of Sills in an Event, Based on Assessments of Michael Sheridan



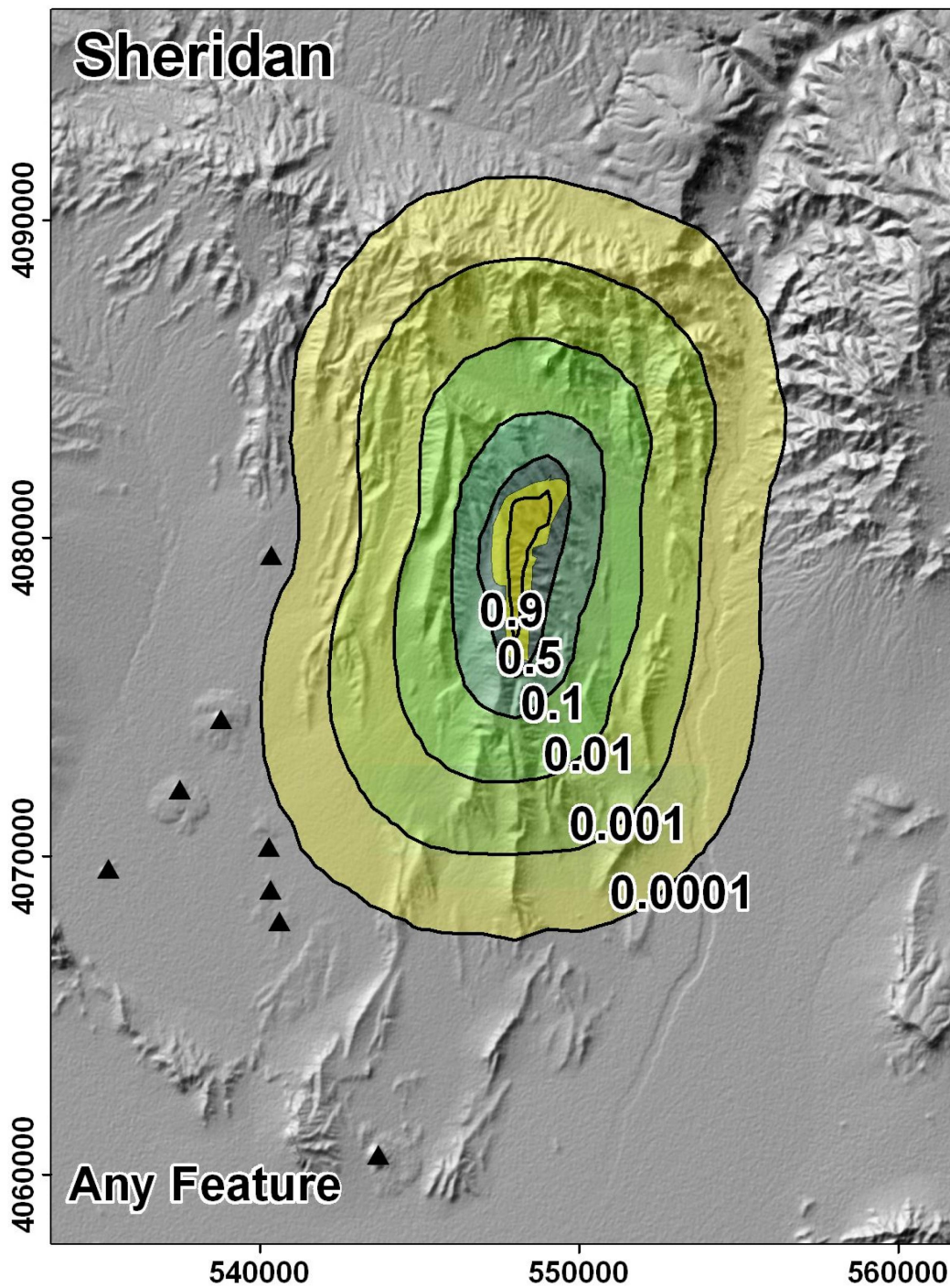
NOTE: Top graph is a cumulative distribution function; bottom graph is a probability density function. For values less than 0.01 on the y-axis, suffix notation is used ($m = 10^{-3}$, so 5m = 0.005; $u = 10^{-6}$, so 500u = .0005)

Figure 3.2.6-15. Simulated Distribution for the Length of a Sill in an Event Based on Assessments of Michael Sheridan



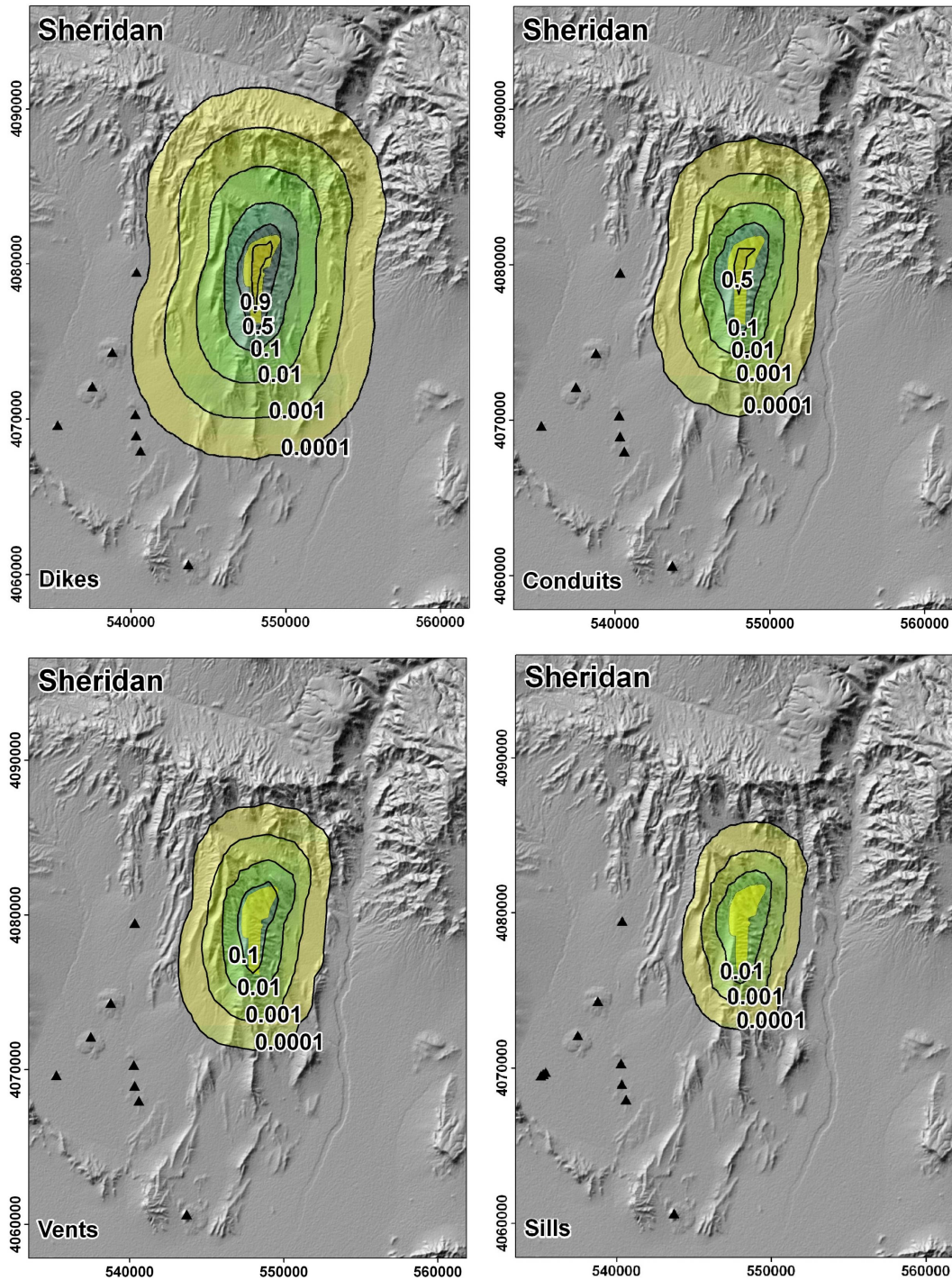
NOTE: Dikes are represented as black lines; their lengths on the figure are the lengths of the simulated dike. Conduits and vents are represented as small red circles; they are not differentiated and their diameters are not represented. Sills, if they exist, are represented by light yellow ovals or polygons.

Figure 3.2.6-16. Examples of Simulated Events from the PVHA-U Model for Michael Sheridan



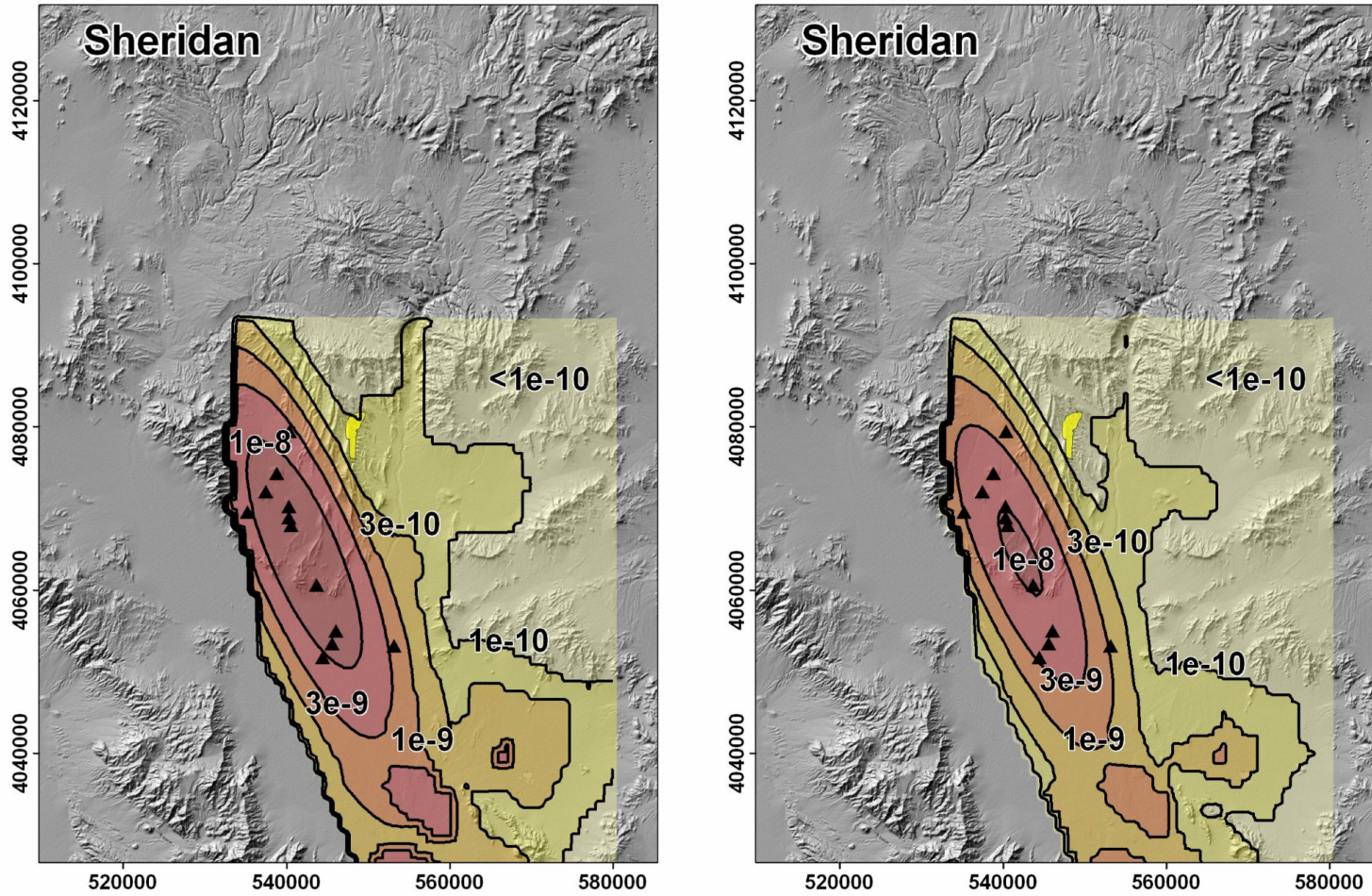
NOTE: Yellow polygon represents the repository footprint. Black triangles represent past events (MS's most likely event set). Map grid ticks are UTM meters; tick intervals are 10 km.

Figure 3.2.6-17. Conditional Probability of Intersection of Any Feature with the Repository Footprint Based on Event Descriptions Developed by Michael Sheridan



NOTE: Yellow polygon represents the repository footprint. Black triangles represent past events (MS's most likely event set). Map grid ticks are UTM meters; tick intervals are 10 km.

Figure 3.2.6-18. Conditional Probability of Intersection of Each Igneous Feature with the Repository Footprint Based on Event Descriptions Developed by Michael Sheridan



NOTE: The left figure is the mean rate density for the 10,000-year assessment, the right figure is the mean rate density for the 1-My assessment. Yellow polygon represents the repository footprint. Black triangles represent past events (MS's most likely event set). Map grid ticks are UTM meters; tick intervals are 20 km.

Figure 3.2.6-19. Mean Rate Density for the 10,000-Year Assessment and the 1-My Assessment Based on the Assessments of Michael Sheridan

Table 3.2.6-1. Data Used to Define Spatial Distribution and Event Rates for Future Volcanic Events for Michael Sheridan's PVHA-U Model

Center	Number of Events	Age (Ma)
Lathrop Wells	1	0.08
Makani Cone	1, 2, or 3 events (weights of 0.05, 0.20, and 0.75)	1.07
Black Cone		1.07
Red Cone		1.07
Little Cones	1 or 2 events (weights of 0.75 and 0.25)	0.78
Pliocene Basalt of Crater Flat	1, 2, or 3 events (weights of 0.05, 0.20, and 0.75)	3.8
Anomaly B	1	3.85
Anomaly F	1, 2, or 3 events (weights of 0.05, 0.20, and 0.75)	3.9
Anomaly G		3.9
Anomaly H		3.9
Anomaly C		4.8
Anomaly D	0, 1, or 2 events (weights of 0.8, 0.1, and 0.1)	4.8

Table 3.2.6-2. Frequency of Number of Dikes and Conduits or Vents in Simulated Events Based on the Assessments of Michael Sheridan

		Number of Conduits and Vents in an Event		
		1	2	3
Number of Dikes in an Event	0	0.8%	0.0%	0.0%
	1	65.2%	3.9%	0.2%
	2	9.0%	10.1%	0.7%
	3	0.0%	4.0%	2.0%
	4	0.0%	2.0%	1.0%
	5	0.0%	0.0%	0.5%
	6	0.0%	0.0%	0.5%

3.2.7 Frank Spera

Spatial and Temporal Models

Figure 3.2.7-1 presents the logic tree describing the basic structure of the spatial and temporal models developed by Frank Spera (FS) for PVHA-U. FS specified several alternative characterizations of past events, and his spatial and temporal models are dependent on those alternative event sets. Table 3.2.7-1 lists the past events in the region of interest judged relevant by FS to his spatial and temporal models. Figure 3.2.7-2 illustrates the region of interest that FS identified as being relevant to his model, and past events in the region. The table includes alternative interpretations of some events, along with the relative probability FS assigned to each interpretation. In combination, 10 unique interpretations of the number of past events in the region of interest are identified. These are represented schematically in the first node of the logic tree; separate spatial and temporal models are fitted to each of these alternative event sets. The probability for each event set is calculated from the probabilities given to different interpretations as summarized in Table 3.2.7-1.

Two alternative approaches to modeling the spatial distribution of future events were specified: (1) spatial smoothing using kernel density estimation and (2) models based on the interpretation of three different sets of geologic data. These are represented by the second and third nodes in the logic tree; each of the three geologic data sets is combined with a kernel density estimate with probability of 75% on the kernel density and 25% on the geology-derived estimate, and then the three combined models are assigned probabilities as shown in the logic tree.

For the kernel density estimate of conditional spatial intensity, FS specified two alternative parameterizations of the kernel density estimator: a Gaussian kernel function with a bandwidth of either 5 km (probability of 75%) or 10 km (probability of 25%). Past events are weighted by the inverse of the age of the event and the volume of the events, equally weighted. For the 1-My assessment, the ages of past events used for weighting are adjusted to reflect the age of the events at 1 My.

For the second modeling approach where spatial density is estimated from geologic data, three relevant data sets were identified: lithostatic pressure and two interpretations of seismic velocity/tomography. These datasets are assigned probabilities of 50% for lithostatic pressure and 25% each for the two interpretations of the tomography data.

FS provided an assessment of the likely values of lithostatic pressure at the location of a hypothetical future event in his region of interest, as illustrated in Figure 3.2.7-3. This assessment was combined with the lithostatic pressure at each point in the region of interest through the Bayesian updating approach described in Section 3.1 and Appendix E to create a spatial density estimate based on lithostatic pressure.

Similarly, FS provided an assessment of the likely seismic velocity at the location of a hypothetical future event in the region of interest: 25% chance of velocity being “high,” 35% of it being “intermediate,” and 40% of it being “low.” High, intermediate, and low velocities were defined by FS based on maps of seismic velocity across his region of interest, as described in his Elicitation Summary in Appendix D. His assessment was combined with the seismic velocity at

each point in the region of interest to create a spatial density estimate based on tomography. Two interpretations of tomography were provided, and FS used both.

Each spatial density estimate based on geology data is combined with the conditional spatial density estimate from the kernel smoothing approach with probabilities as specified in the logic tree.

For each spatial model, additional uncertainty exists in the spatial density resulting from fitting the kernel density estimators to the relatively small datasets. As described in Section 3.1 and Appendix E, uncertainty in the spatial density is modeled through a simulation approach known as bootstrapping. This is represented conceptually by the “Uncertainty in Spatial Density” node in the logic tree of Figure 3.2.7-1; in the actual bootstrapping analyses, more than three representations are used.

A time-volume approach is used to estimate the rate of future events. The time-volume model requires two estimates: the rate of magma generation (the rate of change of cumulative volume), and the volume per event. Both estimates may be functions of time. FS specified two alternative models for cumulative volume over time: (1) a linear function of time fit to Quaternary events (probability 25%), and (2) a linear function of time fit to post-3 Ma events (probability 75%). Volumes are cumulated over all events listed in Table 3.2.7-1.

Fitting the model to the cumulated estimated volumes of Quaternary events with linear regression yields the following:

$$CV(t) = 5.2 + 0.116 \times t$$

Fitting to post-3 Ma events yields:

$$CV(t) = 5.34 + 0.08 \times t$$

where t is the time at which cumulative volume (CV) is to be predicted and is given in millions of years from today. For example, $CV(-1)$ is the estimated cumulative volume 1 Ma before the present (and equals 5.084 km^3), and $CV(1)$ is the estimated cumulative volume 1 My from the present. The 90% confidence interval for the slope of the regression line is used to represent uncertainty in the cumulative volume estimate.

FS specified two alternative approaches for estimating the average volume per event for future events: (1) his direct assessment of the volume per event, as described below (probability 50%), and (2) an estimate fit to the mean and variance of the volume of Quaternary events (probability 50%).

The volume per event is modeled as a mixture of exponential distributions, as described below. The mean volume per event from this assessment is 0.159 km^3 . Uncertainty in the volume per event is modeled using the 5th, 50th, and 95th percentiles of the distribution on volume. The mean volume per event based on Quaternary events for the most likely event set is 0.031 km^3 . The mean differs for different event sets. Uncertainty in the volume per event under this approach is modeled using the 5th, 50th, and 95th percentiles of a lognormal distribution with a

mean and standard deviation matching the mean and standard deviation of the relevant Quaternary events.

Mean rates under the four basic time-volume rate models for the most likely event set are summarized in Table 3.2.7-2. Figure 3.2.7-4 illustrates uncertainty in the estimated rate for each of the temporal models based on one event set. In all cases, the bar represents the 5th to 95th percentiles of the distribution on rate for models based on the most likely event set from Table 3.2.7-1.

Mean Rate Density and Mean Recurrence Rate

Figure 3.2.7-5 illustrates the mean rate density for igneous events calculated from FS's spatial and temporal models for the 10,000-year assessment. The effect of both inverse-age and volume weighting of events is evident in the location and shape of the $3e-9$ contour. The contour labeled $3e-10$ on the northeast side of the region of interest shows the effect of incorporating geology data into the spatial model.

A mean recurrence rate for events in the region of interest can be calculated by summing the mean rate density at each grid point. Based on the mean rate density shown in Figure 3.2.7-5, the mean recurrence rate for events in this region is $5.1e-6$ events per year, giving recurrence intervals between 10,000 and 587,000 years (5th to 95th percentile of the distribution on recurrence interval), with a mean recurrence interval of about 196,000 years for events in the region illustrated.

Event Simulation Model

Figure 3.2.7-6 illustrates the key features of an event simulator for FS's PVHA-U model. In this model an *event* is characterized by a combination of dikes, conduits, and sills; the number, locations and dimensions of each of these features define the event.

Many event characteristics are defined as functions of the eruptive volume of magma for an event. Figure 3.2.7-7 illustrates the distribution used to represent the volume of an event. The total length of dikes in an event was defined by an assessed distribution and correlation with volume; the resulting distribution on total dike length is shown in Figure 3.2.7-8. The number of dikes in an event was defined as a function of event volume; Figure 3.2.7-9 illustrates the number of dikes in simulated events based on the assessments provided by FS of volume and the number of dikes as a function of volume. When multiple dikes exist in the event, the total length of dikes is divided among the dikes such that individual dikes have approximately equal length. Individual dikes are located randomly in an elongate ellipse with length equal to the total dike length and having an aspect ratio between 4:1 and 12:1. Dikes must be separated by at least 50 m. The long axis of the ellipse is oriented in the same direction as dike azimuth, which is illustrated in Figure 3.2.7-10.

Any future event is defined to have at least one conduit. The number of conduits in an event was defined as a function of the volume. Figure 3.2.7-11 shows the number of conduits in simulated events based on the assessments provided by FS of volume and the number of conduits as a function of volume. For events with one conduit, that conduit is located on the longest single dike in the event following the distribution shown in Figure 3.2.7-12. For events with more than

one conduit, additional conduits are located on the longest remaining dike segment in the event. Conduits must be separated by a distance equal to at least three conduit diameters. Conduit diameter is defined as a function of magma volume and the number of conduits and sills in an event. Figure 3.2.7-13 illustrates the distribution of conduit diameters for simulated events based on those assessments. The probability that any conduit in an event would be a column-producing conduit is 0.8.

A sill can occur in an event; based on FS's assessment of the probability of sill formation, approximately 5% of events include a sill. Sills are assumed to be roughly tabular, with length defined as a function of event volume and sill thickness. Figure 3.2.7-14 illustrates the distribution of sill length for simulated events based on those assessments.

Figure 3.2.7-15 illustrates two examples of the simulated events, and Table 3.2.7-3 describes the number of dikes and the number of conduits and vents (combined) in an event, and how frequently such events occur in the event simulation. The table indicates, for example, that the most common type of event consists of one dike with one conduit or vent – about 54% of simulated events are of this type (as shown by the bolded number in the table). The top half of Figure 3.2.7-15 illustrates an example of a one-dike, one-conduit event. Events may contain as many as 8 dikes and 5 conduits or vents, although such events occur much less frequently. Note that events may also include sills, which are not represented in this table.

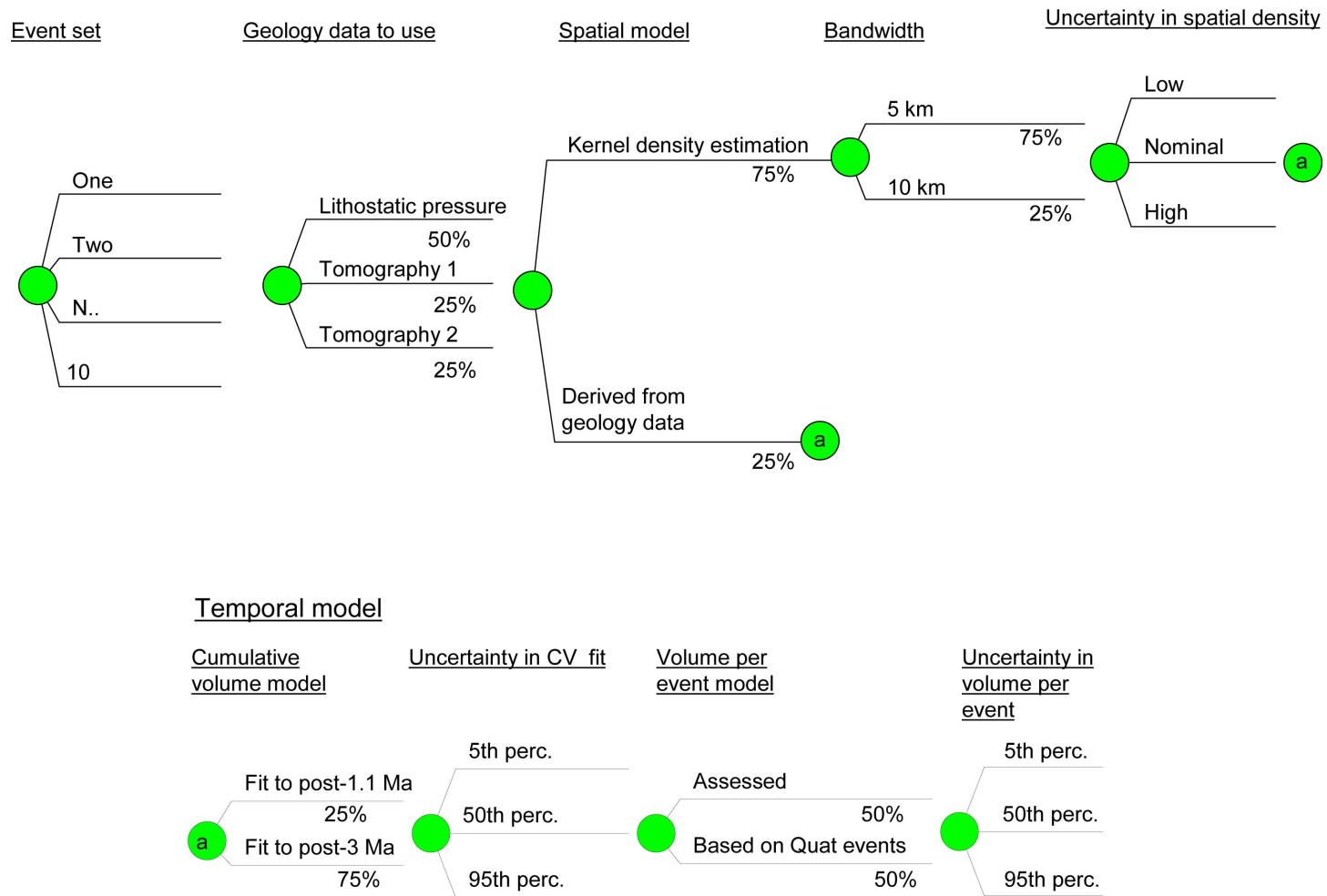
Conditional Probability of Intersection

Figure 3.2.7-16 illustrates the conditional probability of the intersection of any igneous feature with the repository footprint based on FS's event descriptions. The north-south orientation of the contours reflects the preferred direction for dike azimuth.

As described above, FS's events include at least one dike, and may include column-producing conduit(s), vents, and sills. Figure 3.2.7-17 shows the conditional probability of intersection for each of these types of igneous features. These maps reflect the same spatial distribution of features as the intersection of any feature, indicating there is no particular clustering of features within an event. The conditional probability of intersection for conduits and vents is lower than for dikes for an event at any given location due to their smaller size and their distribution along a dike. Sills occur rarely, as reflected in the low probability contours.

Differences Between the 10,000-year and 1-My Assessments

No differences exist in the structure of FS's spatial model, temporal model, or events assessments based on the different assessment periods. Because the spatial model includes weighting of past events by age, the rate density will be different when evaluated at different times. Figure 3.2.7-18 shows the mean rate density for the 10,000-year assessment, which uses the current ages for all past events, and the mean rate density for the 1-My assessment, which uses events assumed to be 1 My older than the current estimated ages. The contours on this figure show the decreased influence of Lathrop Wells (the youngest event) on mean rate density when it (and all other events) is assumed to be 1 My older than it is today.



NOTES: All probabilities shown on the branches are those assigned by the expert. Uncertainty in spatial density and uncertainty in the parameters for the time-volume model (the uncertainty in cumulative volume (CV) fit and the volume per event) are modeled based on the approaches described in Section 3.1.5, and the probabilities for those branches are defined by the modeling approach.

Circles labeled "a" in the upper part of the tree mean that the entire lower tree (the temporal model) is reproduced at those points.

Figure 3.2.7-1. Logic Tree Representing the Spatial and Temporal Components of the PVHA-U Model Specified by Frank Spera

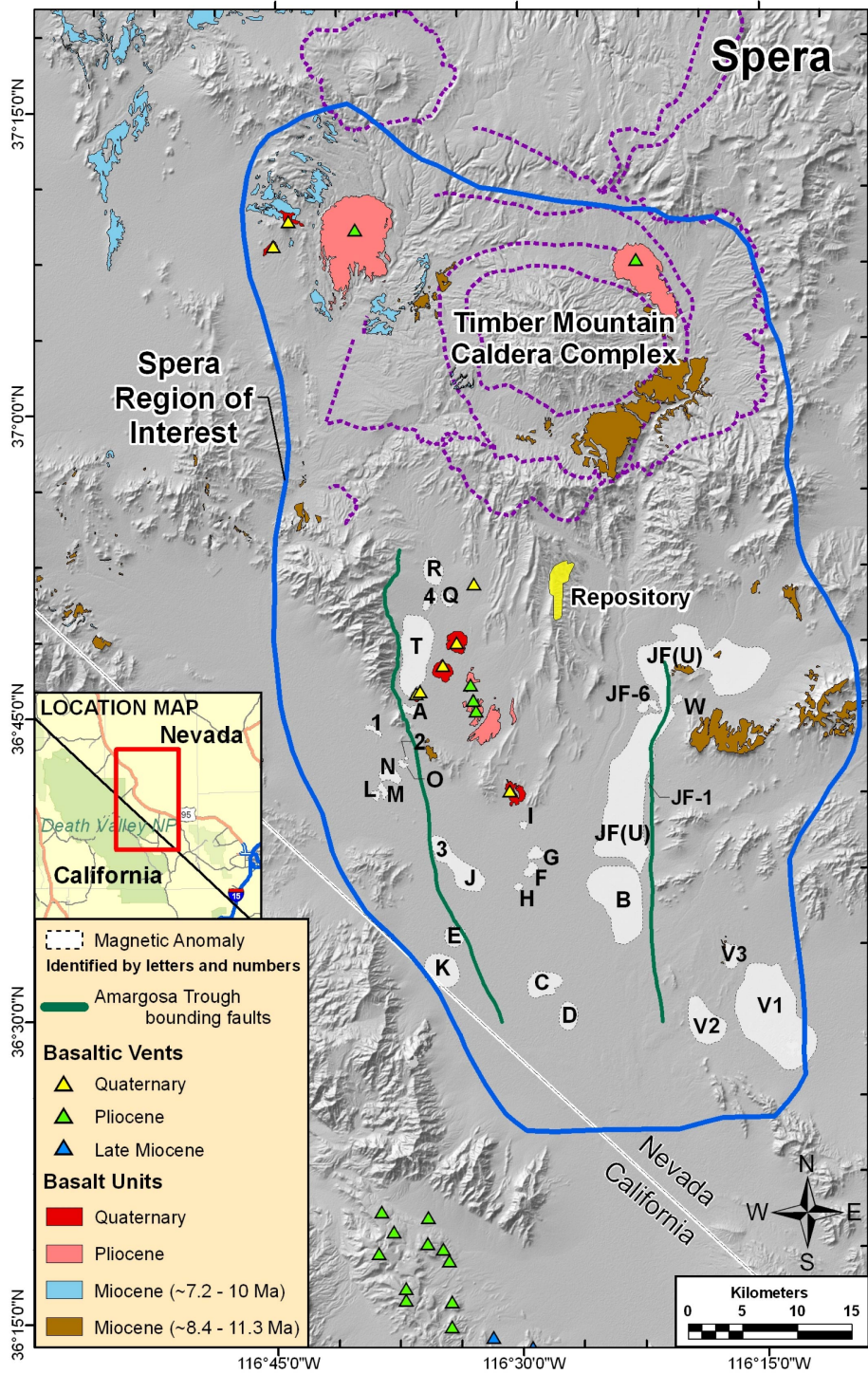
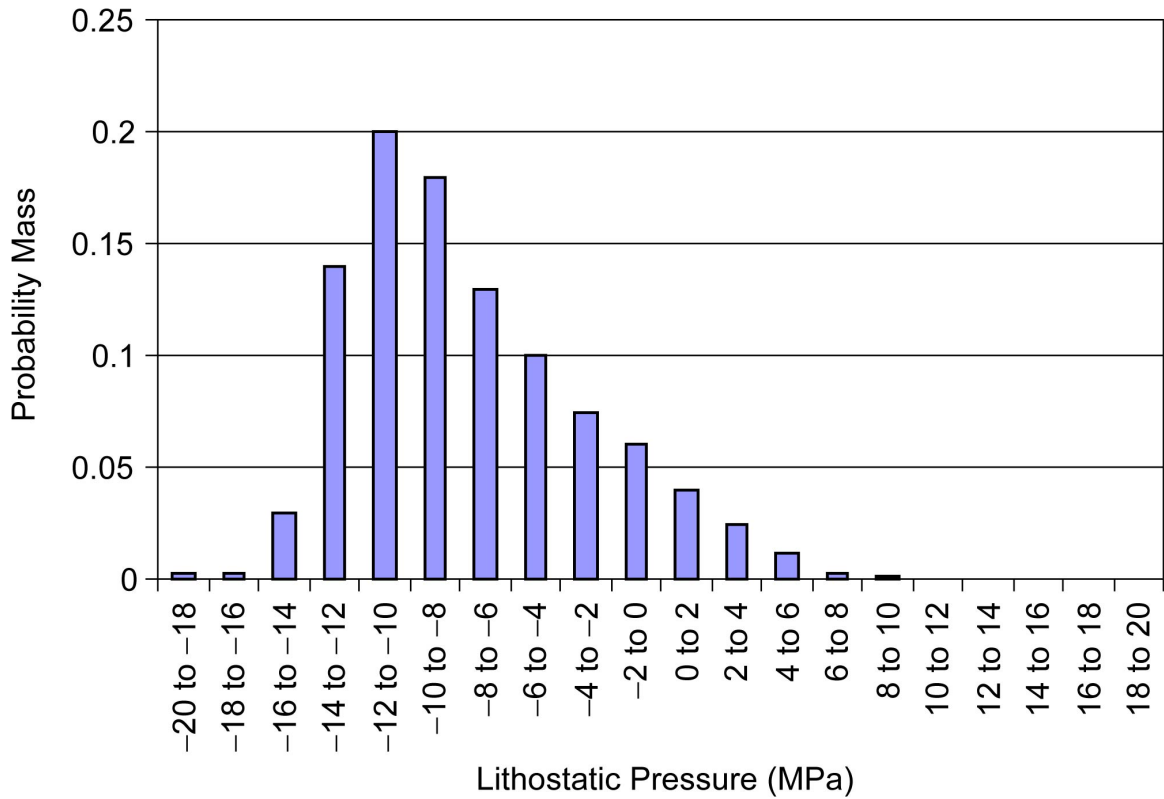
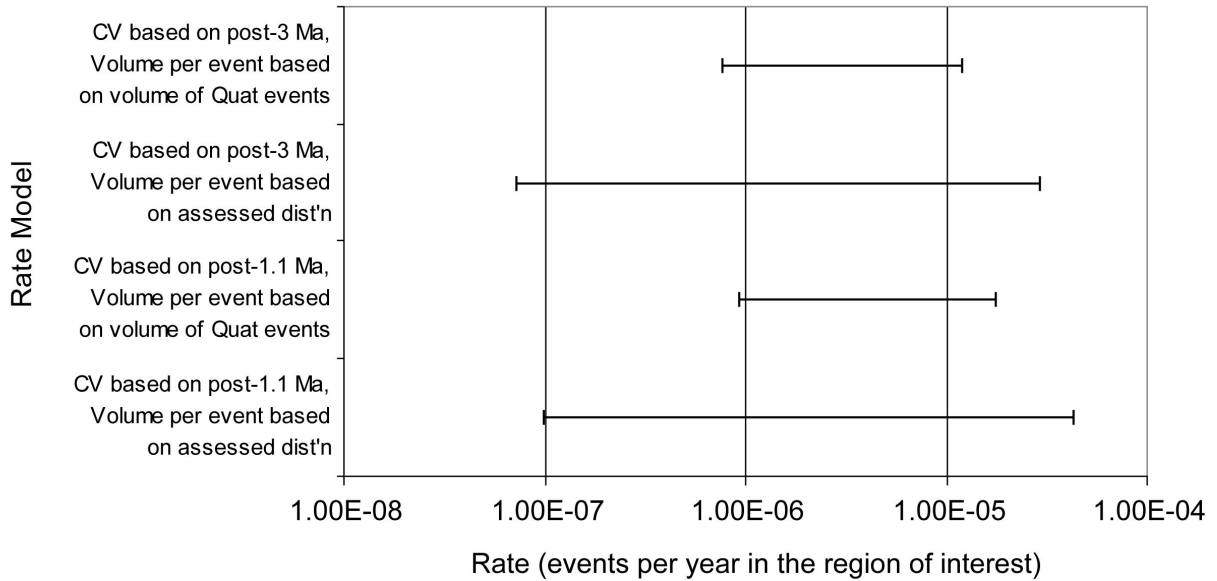


Figure 3.2.7-2. Region of Interest as Specified by Frank Spera



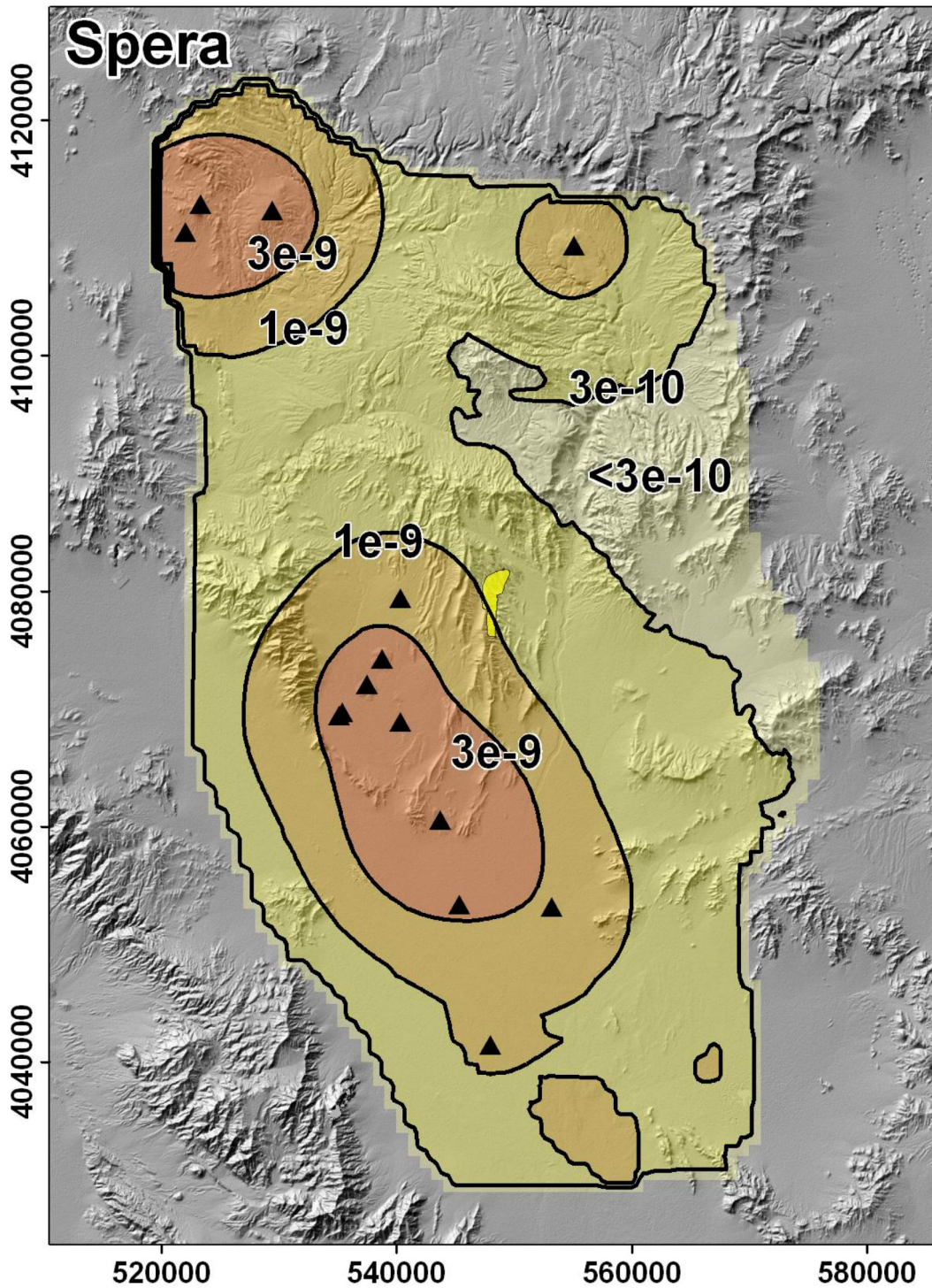
NOTE: Lithostatic pressure in the YMR is one of the data sets provided to the panel and listed in Appendix B. Lithostatic pressure values were calculated from free-air gravity and reflect gravity (mass) excesses (represented as positive lithostatic pressure values) and deficiencies (represented as negative values) relative to a theoretical gravity value at sea level.

Figure 3.2.7-3. Assessment of Lithostatic Pressure at the Location of a Hypothetical Future Event in the Region of Interest, as Specified by Frank Spera



NOTE: Bars represent the 5th to 95th percentile of the uncertainty in the rate for each alternative rate model for estimates based on the most likely event set identified in Table 3.2.7-1.
 CV = cumulative volume; Quat = Quaternary; dist'n = distribution.

Figure 3.2.7-4. Example of Uncertainty in Estimated Rate Based on a Single Interpretation of Past Events for Alternative Temporal Models Specified by Frank Spera

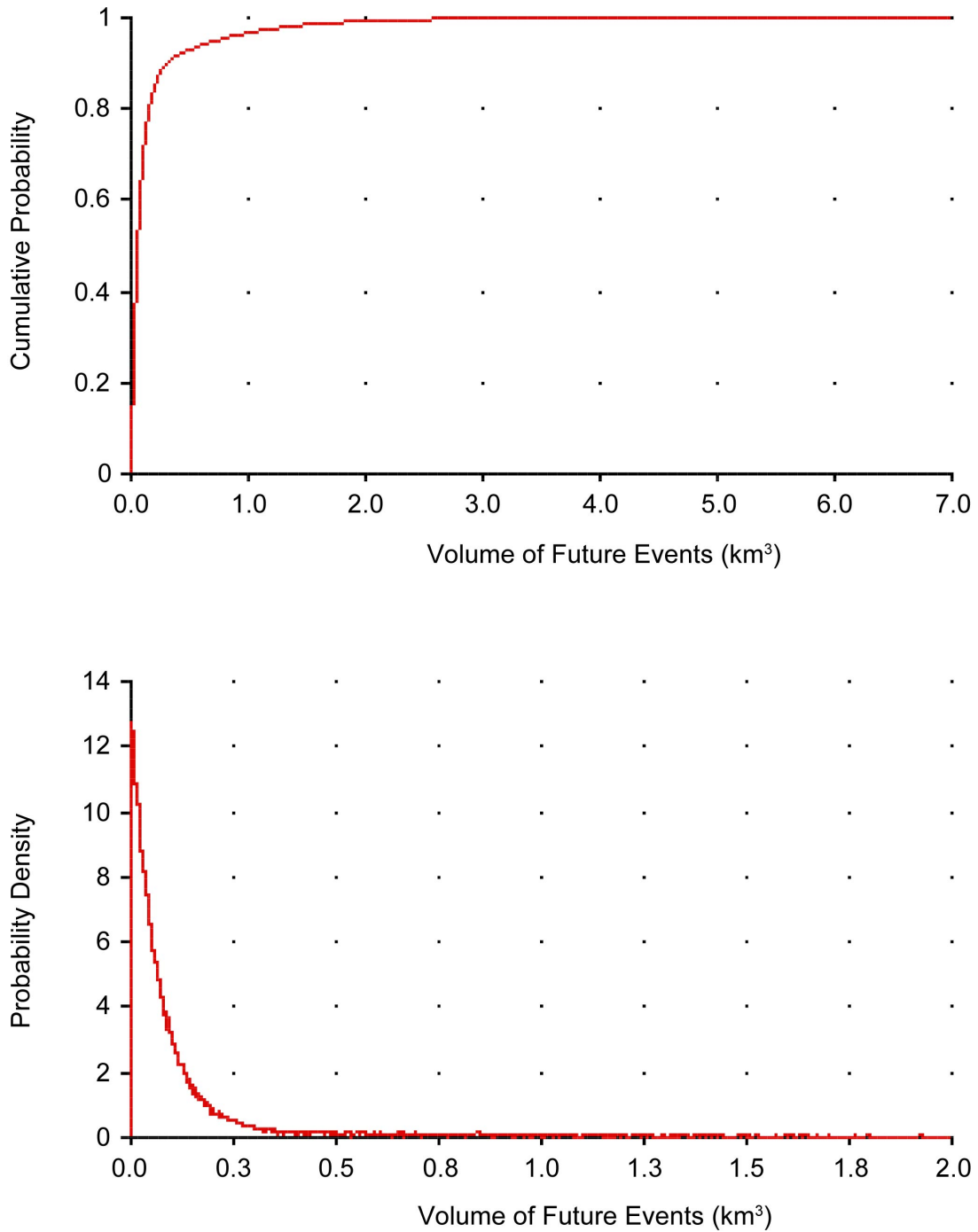


NOTE: Contours show the mean rate density in events per year per km². Yellow polygon represents the repository footprint; black triangles represent past events (FS's most likely event set). Map grid ticks are UTM meters; tick intervals are 20 km.

Figure 3.2.7-5. Mean Rate Density for the 10,000-Year Assessment Based on Models Specified by Frank Spera



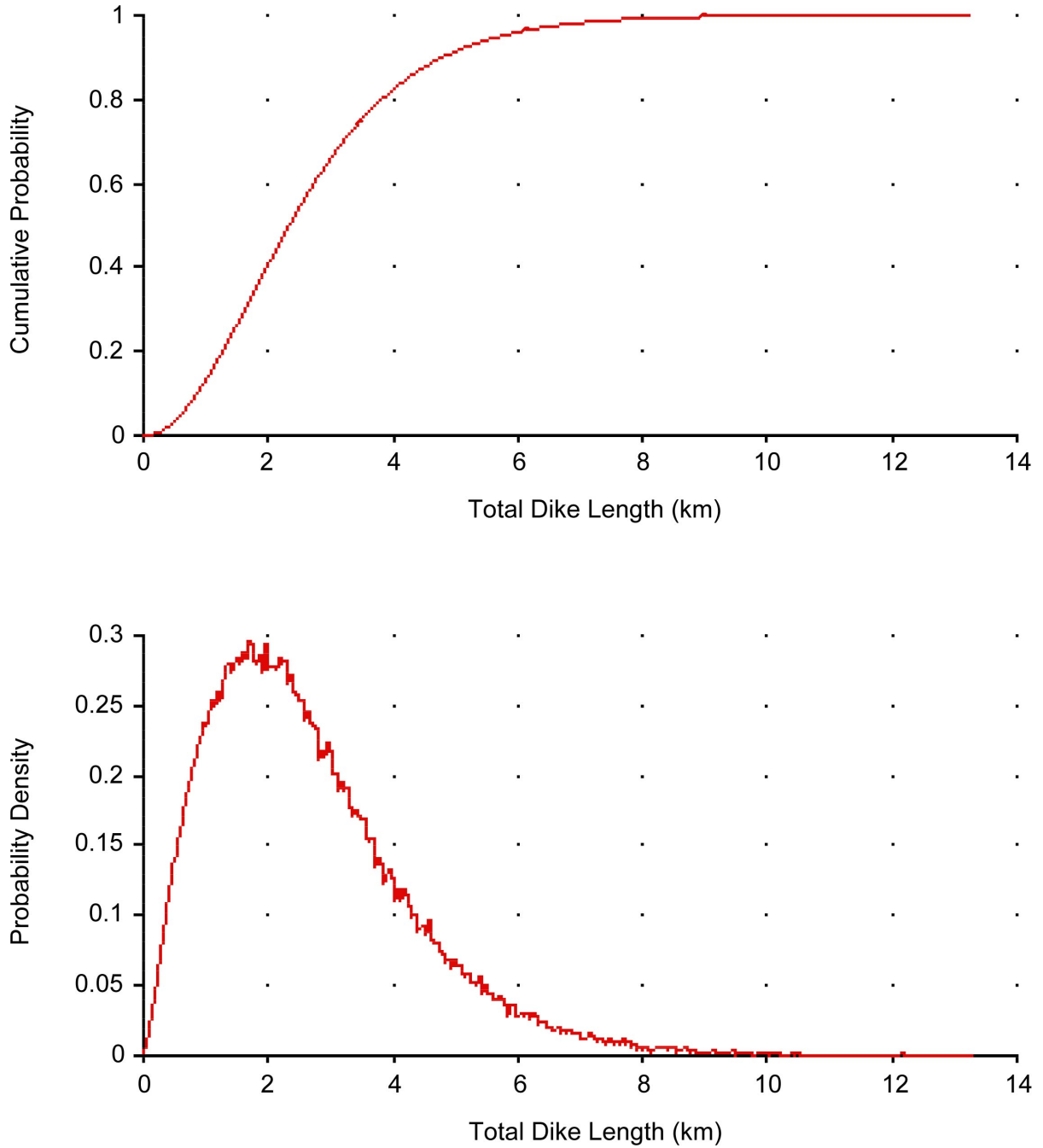
Figure 3.2.7-6. Components of an Event Simulator Based on the Characteristics of Future Events Described by Frank Spera



NOTES: Top graph is a cumulative distribution function; bottom graph is a probability density function. Note the change in scale.

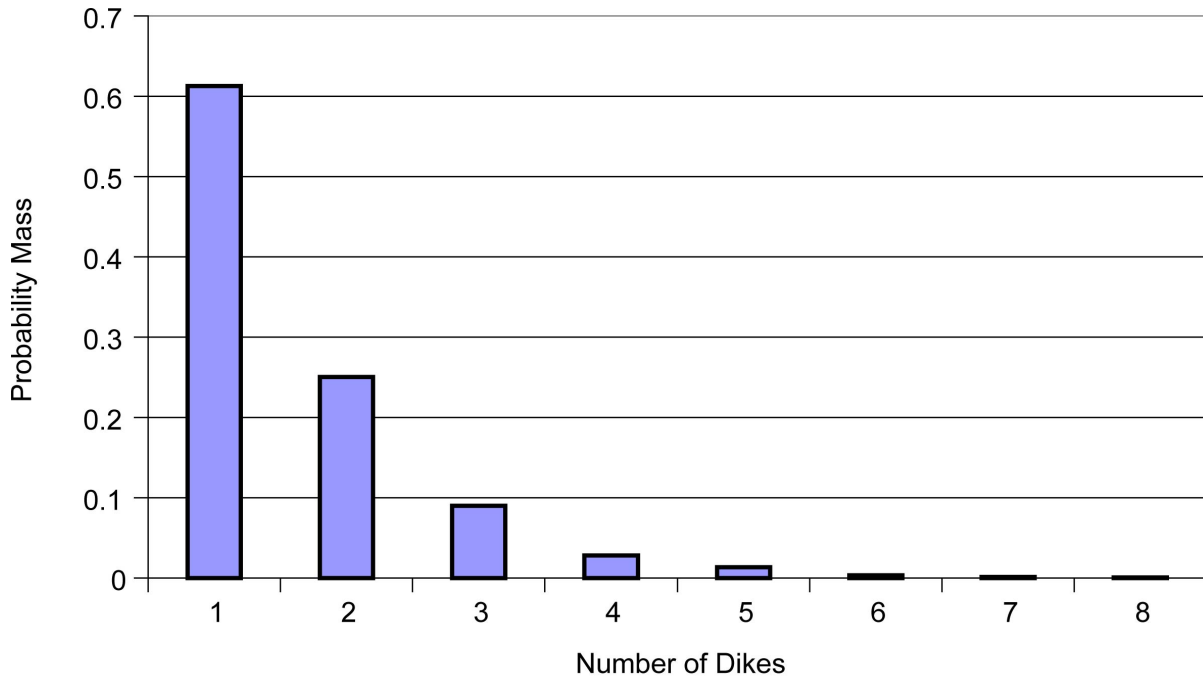
Graphs show results of simulation from a mixture of two exponential distributions.

Figure 3.2.7-7. Distribution for the Eruptive Volume of an Event as Assessed by Frank Spera



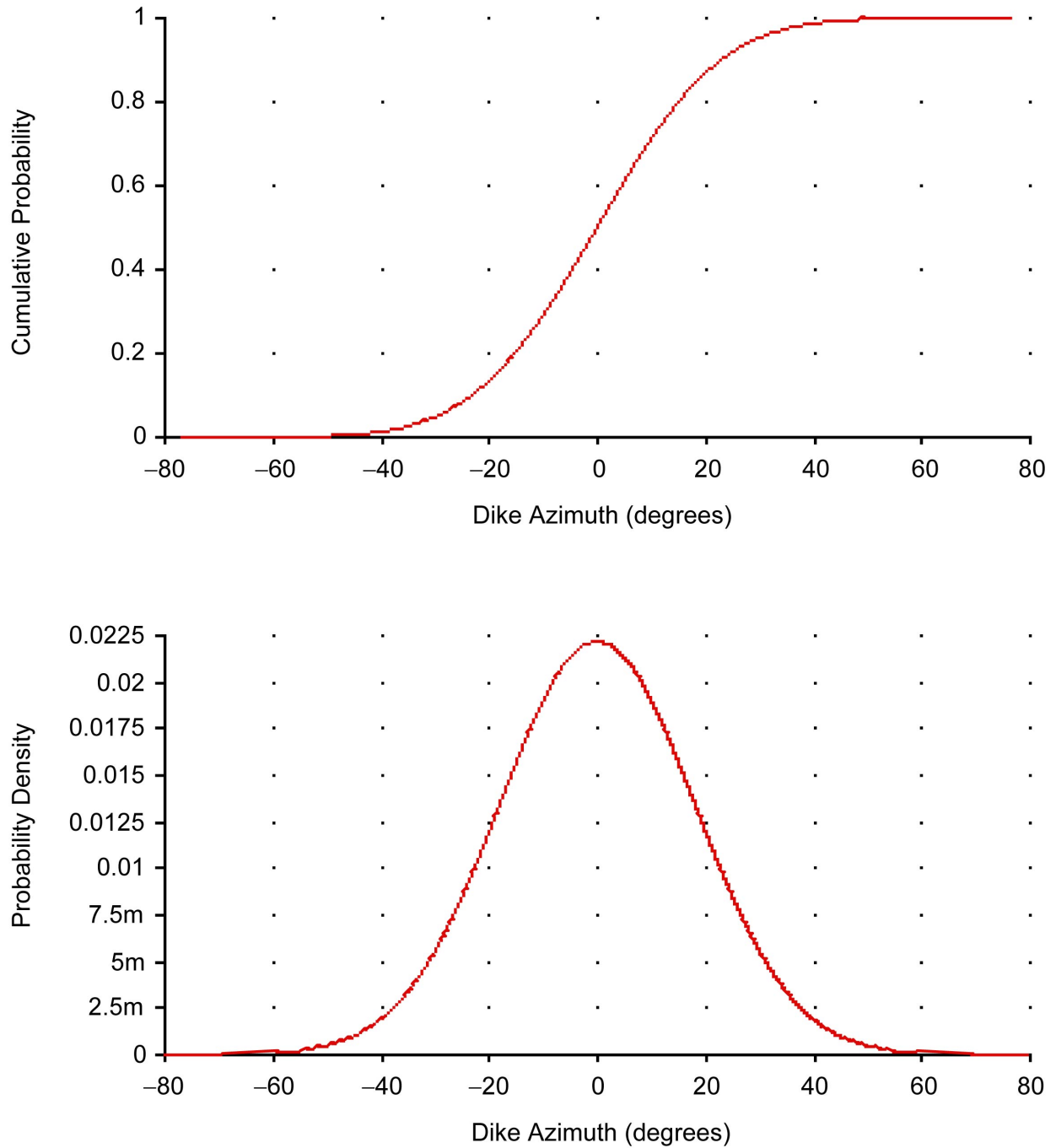
NOTES: Top graph is a cumulative distribution function; bottom graph is a probability density function.
Graphs show results of simulation from a mixture of lognormal distributions, correlated with volume per event.

Figure 3.2.7-8. Distribution for the Total Length of Dikes in an Event Based on Assessments of by Frank Spera



NOTE: Number of dikes is simulated based on the assessments of the volume of an event and the number of dikes as a function of event volume. This graph is based on 30,000 simulations. The probability of 6, 7, or 8 dikes in an event is less than 1%.

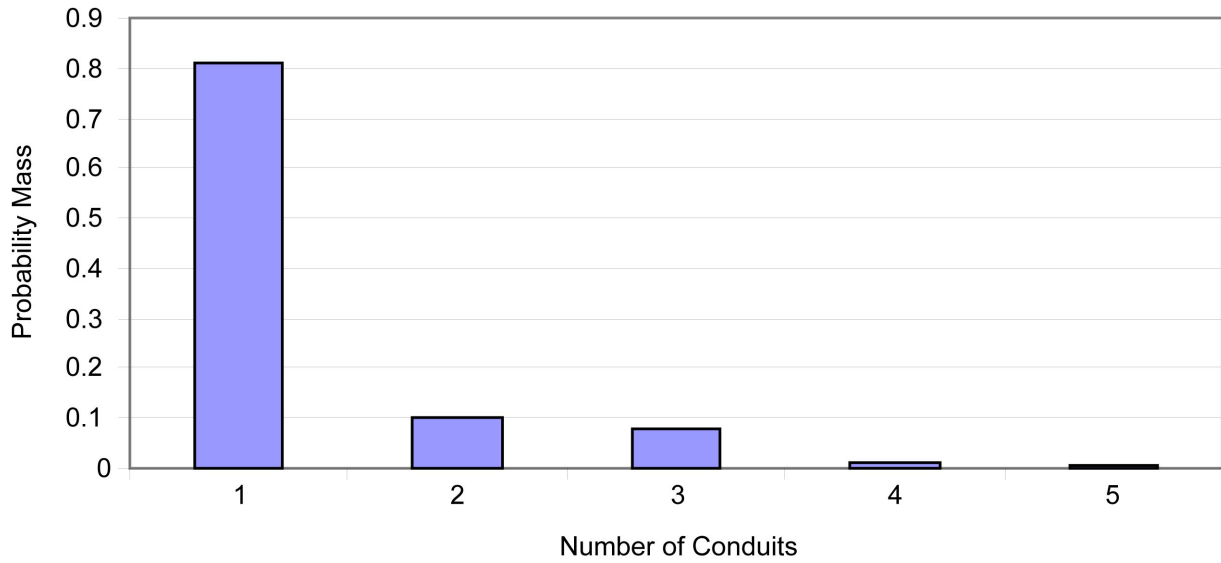
Figure 3.2.7-9. Distribution of the Number of Dikes in an Event, Based on Assessments of Frank Spera



NOTE: Top graph is a cumulative distribution function; bottom graph is a probability density function. For values less than 0.01 on the y-axis, suffix notation is used ($m = 10^{-3}$, so 5m = 0.005, etc).

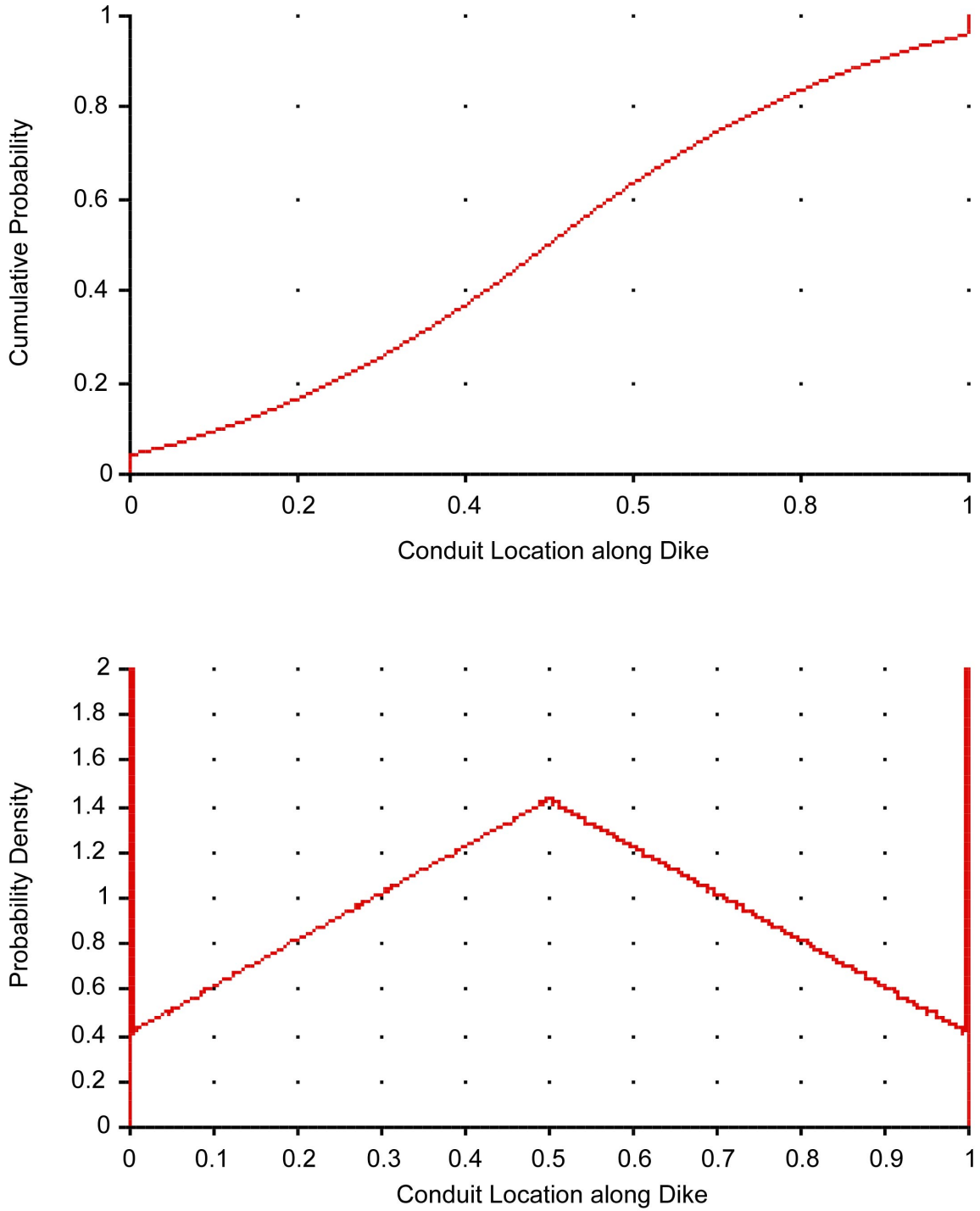
Zero represents North

Figure 3.2.7-10. Distribution for Dike Azimuth as Assessed by Frank Spera



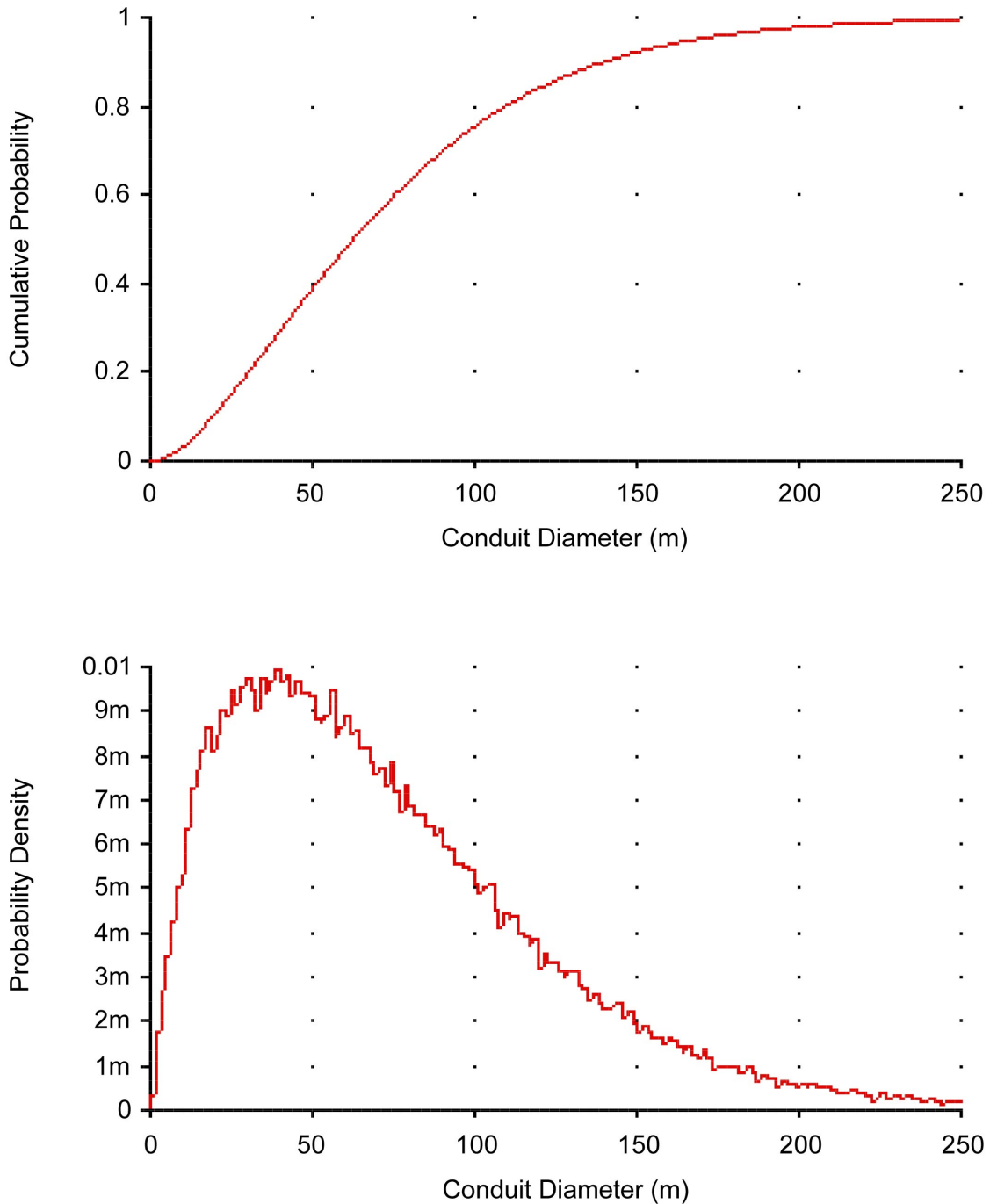
NOTE: Distribution is simulated from the assessment of the event volume and the number of conduits as a function of volume. This result is based on 30,000 iterations. Probability of 4 conduits is 0.8%; probability of 5 conduits is less than 0.5%.

Figure 3.2.7-11. Simulated Distribution for the Number of Conduits in an Event, Based on Assessments of Frank Spera



NOTE: Top graph is a cumulative distribution function; bottom graph is a probability density function. Distribution is a mixture of a discrete and continuous distribution; there is discrete probability mass at 0 and 1, representing the dike endpoints.

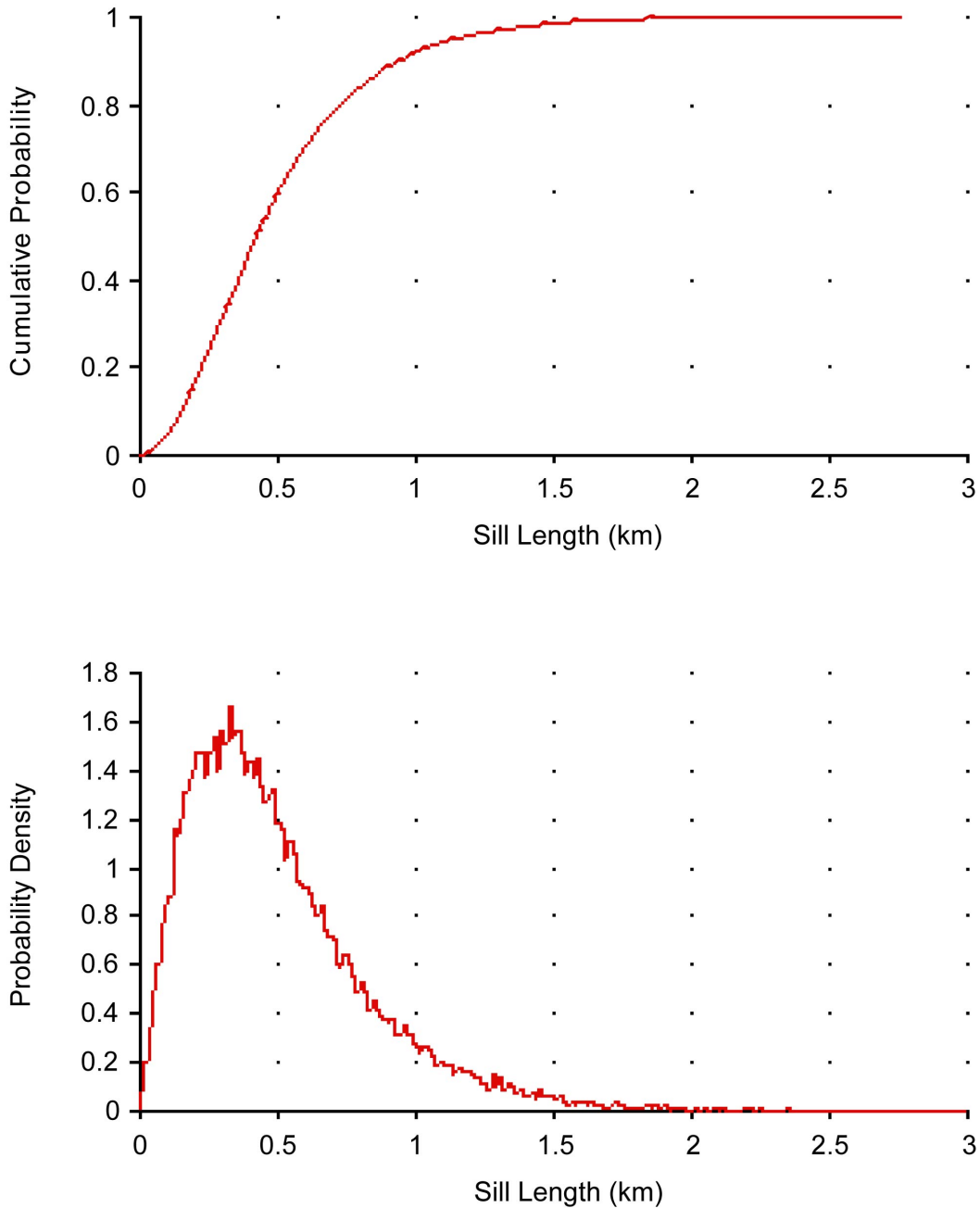
Figure 3.2.7-12. Distribution for the Location of a Conduit along a Dike as Assessed by Frank Spera



NOTES: Top graph is a cumulative distribution function; bottom graph is a probability density function. For values less than 0.01 on the y-axis, suffix notation is used ($m = 10^{-3}$, so 5m = 0.005, etc.).

Distributions are simulated results with 30,000 iterations based on assessment of event volume and the relationship with number and diameter of conduits.

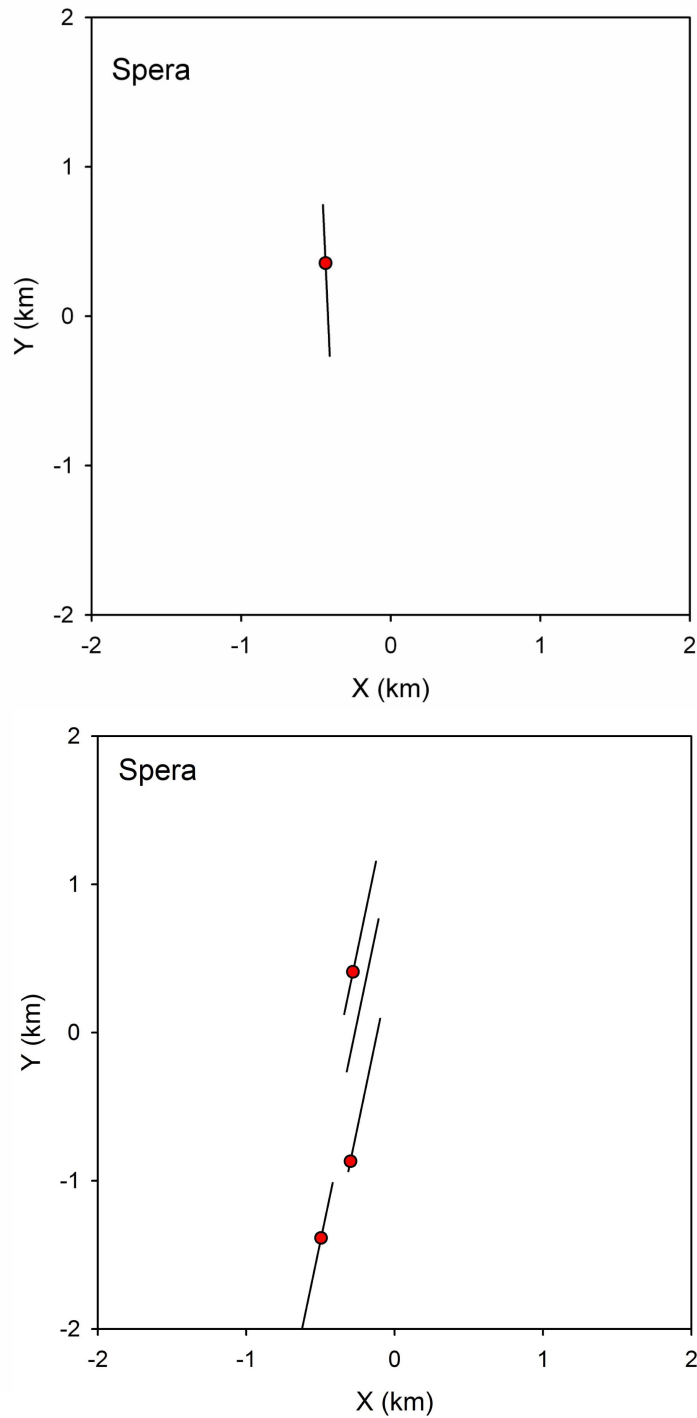
Figure 3.2.7-13. Simulated Distribution for Conduit Diameter in an Event Based on Assessments of Frank Spera



NOTES: Top graph is a cumulative distribution function; bottom graph is a probability density function.

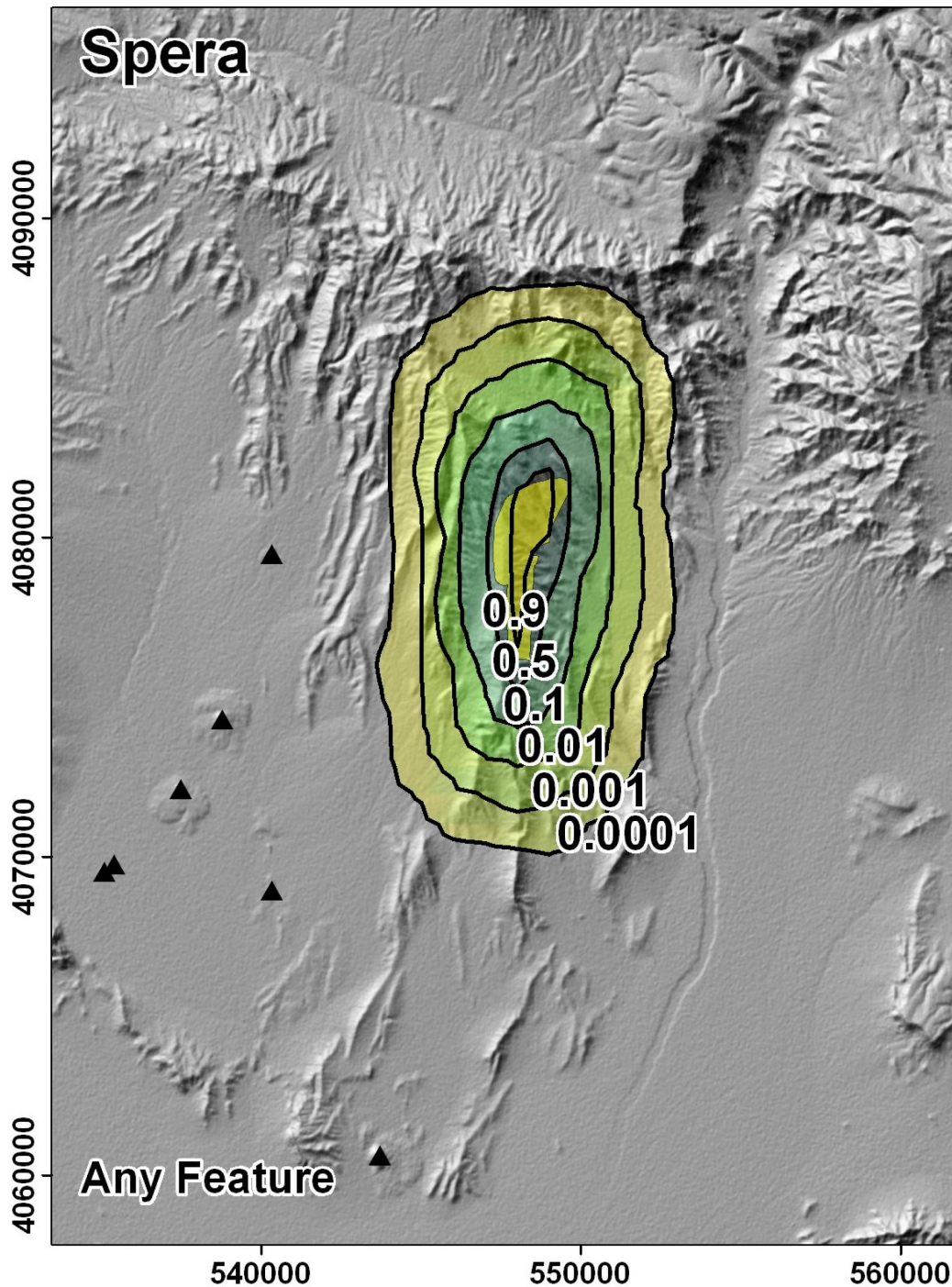
Distributions are simulated results with 30,000 iterations based on assessment of probability of sill formation, event volume, number of dikes, and the relationship between dike volume, sill volume, and sill dimensions.

Figure 3.2.7-14. Simulated Distribution for the Length of a Sill in an Event Based on Assessments of Frank Spera



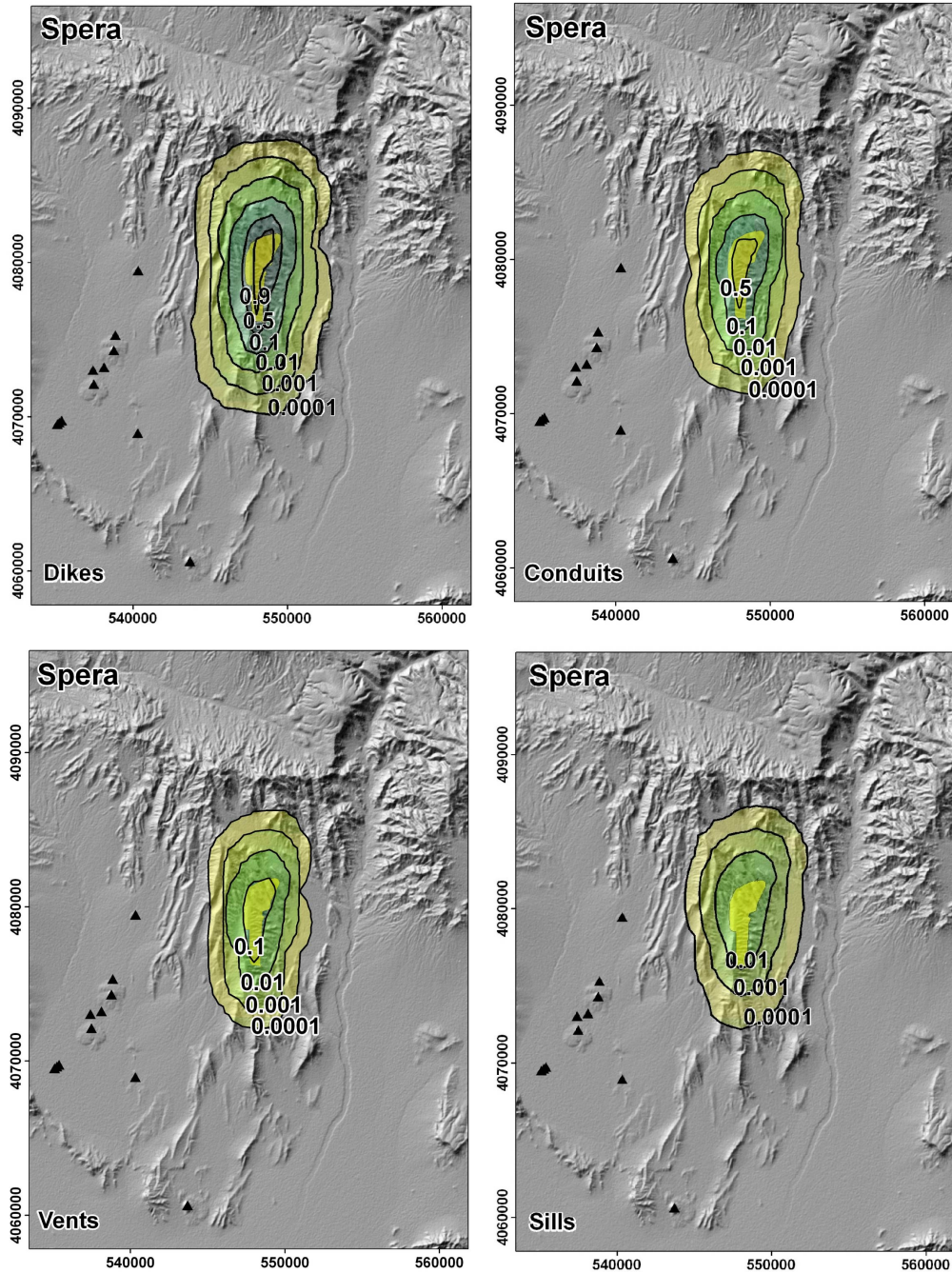
NOTE: Dikes are represented as black lines; their lengths on the figure are the lengths of the simulated dikes. Conduits and vents are represented as small red circles; they are not differentiated and their diameters are not represented. Sills, if they exist, are represented by light yellow ovals or polygons.

Figure 3.2.7-15. Examples of Simulated Events from the PVHA-U Model for Frank Spera



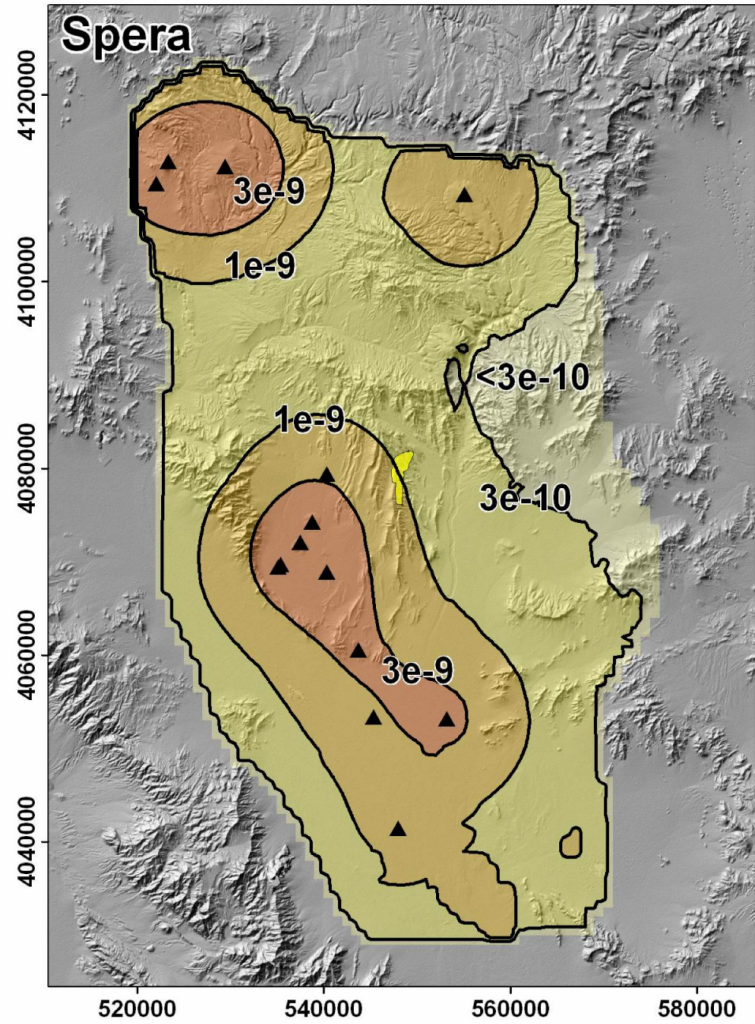
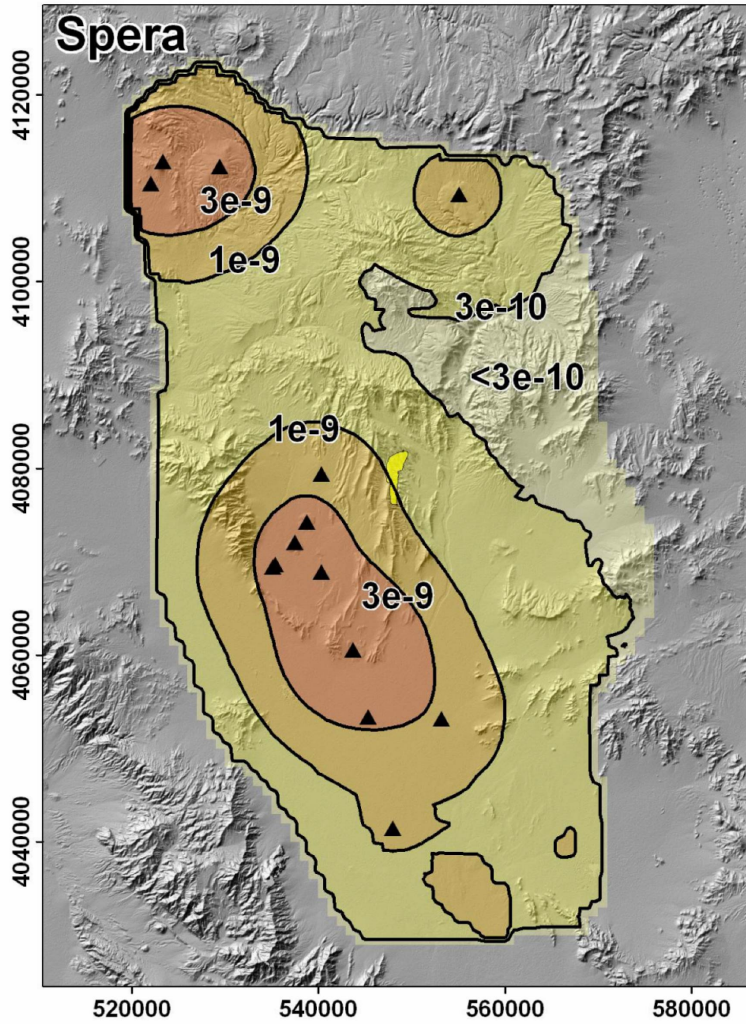
NOTE: Yellow polygon represents the repository footprint. Black triangles represent past events (FS's most likely event set is shown). Map grid ticks are UTM meters; tick intervals are 10 km.

Figure 3.2.7-16. Conditional Probability of Intersection of Any Feature with the Repository Footprint Based on Event Descriptions Developed by Frank Spera



NOTE: Yellow polygon represents the repository footprint. Black triangles represent past events. (FS's most likely event set is shown). Map grid ticks are UTM meters; tick intervals are 10 km.

Figure 3.2.7-17. Conditional Probability of Intersection of Each Igneous Feature with the Repository Footprint Based on Event Descriptions Developed by Frank Spera



NOTE: The left figure is the mean rate density for the 10,000-year assessment; the right figure is the mean rate density for the 1-My assessment. Yellow polygon represents the repository footprint. Black triangles represent past events (FS's most likely event set). Map grid ticks are UTM meters; tick intervals are 20 km.

Figure 3.2.7-18. Mean Rate Density for the 10,000-Year Assessment and the 1-My Assessment Based on the Assessments of Frank Spera

Table 3.2.7-1. Data Used to Define Spatial Distribution and Event Rates for Future Volcanic Events for Frank Spera's PVHA-U Model

Center or Cone	Number of Events	Age (Ma)	Volume (km ³)
Anomalies C and D	0 (weight = 0.2) 1 (weight = 0.8)	4.2	0.19
Thirsty Mountain	1	4.63	2.63
Pliocene SE Crater Flat (PSECF)	1	3.8	0.59
Anomalies F,G, and H	1	3.91	0.06
Anomaly B	1	3.85	1.2
Buckboard Mesa	1	2.87	0.84
Quaternary Crater Flat	1 (weight = 0.05)		Total V = 0.15
Makani Cone	2 (weight = 0.14)	1.09	0.002
Black Cone	3 (weight = 0.06)	1.07	0.06
Red Cone	4 (weight = 0.37)	1.07	0.055
SW Little Cone	5 (weight = 0.38)	0.95	0.02
NE Little Cone		0.95	0.014
Hidden Cone	1	0.35	0.032
Little Black Peak	1	0.35	0.014
Lathrop Wells	1	0.077	0.05

NOTE: Derived from Table D.7-1 in Frank Spera's Elicitation Summary in Appendix D.

Table 3.2.7-2. Alternative Models of Cumulative Volume over Time and Volume per Events as Specified by Frank Spera

Cumulative Volume Model	Volume per Event Model	Mean Estimate Rate (events per year in the region of interest)
Linear fit to post-1.1 Ma events	Assessed distribution	1.7e-5
Linear fit to post-1.1 Ma events	Fit to volume of Quaternary events	5.4e-6
Linear fit to post-3 Ma events	Assessed distribution	1.3e-5
Linear fit to post-3 Ma events	Fit to volume of Quaternary events	3.9e-6

Table 3.2.7-3. Frequency of Number of Dikes and Conduits or Vents in Simulated Events Based on the Assessments of Frank Spera

		Number of Conduits and Vents in an Event				
		1	2	3	4	5
Number of Dikes in an Event	1	54.3%	4.8%	2.7%	0.02%	0.01%
	2	20.5%	2.5%	1.6%	0.1%	0.03%
	3	5.4%	1.5%	1.5%	0.2%	0.1%
	4	0.8%	0.7%	1.1%	0.2%	0.2%
	5	0.1%	0.2%	0.6%	0.2%	0.1%
	6	0.03%	0.1%	0.2%	0.1%	0.04%
	7	0.02%	0.03%	0.1%	0.03%	0.01%
	8	0.01%	0.01%	0.05%	0.02%	0.01%

3.2.8 George Thompson's PVHA Model

Spatial and Temporal Models

Figure 3.2.8-1 presents the logic tree describing the basic structure of the spatial and temporal models developed by George Thompson (GT) for PVHA-U.

GT specified a locally homogenous spatial zones model, with two zones: a "Crater Flat / Amargosa Desert (CV/AD) Volcanic Domain" and a "Yucca Mountain Fault Domain" as illustrated in Figure 3.2.8-2. The Yucca Mountain Fault Domain contains no past events younger than 4 Ma, which GT defines as the time period of interest. Accordingly, to estimate an event rate outside the Crater Flat-Amargosa Desert (CF-AD) zone, GT identified a "background zone" as illustrated in Figure 3.2.8-3. The transition in rate density between the zones is gradual, and the start of the rate transition area is uncertain. GT defined three alternative rate transition boundaries, as shown in Figure 3.2.8-2. The uncertainty in the location of the rate transition boundary is represented by the second node along the top branch of the logic tree.

The event rate within the CF/AD zone and within the background zone is based on the number of events in each region that have occurred in the last 4 Ma. Table 3.2.8-1 lists the past events in each zone judged relevant by GT. The table includes alternative interpretations of some events, along with the relative probability GT assigned to each interpretation. In combination, 8 unique interpretations of the number of past events in the CF/AD zone are identified. These are represented schematically in the third node along the top branch of the logic tree. The probabilities for each event set are determined by the probabilities assigned to alternative interpretations in Table 3.2.8-1.

Two alternative conceptual models were specified for estimating the rate of future events: a homogenous Poisson model for both the CF-AD zone and the background zone, and a time-volume model for the rate within the CF-AD zone, as illustrated in the logic tree.

For the homogenous Poisson model, the rate is estimated based on the number of events in the relevant region and the age of the oldest relevant event using the approach described in Section 3.1. Based on the most likely event set from Table 3.2.8-1, the mean of the estimated rate in the CF/AD zone is $1e-6$ events per year. The mean of the estimated rate in the background zone is $1e-6$ events per year (note that the different areas of the two zones mean that the rate per km^2 is higher in the CF/AD zone than outside). In the logic tree formulation of Figure 3.2.8-1, uncertainty in the rate is represented by the 5th, 50th, and 95th percentiles of the Gamma distribution with the appropriate parameters as described in Section 3.1.

To develop a rate estimate based on the time-volume model, GT specified that a model of cumulative volume as a function of time should be fit to the events he specified in Table 3.2.8-1, and that the model should be consistent with a conductive heat loss model. Two alternative functions were fit to his data: cumulative volume as a function of the square-root of time, as suggested by Rick Carlson in the 1996 PVHA study (CRWMS M&O 1996, and presentations at Workshop 2) and cumulative volume as a function of the natural log of time. The latter model provided a better statistical fit to the data and is used here. The best-fit linear regression was:

$$CV(t) = 1.87 + 0.282 \times \ln(3.91 + t) \quad (\text{Eq. 3.2.8-1})$$

In all cases, t is the time at which CV is to be estimated, in millions of years from the present. So for 2 Ma prior to the present, $t = -2$, and for 1 My in the future, $t = 1$.

The 90% confidence interval on the slope of the regression lines is used to represent the uncertainty in the estimated magma generation rate, as described in Section 3.1.

The volume per event for future events is estimated based on the mean and variance of the volume of Quaternary events. To incorporate uncertainty in the volume per event for future events, volume per event is modeled with a lognormal distribution with mean and variance matching the mean and variance of the volume of relevant events, and the 5th, 50th, and 95th percentiles of that distribution are used in the logic tree. The volume per event differs for different event sets.

Figure 3.2.8-4 illustrates uncertainty in the estimated rate for each of the alternative temporal modes specified by GT, based on one event set. In all cases, the bar represents the 5th to 95th percentiles of the distribution on rate for the specified model based on the most likely event set from Table 3.2.8-1.

Mean Rate Density and Mean Recurrence Rate

Figure 3.2.8-5 illustrates the mean rate density for igneous events calculated from GT's spatial and temporal models for the 10,000-year assessment. The locally homogenous zone model can be seen clearly: within the zone boundary, one rate applies, outside the boundary another, lower rate applies, and in the transition zone between zones, the rate changes gradually from the inside-the-zone rate to the outside-the-zone rate. The color-shaded area represents the model domain, which includes both the Crater Flat zone defined by GT and a portion of the background zone. The model domain was chosen for modeling convenience, although constrained to encompass the defined zone and to be no smaller than the region where the conditional probability of intersection of an event with the repository footprint is non-zero (discussed below).

A mean recurrence rate for events in the region of interest can be calculated by summing the mean rate density at each grid point. Based on the mean rate density shown in Figure 3.2.8-5, the mean recurrence rate for events in this region is 1.1×10^{-6} events per year, giving recurrence intervals between 47,000 and 2.7 million years (5th to 95th percentile of the distribution on recurrence interval), with a mean recurrence interval of about 909,000 years for events in the region illustrated.

Event Simulation Model

Figure 3.2.8-6 illustrates the key features of an event simulator for GT's PVHA-U model. In this model, an *event* consists of one or more dikes and one or more conduits.

The total length of dikes in an event is defined by the distribution illustrated in Figure 3.2.8-7. The number of dikes in an event is defined as a function of the total dike length, as illustrated in Figure 3.2.8-8. When multiple dikes exist, the length of each is random, with the restriction that the minimum dike length is 400m and the length of all the dikes in the event must match the total dike length sampled from the distribution above. All dikes in an event have the same azimuth, with the distribution as illustrated in Figure 3.2.8-9. Individual dikes in an event are arranged in

a right-stepping en echelon pattern, with the overlap between dikes in the direction of dike azimuth ranging from 0 (no overlap) to 10% of the length of the shorter of the overlapping segments. The total width of the event is defined as a function of the total dike length. Figure 3.2.8-10 shows the distribution of the dike system width for simulated events, based on GT's assessment of total dike length and the relationship between dike system length and dike system width.

The number of conduits that may occur in a single event is a function of the total length of dikes in an event; the full assessment is included in GT's Elicitation Summary in Appendix D. Figure 3.2.8-11 shows the simulated distribution of the number of conduits in an event, based on GT's assessments of total dike length and the relationship between total dike length and the number of conduits. Conduits are located along dikes, following the distribution shown in Figure 3.2.8-12. Each dike can have no more than one conduit. The diameter of a conduit was defined as a function of the width of the dike on which that conduit is located. Figure 3.2.8-13 shows the simulated distribution on conduit diameter, based on GT's assessment of dike width and the relationship between dike width and conduit diameter.

Figure 3.2.8-14 illustrates two examples of the simulated events, and Table 3.2.8-2 describes the number of dikes and the number of conduits and vents (combined) in an event, and how frequently such events occur in the event simulation. The table indicates, for example, that the most common type of event (30.8% of simulated events, as indicated by bold in the table) consists of one dike with one conduit or vent. The top half of Figure 3.2.8-14 illustrates an example of a one-dike, one-conduit event. Events may contain as many as 30 dikes (not shown in the table) and 8 conduits or vents, although such events occur very rarely in simulated events. Events with more than 10 dikes (not shown in the table) occur in about 1.2% of the simulations.

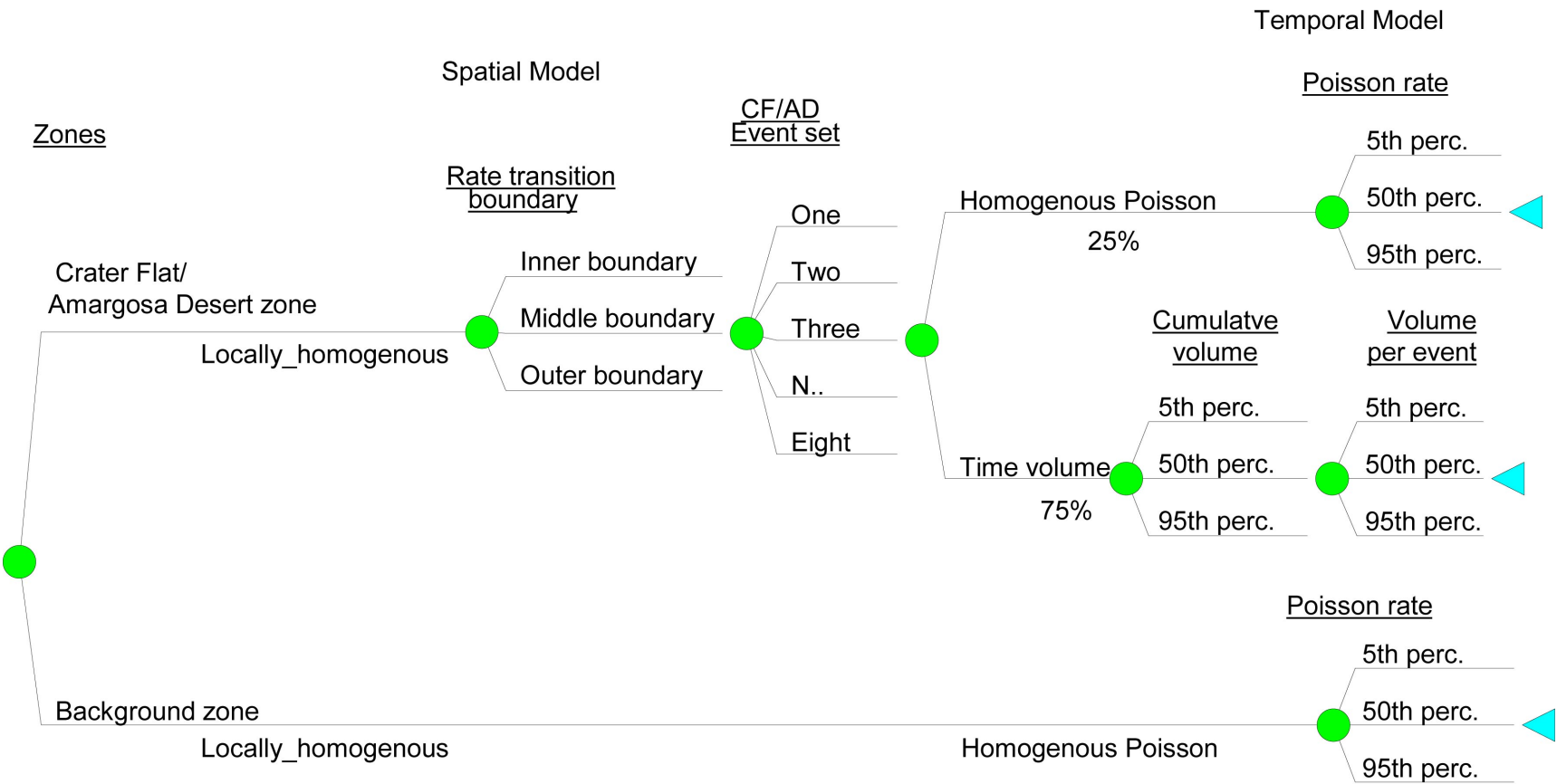
Conditional Probability of Intersection

Figure 3.2.8-15 illustrates the conditional probability of the intersection of any igneous feature with the repository footprint based on GT's event descriptions. The effect of his widely spaced, right-stepping en echelon dike system can be seen in the right-stepping shape of the contours.

Figure 3.2.8-16 shows the conditional probability of intersection for each type of igneous feature that may occur in events described by GT (dikes and column-producing conduits). The two maps show the same spatial pattern, although the probability of a conduit intersection is lower than the probability of a dike intersection for an event at a given location, reflecting the smaller geometry and the spatial distribution of conduits.

Differences Between the 10,000-year and 1-My Assessments

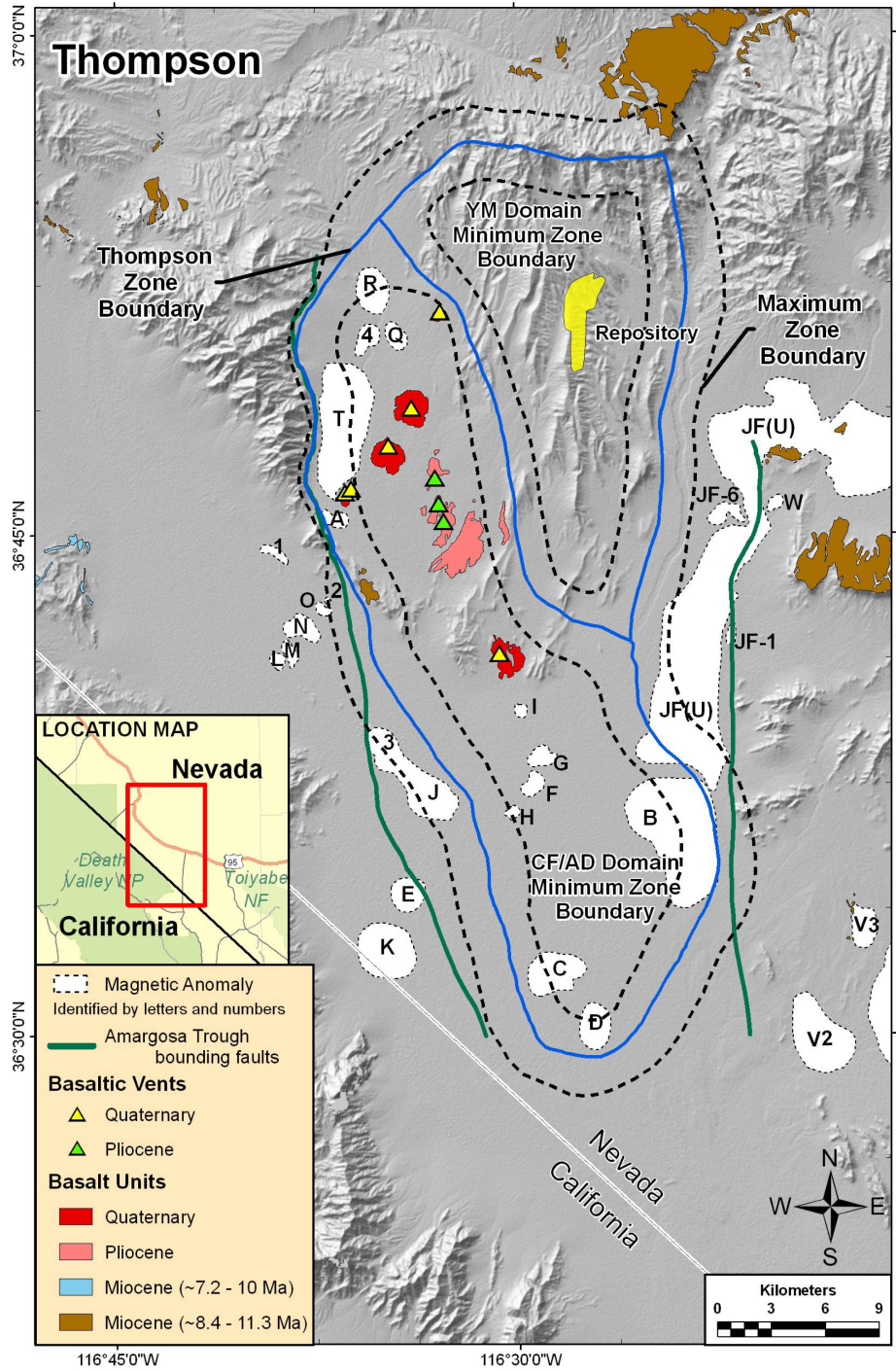
No differences exist in GT's models or assessments based on the different assessment periods. Although the time-volume temporal model described above results in a rate estimate that varies over time, the changes are sufficiently small as to make the mean rate density map for the 1-My assessment indistinguishable from the map for the 10,000-year assessment (Figure 3.2.8-17).



NOTES: All probabilities shown on the branches are those assigned by the expert. Uncertainty in spatial density, uncertainty in the Poisson rate and uncertainty in the cumulative volume and volume per event are modeled based on the approaches described in Section 3.1.5, and the probabilities for those branches are defined by the modeling approach.

A homogenous spatial and temporal model for the rate within the background zone was specified, so the only uncertainty along the bottom branch is the estimated rate. CF/AD = Crater Flat/Amargosa Desert

Figure 3.2.8-1. Logic Tree Representing the Spatial and Temporal Components of the PVHA-U Model Specified by George Thompson



NOTE: Blue line represents the zone boundary. Dashed black lines represent uncertainty in the rate transition distance. For one model, the rate transition begins at the innermost black line and ends at the blue line; for the second, the transition begins and ends halfway between each black line and the red line; and for the third, the transition distance begins at the red line and ends at the outer black dashed line.

Figure 3.2.8-2. Crater Flat / Amargosa Desert Zone as Specified by George Thompson

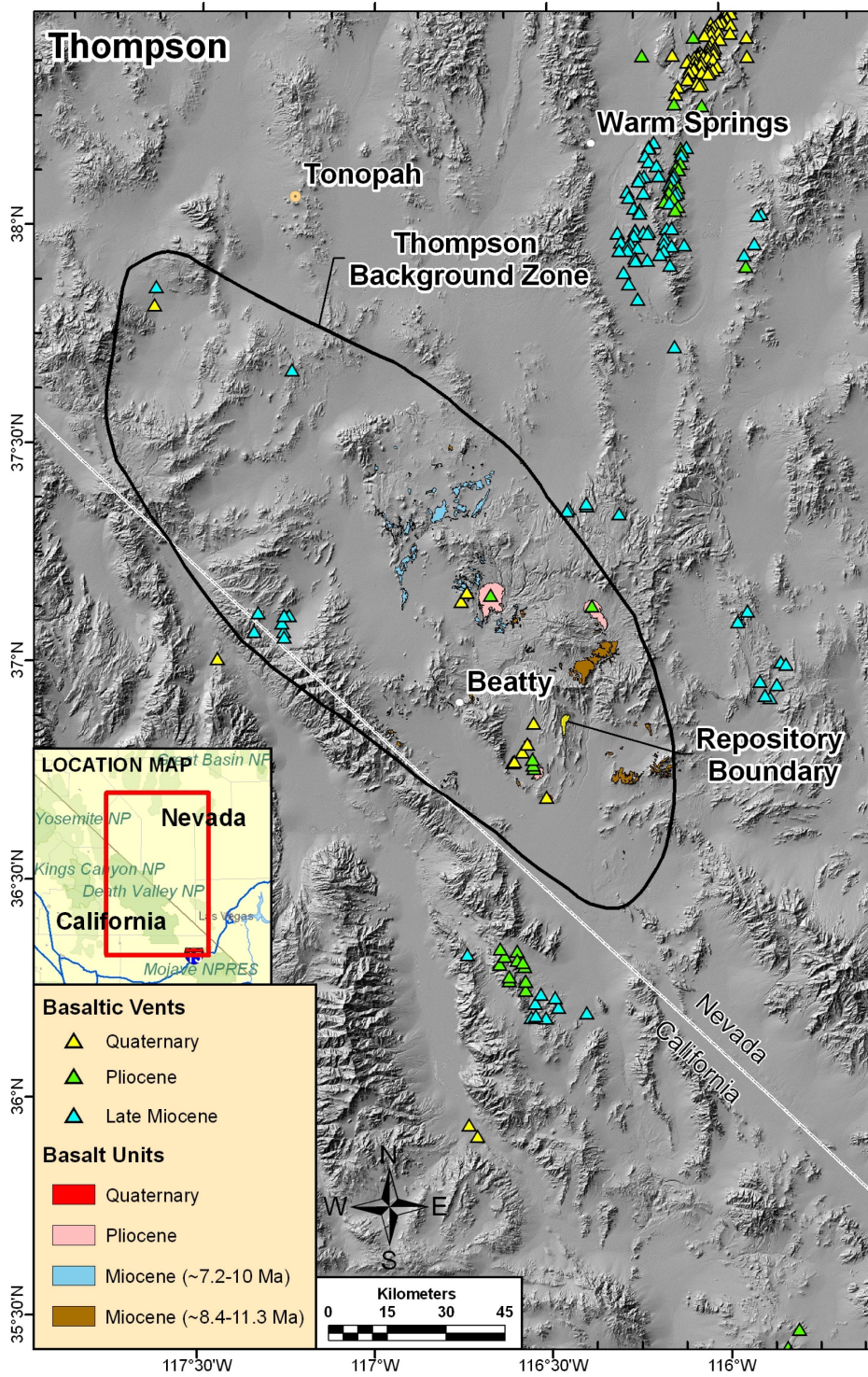
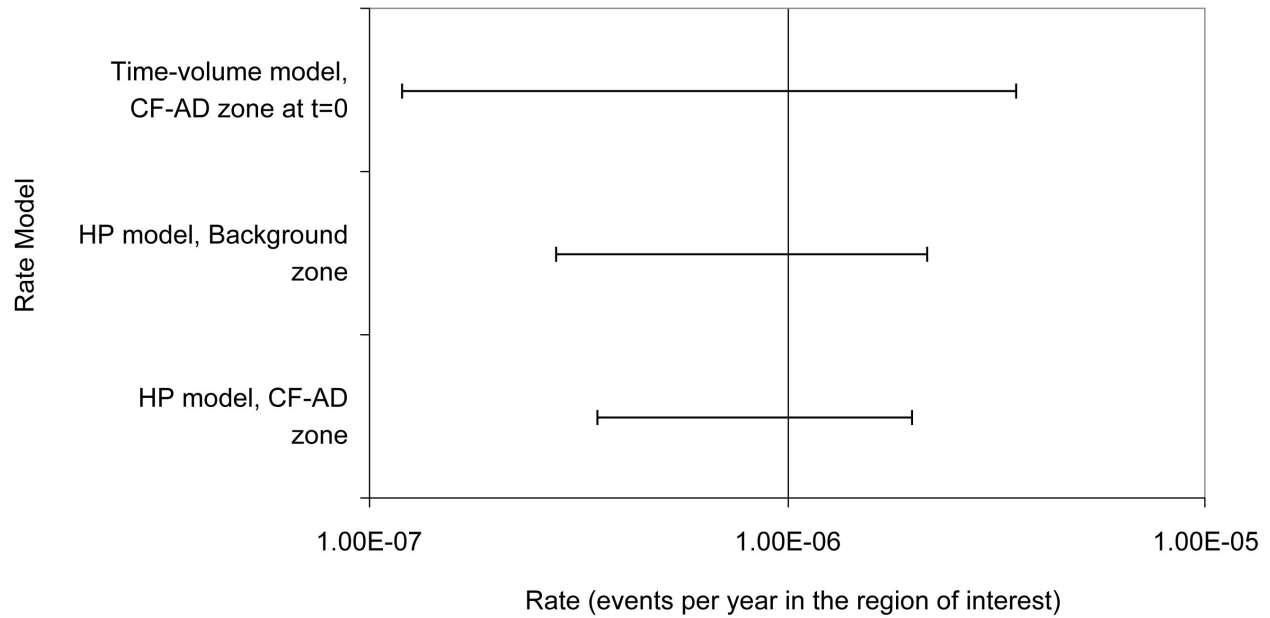


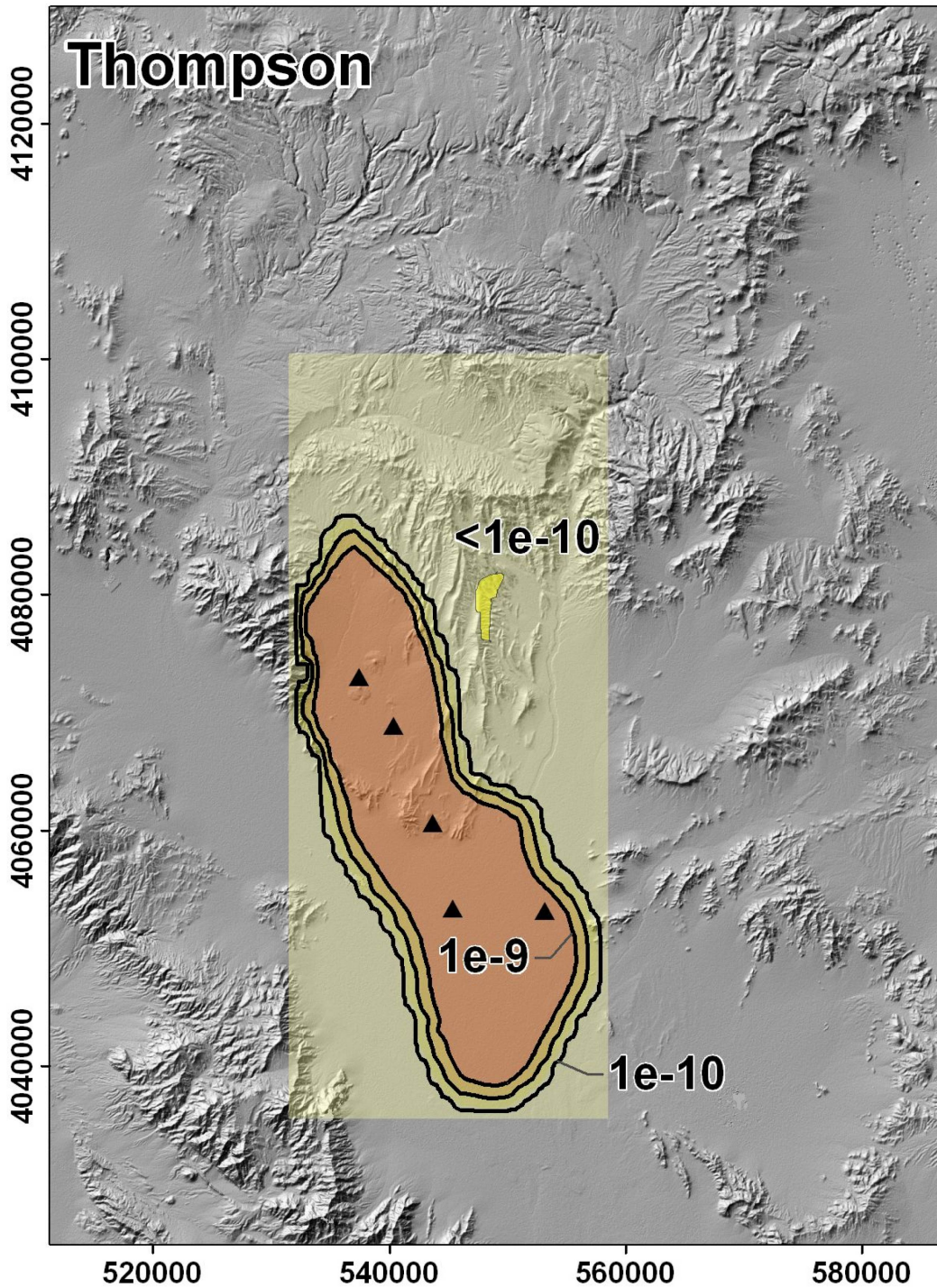
Figure 3.2.8-3. Background Zone as Specified by George Thompson



NOTES: Bars represent the 5th to 95th percentile of the uncertainty in the rate for each alternative rate model, for estimates based on the most likely event set identified in Table 3.2.7-1.

Caution is recommended in comparing these rate distributions. Note that for each model, the estimated rate applies to the specific zone (CF-AD = Crater Flat/Amargosa Desert domain/zone, Background = background zone), the areas of which vary, implying different rate densities. HP = homogenous Poisson rate model

Figure 3.2.8-4. Example of Uncertainty in Estimated Rate Based on a Single Interpretation of Past Events for Alternative Temporal Models Specified by George Thompson



NOTE: Contours show the mean rate density in events per year per km². Yellow polygon represents the repository footprint; black triangles represent past events (GT's most likely event set). Map grid ticks are UTM meters; tick intervals are 20 km.

Figure 3.2.8-5. Mean Rate Density for the 10,000-Year Assessment Based on Models Specified by George Thompson

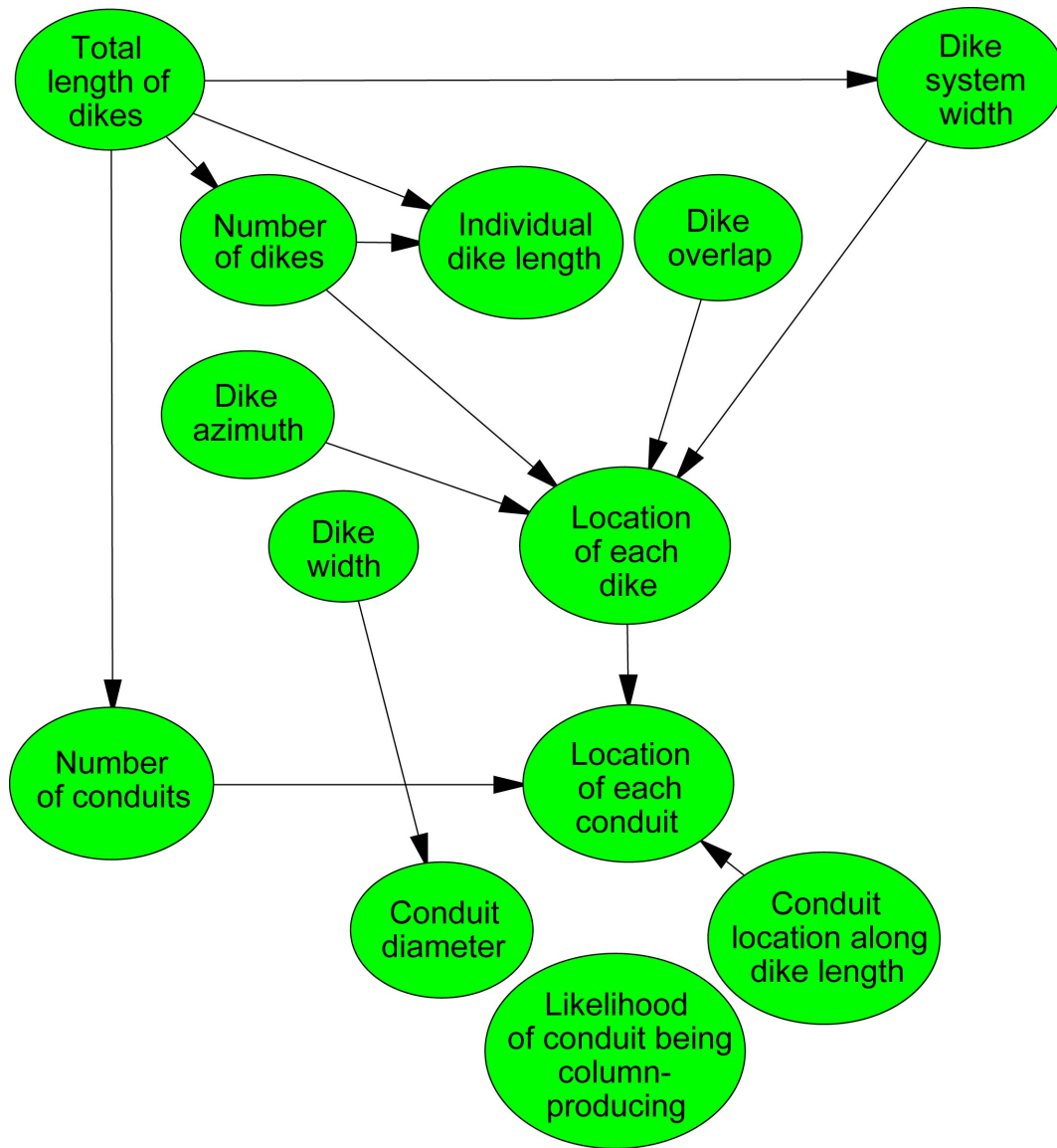
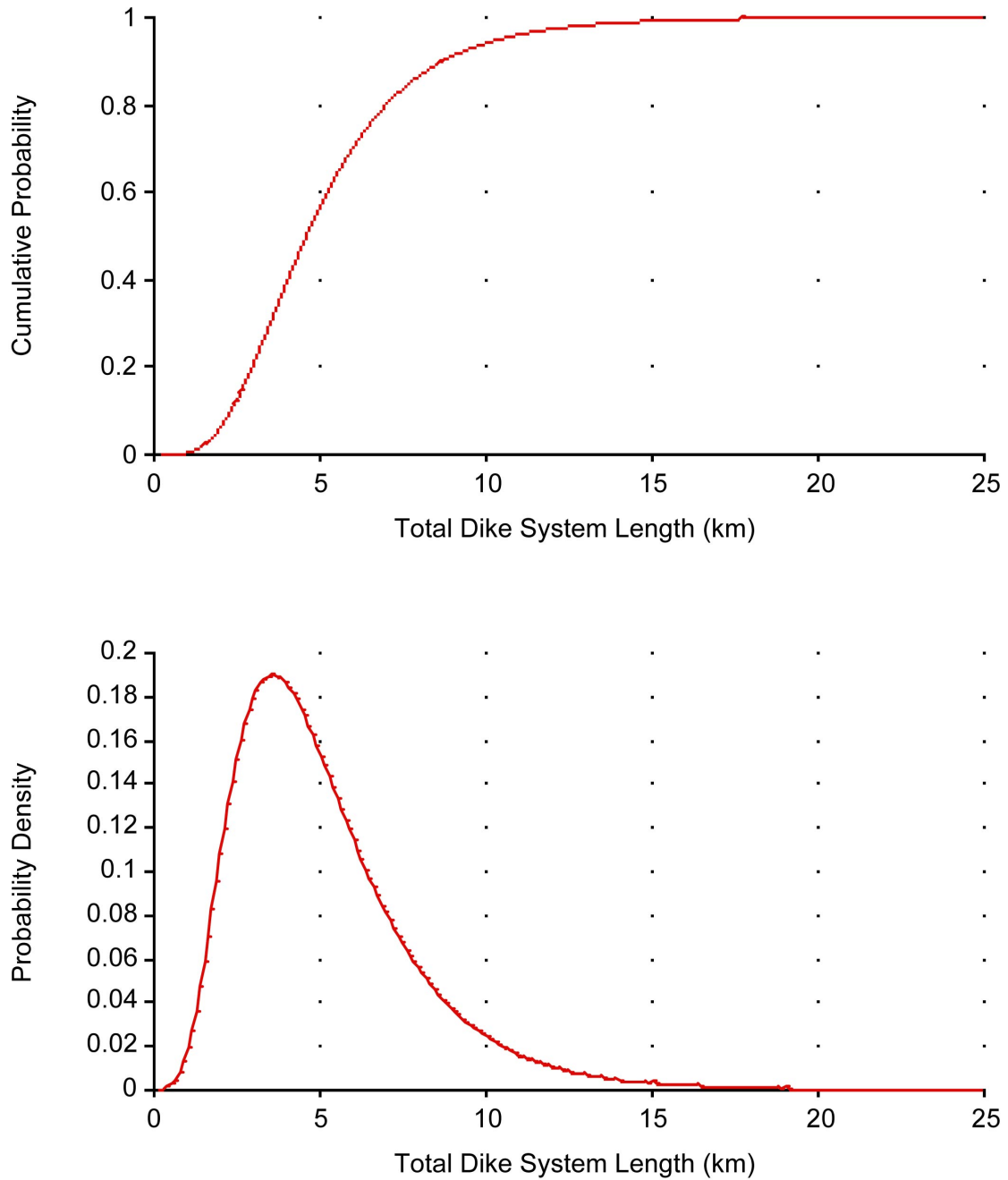
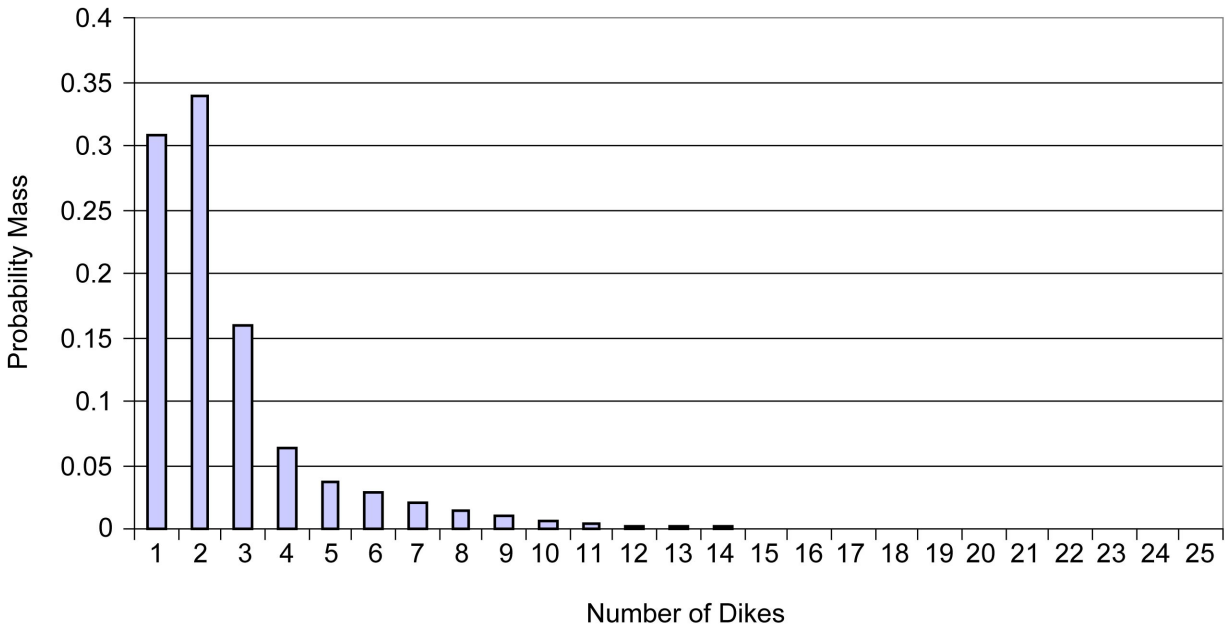


Figure 3.2.8-6. Components of an Event Simulator Based on the Characteristics of Future Events Described by George Thompson



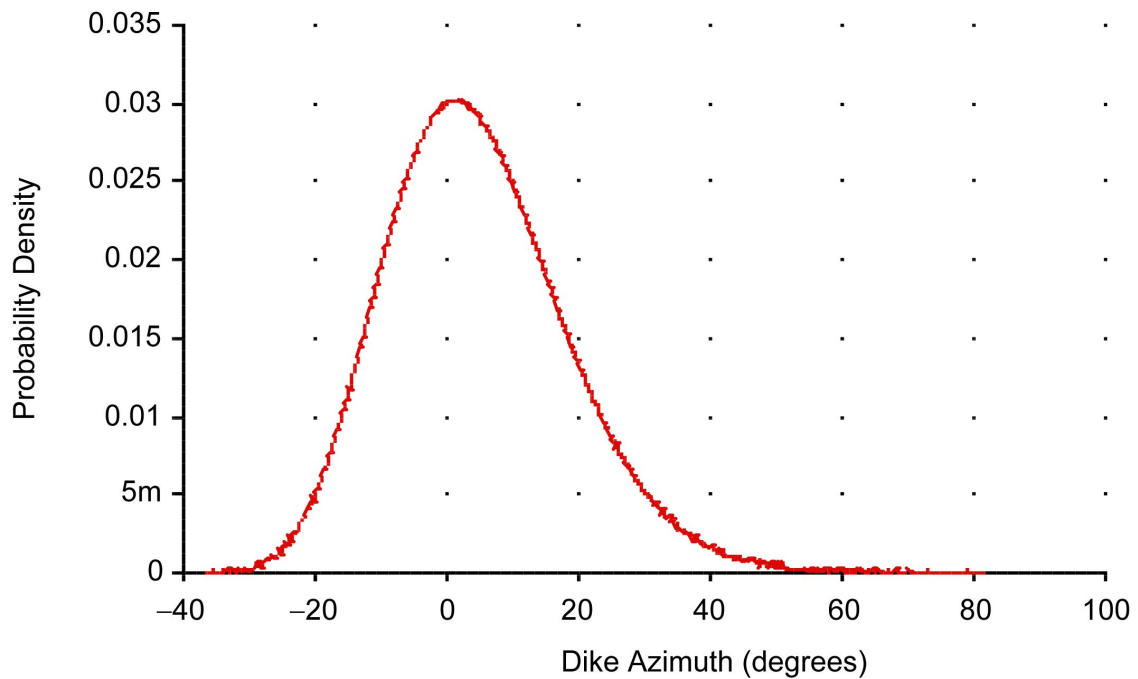
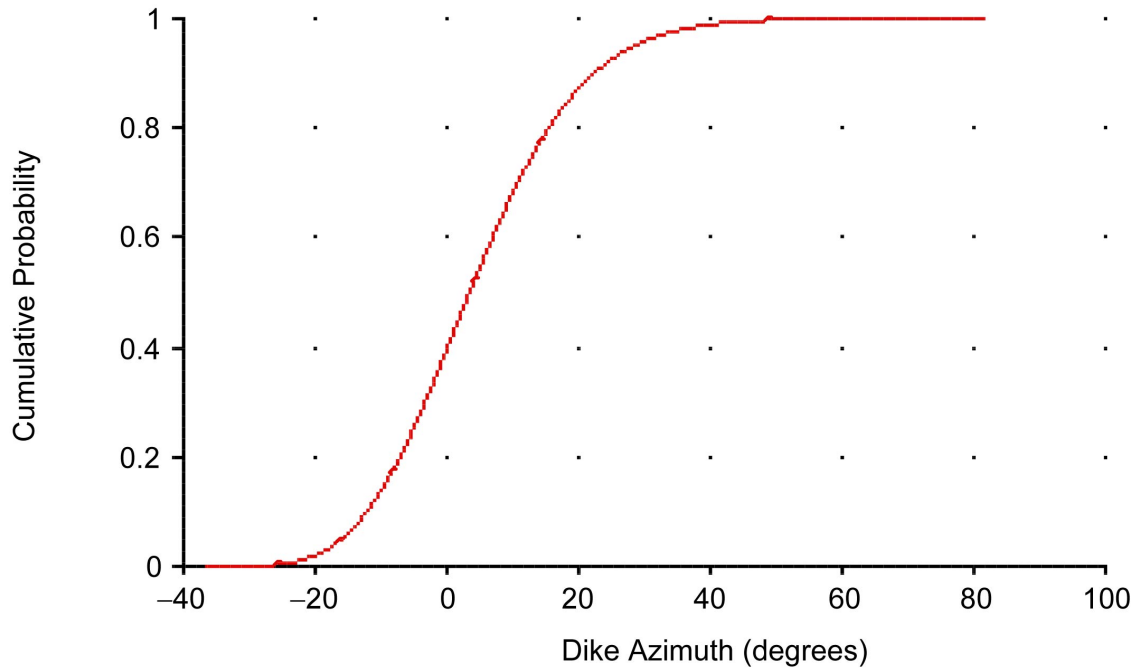
NOTE: Top graph is a cumulative distribution function; bottom graph is a probability density function.

Figure 3.2.8-7. Distribution for the Total Length of Dikes in an Event as Assessed by George Thompson



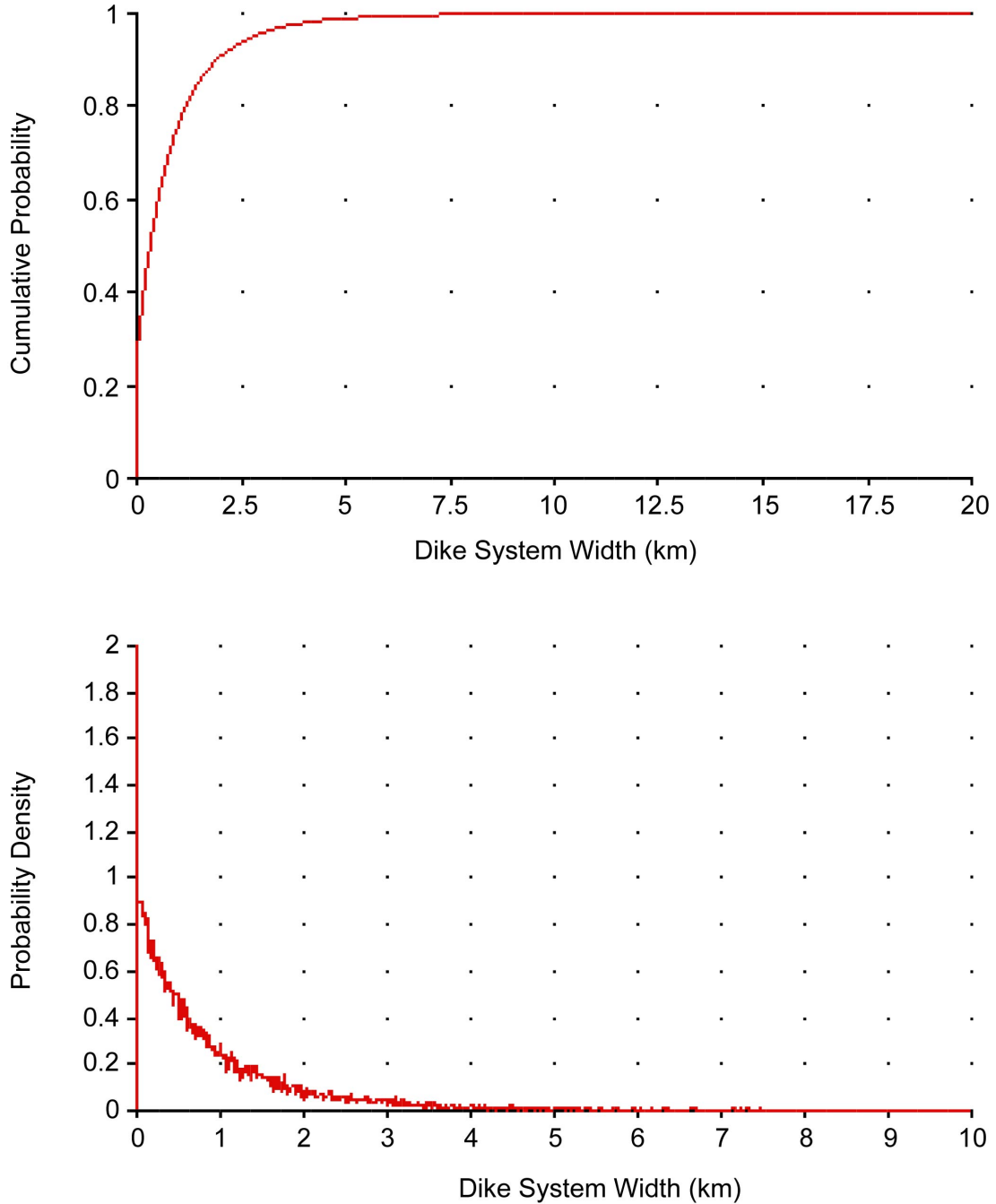
NOTE: Results from 30,000 iterations of the event simulator. Number of dikes is a function of the total dike length and the assessed relationship between total length and number. The probability of 10 dikes is less than 1%. The probability of 11 or more dikes is less than 0.5%.

Figure 3.2.8-8. Simulated Distribution of the Number of Individual Dikes in an Event Based on Assessments of George Thompson



NOTE: Top graph is a cumulative distribution function; bottom graph is a probability density function. Zero represents north.

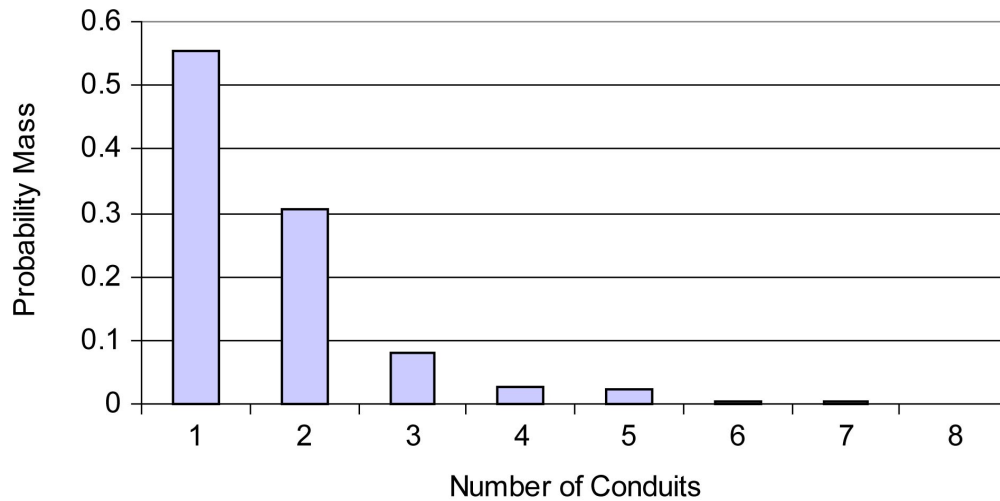
Figure 3.2.8-9. Distribution for Dike Azimuth as Assessed by George Thompson



NOTES: Top graph is a cumulative distribution function; bottom graph is a probability density function. Note change in scale.

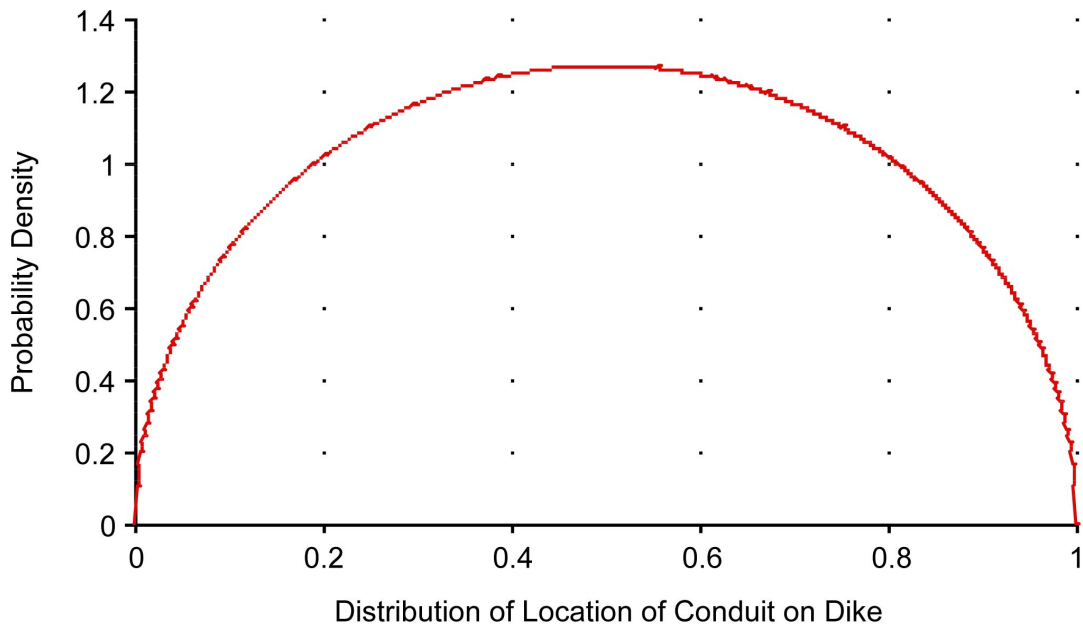
Results of 30,000 iterations of the event simulator; dike system width is a function of the total dike length and the assessed relationship between dike system length and dike system width. Events with a single dike have a dike system width of zero.

Figure 3.2.8-10. Simulated Distribution for Dike System Width Based on Assessments of George Thompson



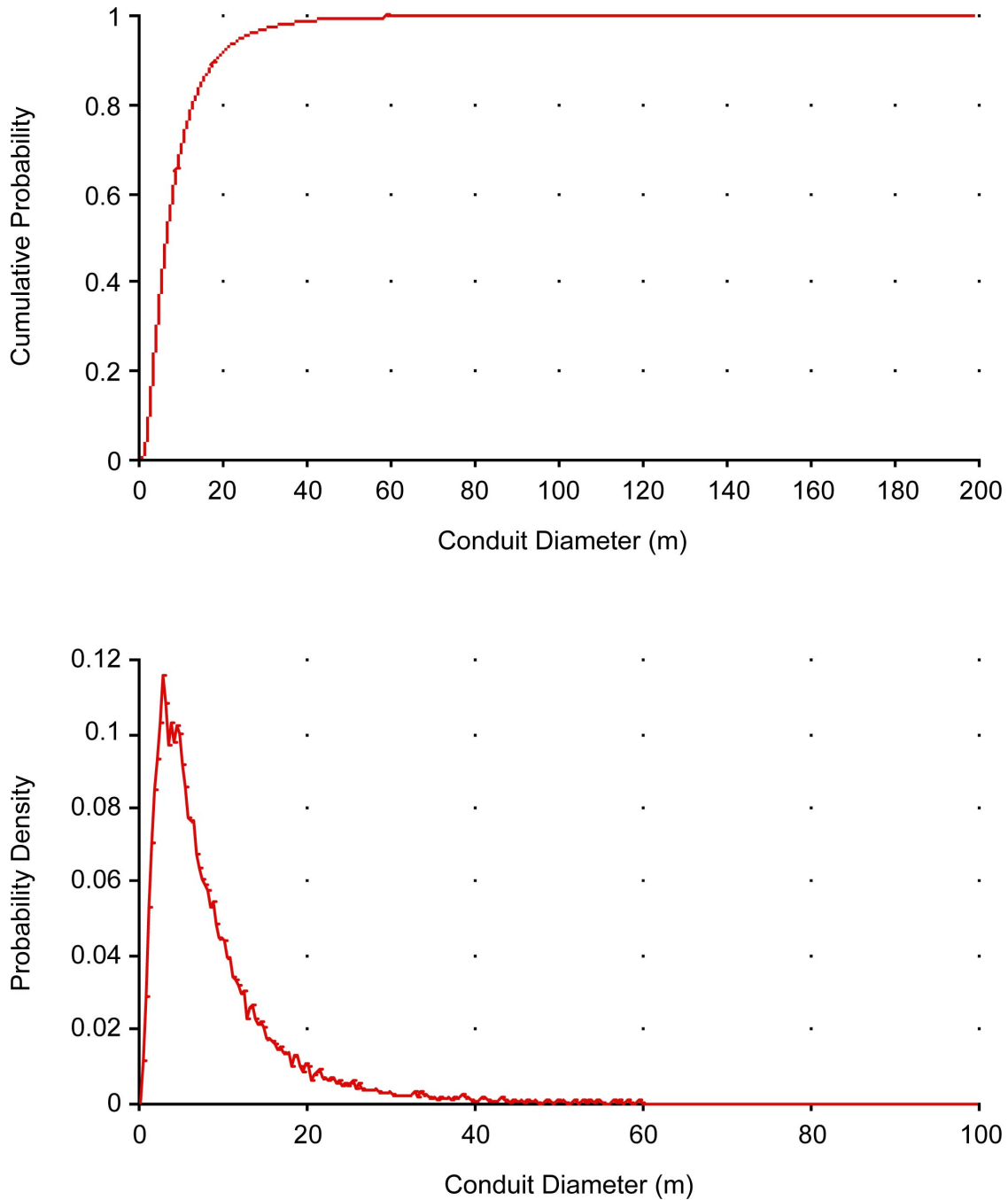
NOTE: Graph shows the results of 30,000 iterations of the event simulator. Number of conduits is a function of the total dike length and the number of dikes.

Figure 3.2.8-11. Simulated Distribution of the Number of Conduits in an Event Based on Assessments of George Thompson



NOTE: Graph shows the relative likelihood of a conduit being located at any position along the dike length, with zero and one representing the ends of the dike.

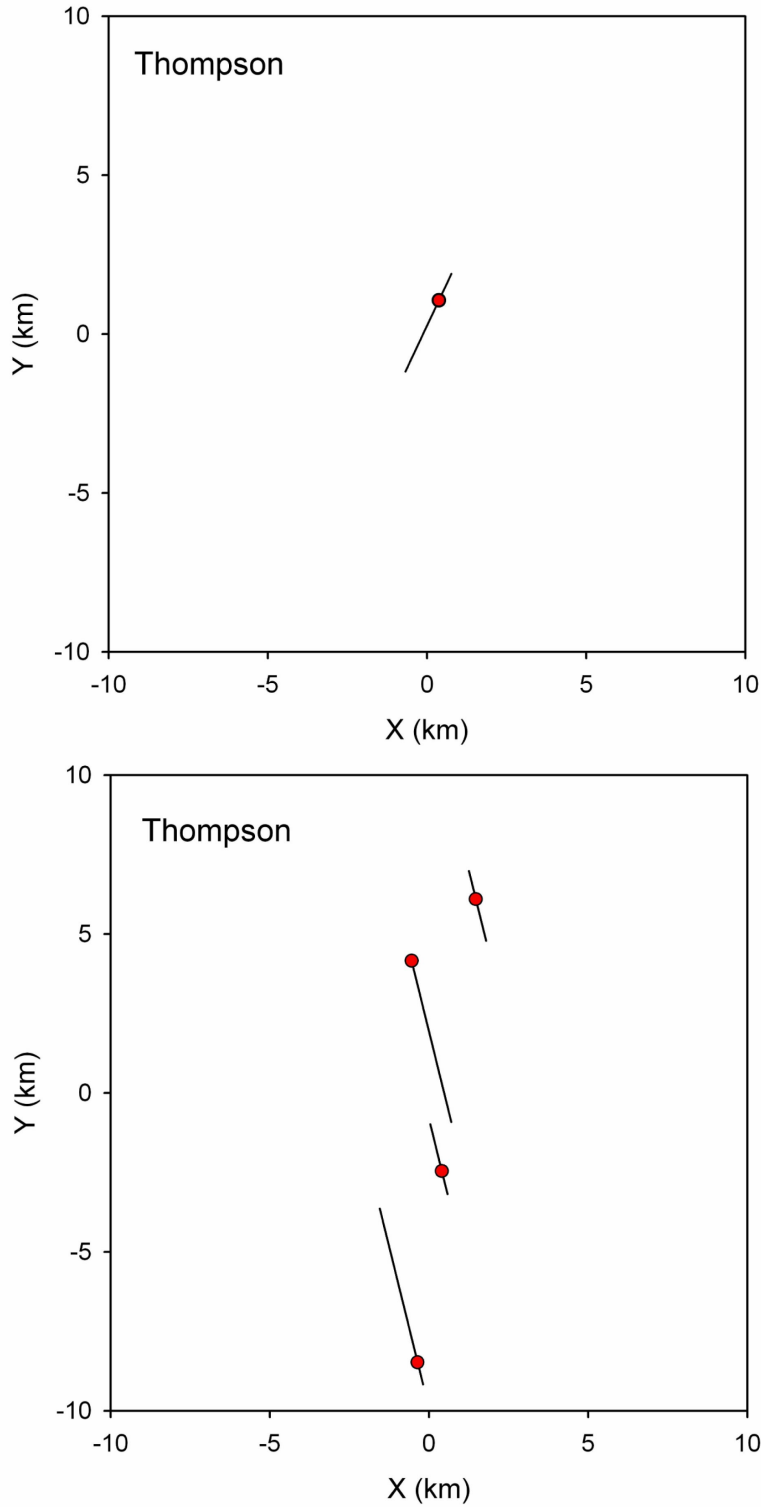
Figure 3.2.8-12. Distribution for the Location of a Conduit along the Length of a Dike as Assessed by George Thompson



NOTES: Top graph is a cumulative distribution function; bottom graph is a probability density function. Note change in scale.

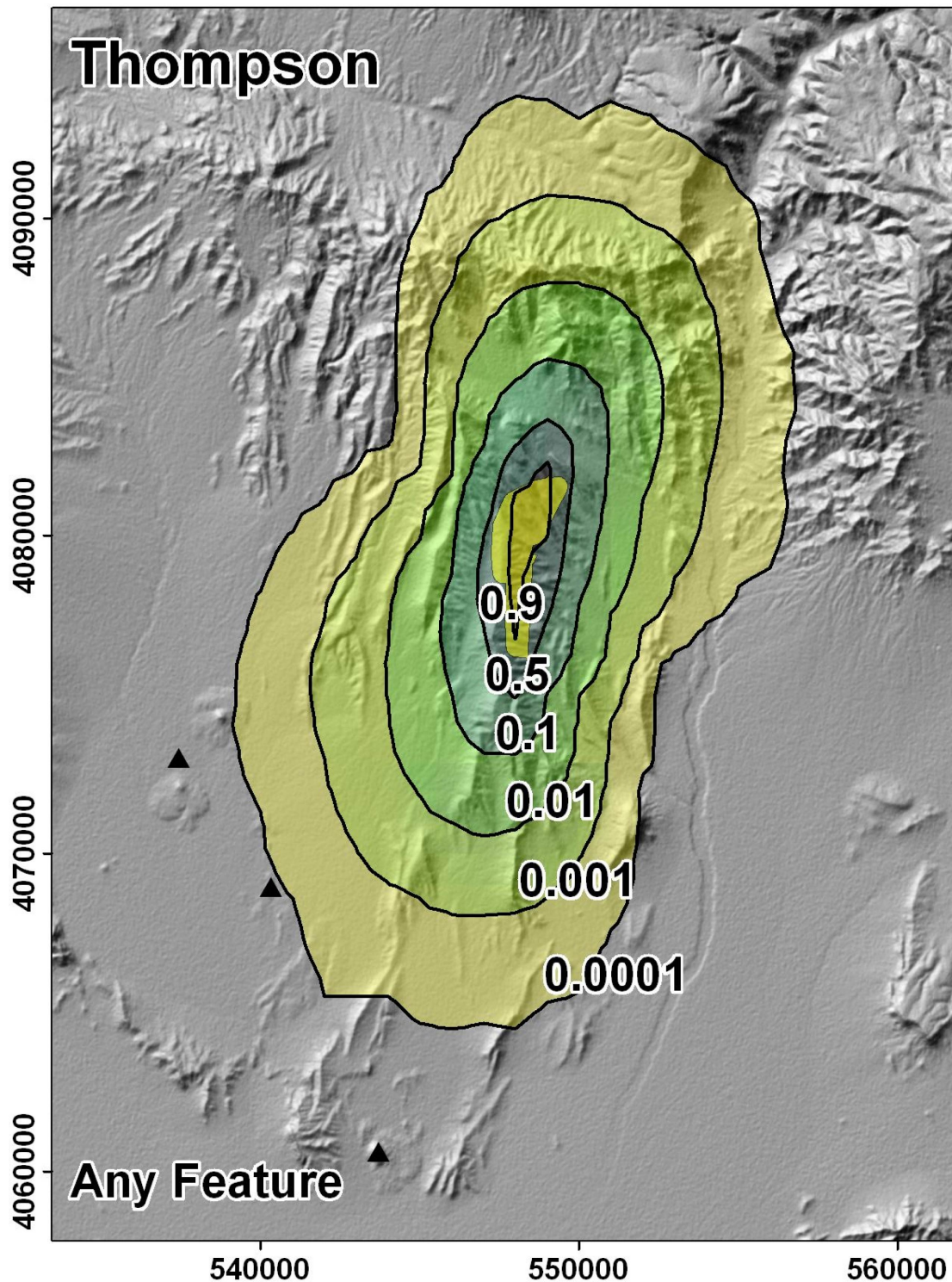
Graphs show the results of 30,000 iterations of the event simulator, which generates conduit diameter based on the dike width and the assessed relationship between dike width and conduit diameter.

Figure 3.2.8-13. Simulated Distribution for Conduit Diameter Based on Assessments of George Thompson



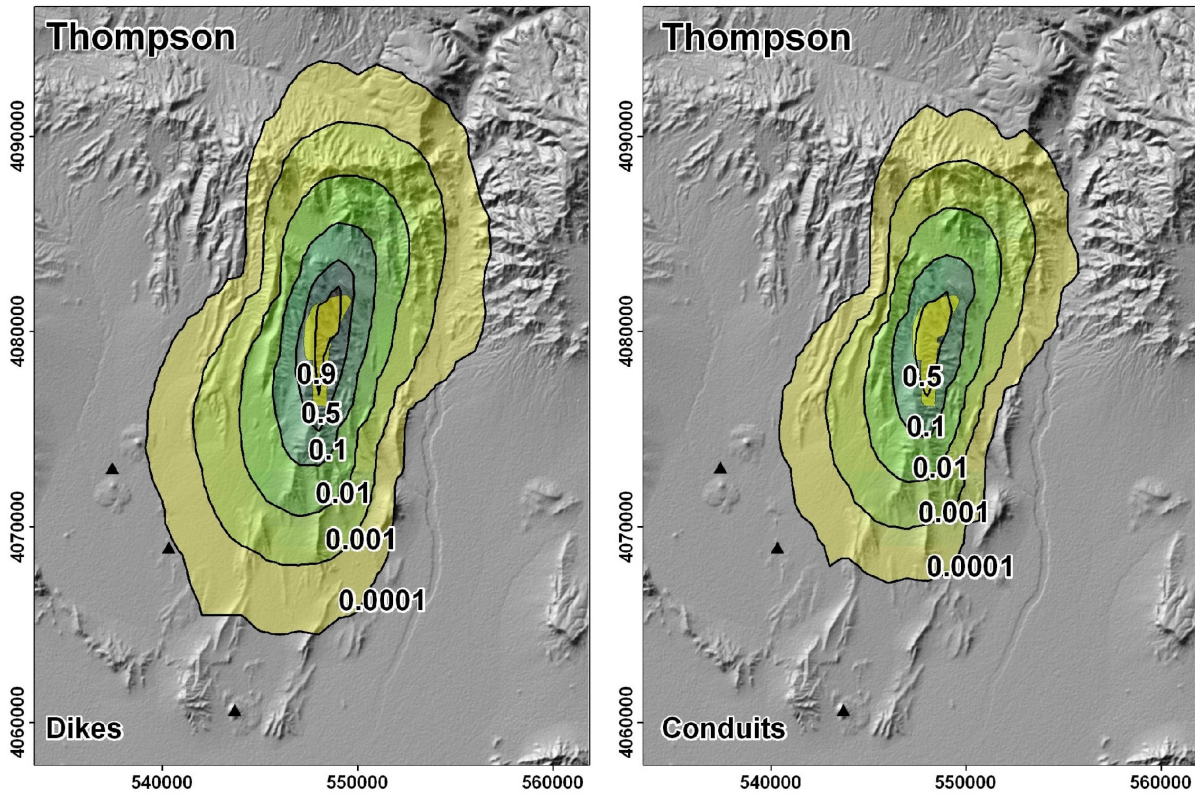
NOTE: Dikes are represented as black lines; their lengths on the figure are the lengths of the simulated dike. Conduits are represented as small red circles; the diameter of the conduit is not represented. Sills, if they exist, are represented by light yellow ovals or polygons.

Figure 3.2.8-14. Examples of Simulated Events from the PVHA-U Model for George Thompson



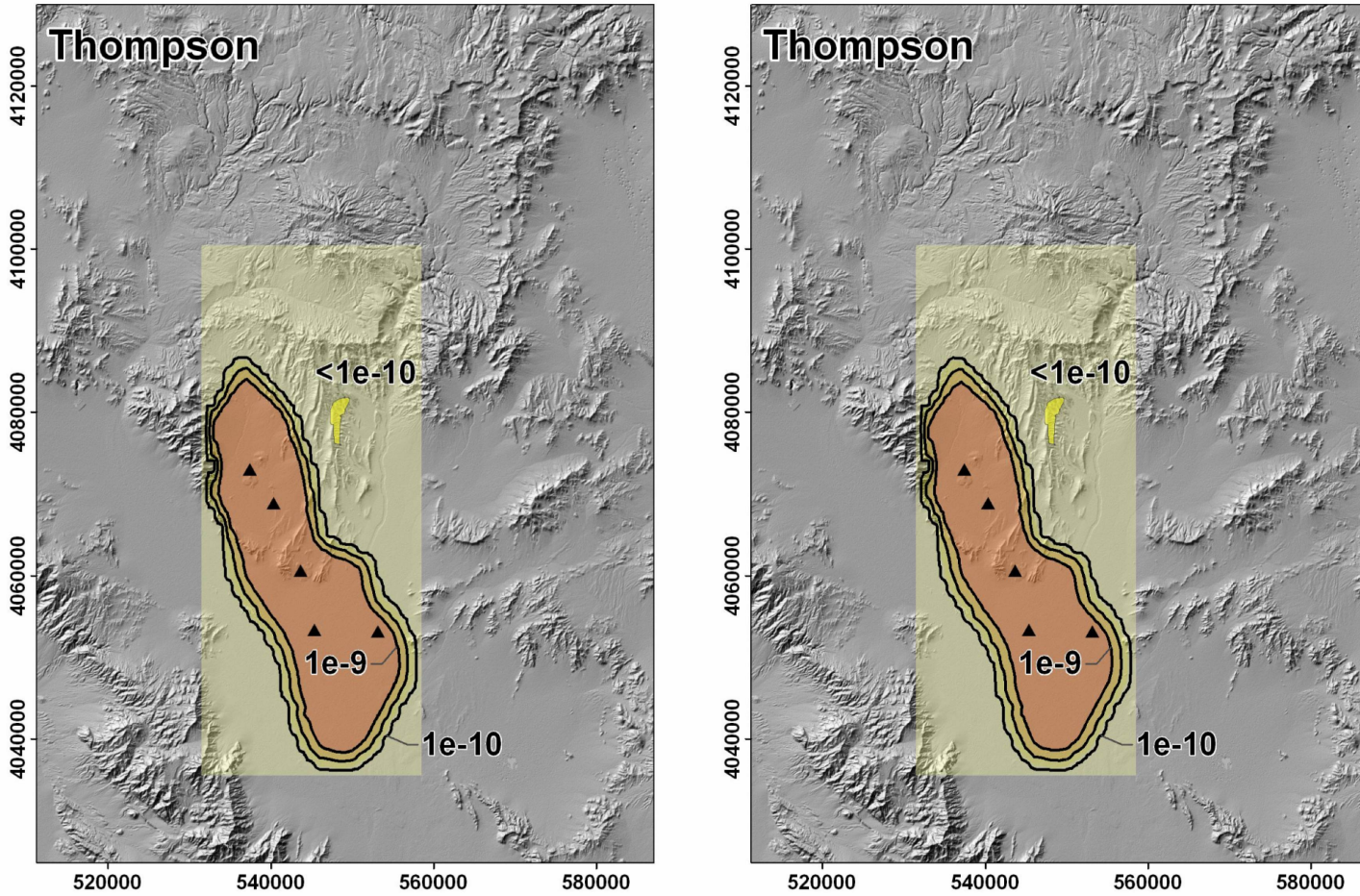
NOTE: Yellow polygon represents the repository footprint. Black triangles represent past events (GT's most likely event set). Map grid ticks are UTM meters; tick intervals are 10 km.

Figure 3.2.8-15. Conditional Probability of Intersection of Any Feature with the Repository Footprint Based on Event Descriptions Developed by George Thompson



NOTE: Yellow polygon represents the repository footprint. Black triangles represent past events (GT's most likely event set). Map grid ticks are UTM meters; tick intervals are 10 km.

Figure 3.2.8-16. Conditional Probability of Intersection of Each Igneous Feature with the Repository Footprint Based on Event Descriptions Developed by George Thompson



NOTE: The left figure is the mean rate density for the 10,000-year assessment, the right figure is the mean rate density for the 1-My assessment. Yellow polygon represents the repository footprint. Black triangles represent past events (GT's most likely event set). Map grid ticks are UTM meters; tick intervals are 20 km.

Figure 3.2.8-17. Mean Rate Density for the 10,000-Year Assessment and the 1-My Assessment Based on the Assessments of George Thompson

Table 3.2.8-1. Data Used to Define Spatial Distribution and Event Rates for Future Volcanic Events for George Thompson's PVHA-U Model

Zone	Name	Number of Events (weight)	Age (Ma)	Volume (km ³)
Crater Flat / Amargosa Desert zone	Lathrop Wells	1	0.077	0.048
	Quaternary Crater Flat	1 (weight = 0.95)		
	Makani Cone	2 (weight = 0.03)	1.07	0.002
	Black Cone	3 (weight = 0.01)	1.07	0.06
	Red Cone	4 (weight = 0.01)	1.07	0.055
	Little Cones		1.07	0.034
	Pliocene Crater Flat	1	3.8	0.585
Anomaly B	1	3.85	1.227	
	Anomalies G, F, and H	1 (weight = 0.95)	3.9	0.028
		3 (weight = 0.05)		0.029
Background zone	Sleeping Butte: Hidden Cone	1	0.35	
	Sleeping Butte: Little Black Peak	1	0.35	
	Clayton Valley Cone	1	0.39	
	Buckboard Mesa	1	2.9	

NOTES: Table derived from GT's Elicitation Summary in Appendix D.

Volumes of events outside the Crater Flat / Amargosa Desert zone are irrelevant for the model and are not included.

Table 3.2.8-2. Frequency of Number of Dikes and Conduits or Vents in Simulated Events Based on the Assessments of George Thompson

		Number of Conduits and Vents in an Event							
		1	2	3	4	5	6	7	8
Number of Dikes in an Event	1	30.8%	0.0%	0.0%	0.0%	0.0%	0.0%	0.0%	0.0%
	2	13.4%	20.6%	0.0%	0.0%	0.0%	0.0%	0.0%	0.0%
	3	6.1%	4.8%	4.9%	0.0%	0.0%	0.0%	0.0%	0.0%
	4	2.1%	1.9%	1.1%	1.3%	0.0%	0.0%	0.0%	0.0%
	5	1.0%	1.0%	0.6%	0.4%	0.8%	0.0%	0.0%	0.0%
	6	0.7%	0.7%	0.4%	0.3%	0.4%	0.2%	0.0%	0.0%
	7	0.5%	0.5%	0.3%	0.2%	0.3%	0.1%	0.1%	0.0%
	8	0.4%	0.3%	0.2%	0.2%	0.2%	0.1%	0.0%	0.0%
	9	0.2%	0.2%	0.2%	0.1%	0.2%	0.1%	0.0%	0.0%
	10	0.1%	0.2%	0.1%	0.1%	0.1%	0.0%	0.0%	0.0%